INVESTIGATING THE TIME-DEPENDENT EFFECTS OF SULFORAPHANE, UROLITHIN A, AND ZLN005 AS INDUCERS OF MITOCHONDRIAL TURNOVER IN MUSCLE

NEUSHAW MORADI

A THESIS SUBMITTED TO THE FACULTY OF GRADUATE STUDIES IN PARTIAL FULFILLMENT OF THE REQUIREMENTS FOR THE DEGREE OF

MASTER OF SCIENCE

GRADUATE PROGRAM IN KINESIOLOGY AND HEALTH SCIENCE

YORK UNIVERSITY

TORONTO, ONTARIO

OCTOBER 2022

ABSTRACT

The mitochondrial profile of skeletal muscle is a strong determinant of whole-body metabolic health. The overarching mechanisms that contribute to organelle maintenance and optimal function involve their production, preservation, and recycling. Impairments in the vast connections between these mechanisms have been reported to develop because of poor signal transduction, thus leading to complications in mitochondrial content and function, resulting in a catabolic phenotype. While the importance of these mechanisms is uncontested, their characterization continues to unfold. We pursued three agents, Sulforaphane, Urolithin A, and ZLN005, which have been partially recognized in their ability to induce the Nrf-2/ARE antioxidant system, mitophagy, or mitochondrial biogenesis, respectively. As a novel approach, we sought to add to their characterization by examining the time-dependent effects on mitochondrial refreshment using an *in vitro* model of skeletal muscle following treatment. Our data indicate the potential of these agents, either alone or in combination, to improve mitochondrial homeostasis in muscle.

ACKNOWLEDGMENTS

"The great tragedy of science – the slaying of a beautiful hypothesis by an ugly fact."

-T.H. Huxley

To my family, thank you. Your support and belief in my aspirations are what sustain my perseverance and ambition to keep going. I endlessly appreciate your faith in my passion. Thank you for enduring my odd hours of work and for understanding my dedication to the field. I hope to make you proud.

To my supervisor, Dr. David Hood, thank you. Your leadership, guidance, and support construct the fundamentals on which I continue to fortify and expand my scientific experience, knowledge, and journey. We have begun since my undergraduate position as an Independent Study student, and it is with great honour to now close the second chapter of my research career, as an MSc. I look forward to this next challenging and exciting climb towards a PhD with you, as well.

To Ashley, Jon, and Matt, thank you. I could not have asked for a better trio of mentors, each of whom I have equally annoyed with endless questions. It has been a privilege to receive your guidance and advice as they have accelerated my understanding of the laboratory life and the realm of research. Thank you for being my teachers and moulding my technique, for your patience, and for your time. You have each calibrated my goals to attain your level of intellectual strength one day.

To Shahir, thank you. You are a talented and inspirational trailblazer who encouraged me to follow the data. The quote above applies to what you have been trying to show me. Thank you for being my pillar and for listening to all my good and bad days. I am honoured to witness your triumph as a great scientist, and I am lucky to have you in my life.

To Mikhaela, thank you. I think of you as the best example for what a persevered and dedicated critical thinker should be. Thank you for supporting me and listening to me. Thank you for the late-night lab jam sessions, for matching my energy for 'The Office', and for the constant vein-popping laughs. It is a privilege to watch you flourish in this field.

To Deb and Rita, thank you. Your vast scientific knowledge and mentorship widened my lens of education in the field. You have both reminded me to avoid neglecting the bigger picture, and to appreciate the general and wide-ranging scientific applications on which I can build and refine my expertise.

To Jenna, Victoria, and Kate, thank you. I am glad you are here and proud to see how each of you are building your knowledge and experience in research. I cannot wait to see the ways in which you will excel with valuable achievements in your arsenal. Thank you for all your help and support. I am grateful to continue sharing what I have learned on my journey so far, and to be a trailblazer for you and others, in the way the people above have been for me.

TABLE OF CONTENTS

ABSTRACT……..ii

ACKNOWLEDGEMENTS……iii

TABLE OF CONTENTS……...iv

LIST OF FIGURES…….vi

LIST OF TABLES……..vii

LIST OF ABBREVIATIONS……...viii

CHAPTER 1 – REVIEW OF LITERATURE **1**

1.0. THE ROLE OF MITOCHONDRIA IN SKELETAL MUSCLE……2

1.1.MITOCHONDRIAL TURNOVER……3

1.1.1. *Mitochondrial Biogenesis*……..3

1.1.2. *Mitophagy: The Autophagosome-Lysosome Pathway*…….....6

1.1.3. *Mitochondrial Preservation via Antioxidant Response*……....10

1.2.MITOCHONDRIAL SIGNAL ENHANCEMENTS AND IMPAIRMENTS……..15

1.2.1. *Exercise: The Ultimate Stimulus for Redundant Pathway Activation*…….15

1.2.2. *The Decline in Mitochondrial Health with Aging*……18

1.2.3. *Metabolic Mimicry: Nutraceutical and Pharmaceutical Agents*…….20

RESEARCH OBJECTIVES……..28

HYPOTHESES……28

REFERENCES……...30

CHAPTER 2 – MANUSCRIPT **43**

MANUSCRIPT AUTHOR CONTRIBUTIONS……..44

SULFORAPHANE, UROLITHIN A, AND ZLN005 INDUCE TIME-DEPENDENT ALTERATIONS FOR ANTIOXIDANT CAPACITY, MITOPHAGY, AND MITOCHONDRIAL BIOGENESIS IN MUSCLE…….45

ABSTRACT……46

INTRODUCTION……47

METHODS…….....49

RESULTS…….....52

DISCUSSION…….....64

CONCLUSIONS…….....68

REFERENCES…….....69

FUTURE DIRECTIONS…….....73

APPENDIX A: SAMPLE DATA AND STATISTICAL ANALYSES…….....74

APPENDIX B: SUPPLEMENTAL DATA…….....78

APPENDIX C: LABORATORY METHODS AND PROTOCOLS…….....79

APPENDIX D: OTHER CONTRIBUTIONS TO THE LITERATURE…….....88

LIST OF FIGURES

CHAPTER 1: REVIEW OF LITERATURE

Fig. 1 – Mechanisms and stimuli that contribute to mitochondrial turnover and homeostasis……..25

Fig. 2 – Schematics summarizing the documented function of the agents [A] Sulforaphane, [B] Urolithin A, and [C] ZLN005. ……..26

CHAPTER 2: MANUSCRIPT

Fig. 1 – Schematic summarizing the documented function of Sulforaphane……54

Fig. 2 – Upstream protein markers observed in the Nrf-2-ARE antioxidant pathway following Sulforaphane treatment…….55

Fig. 3 – Downstream protein markers observed in Nrf-2-ARE antioxidant pathway following Sulforaphane treatment…….56

Fig. 4 – Schematic summarizing the documented function of Urolithin A……..58

Fig. 5 – Whole cell mitophagy markers following Urolithin A treatment……59

Fig. 6 – Mitophagy flux following Urolithin A and Bafilomycin A co-treatment……60

Fig. 7 – Schematic summarizing the documented function of ZLN005……62

Fig. 8 – Analyzing the impact of ZLN005 on the drive for mitochondrial biogenesis……..63

APPENDIX B: SUPPLEMENTAL DATA

Image – Crystal Violet Staining. Diagnostic of cell viability for each treatment and corresponding concentrations using crystal violet staining assay……78

LIST OF TABLES

CHAPTER 1: REVIEW OF LITERATURE

Table 1 – A few of many pharmaceutical and nutraceutical agents and their reported effects on mitochondria…….27

APPENDIX A: DATA AND STATISTICAL ANALYSES

Table 1 **A** – Whole cell Nrf-2 protein content following 4, 24, and 48 hours of SFN treatment……..74

Table 1 **B** – Corresponding Fold-Above-Control for whole cell Nrf-2 protein at each time point…….. ……..74

Table 2 – Nuclear Fraction of Nrf-2 measured after 4 hours of SFN treatment……..75

Table 3 **A** – Whole cell Keap-1 protein content following 4, 24, and 48 hours of SFN treatment……..75

Table 3 **B** – Corresponding Fold-Above-Control for whole cell Nrf-2 protein at each time point…….75

Table 4 – Example of calculations conducted for all 3 time points for proteins related to SFN, UroA, and ZLN treatment. Example procedure provided using NQO1…….76

Table 5 **A** – Mitophagy Flux Data for p62……...76

Table 5 **B** – Mitophagy Flux Data for LC3-II……..76

Table 6 – NTC- and EV-corrected data of ZLN-induced increases in TFAM promoter activity…..……77

APPENDIX B: SUPPLEMENTAL DATA

Table 1 – Luminescence reading of dual luciferase reporter assay following treatment with SFN, UroA, and ZLN005. ZLN has been reported to inhibit luciferase activity.……78

LIST OF ABBREVIATIONS

AMP	Adenosine monophosphate
AMPK	AMP-activated protein kinase
ANOVA	Analysis of variance
ARE	Antioxidant response element
ATG	Autophagy-related protein
ATP	Adenosine triphosphate
CaMK	Ca2+/calmodulin-dependent protein kinase
cAMP	Cyclic AMP
COX	Cytochrome c oxidase
DNA	Deoxyribonucleic acid Drp1 Dynamin-related protein 1
ETC	Electron transport chain
FAD+	Flavin adenine dinucleotide
FADH2	Flavin adenine dinucleotide (reduced)
Fis1	Mitochondrial fission 1
Foxo	Forkhead box O
H+	Hydrogen ion
HO-1	Heme-oxygenase-1
IMM	Inner mitochondrial membrane
IMS	Intermembrane space
K+	Potassium ion
KO	Knockout
kDa	Kilodaltons
LC3	Microtubule-associated proteins 1A/1B light chain 3A
MAPK	Mitogen-activated protein kinase
MEF2	Myocyte enhancer factor 2
Mfn2	Mitofusin-2
mTORC1	Mammalian/mechanistic target of rapamycin complex 1
Na+	Sodium ion
NAD+	Nicotinamide adenine dinucleotide

NADH	Nicotinamide adenine dinucleotide (reduced)
NF-κB	Nuclear factor kappa-light-chain-enhancer of activated B cells
NTC	Non-transfected control
NQO1	Nicotinamide Quinone Oxidoreductase 1
NRF-1/-2	Nuclear respiratory factor-1 and -2
Nrf-2	Nuclear factor (erythroid-derived 2)-like 2
NuGEMPs	Nuclear gene-encoded mitochondrial proteins
OMM	Outer mitochondrial membrane
OPA1	Optic atrophy 1
OXPHOS	Oxidative phosphorylation
p62	Sequestosome-1 (SQSTM1)
PCR	Polymerase chain reaction
PGC-1α	Peroxisome proliferator activator receptor (PPAR) γ coactivator 1 alpha
PINK1	PTEN-induced putative kinase 1
PMF	Proton motive force
RNA	Ribonucleic acid
ROS	Reactive oxygen species
SDS-PAGE	Sodium dodecyl sulfate polyacrylamide gel electrophoresis
SirT	Sirtuin
SR	Sarcoplasmic reticulum
SS	Subsarcolemmal
TCA	Tricarboxylic acid cycle
TFAM	Mitochondrial transcription factor A
TFEB	Transcription factor EB
UCP3	Uncoupling protein 3
ULK1	Serine/threonine protein kinase ULK1
UQ	Ubiquinone
Ub	Ubiquitin
VDAC1	Voltage-dependent anion channel 1

CHAPTER 1

REVIEW OF LITERATURE

1.0 The Role of Mitochondria in Skeletal Muscle

Cellular respiration is an evolutionarily conserved process carried out by virtually all known eukaryotic organisms to sustain their function, maintain homeostasis, and adapt to the energy demands brought on by metabolic or environmental stressors. The mitochondrion is the exceptional organelle responsible for this stunning yet complex procedure, using anaerobic (pyruvate, TCA cycle) and aerobic systems (oxidative phosphorylation) to generate adenosine triphosphate (ATP), the metabolic currency that drives a plethora of cellular processes for survival. ATP fuels most of the biological pathways that sustain broad and important functions, such as muscle contraction, neural action potential propagation, photosynthesis, and protein synthesis [1-5]. Therefore, the mitochondrial phenotype can differ between cell or tissue types as the volume of ATP required changes with respect to functional and metabolic demands [5-6].

While the organelle can differ in size, morphology, and content between tissues [5,7-9], mitochondrial plasticity is arguably most animated in skeletal muscle, owing to the varying energy demands from movement and locomotion. Further, the mitochondrial profile observed in skeletal muscle is a direct determinant of not only its endurance capacity, but also its capability to adapt to the metabolic or environmental insults against the cell [10-12]. Exceptional and unfaltering research has shown that regular endurance exercise can enhance the mitochondrial pool in skeletal muscle to 1) develop a reticular morphology that is higher in content compared to untrained muscle [13-15], 2) tightly couple oxidative phosphorylation (OXPHOS) with ATP generation [16-17], and 3) attain physical proximity to other mitochondrial reticula and myofibres for efficient substrate exchange [18-19]. Together, these equip the cell with the metabolic foundation to effectively perform under duress and achieve enhanced basal respiration and homeostasis at rest. Meanwhile, physical inactivity and aging have been found to impair the signaling cascades that govern mitochondrial dynamics and

turnover, thus compromising the reticulum, impairing function, and shifting the cell's equilibrium to favour a catabolic phenotype [5,8-9,13,20-22].

While it is important to acknowledge the integral role of mitochondria in all cell and tissue types within the eukaryotic domain, this review of literature will focus on mammalian skeletal muscle mitochondria and discuss the shifts in their milieu following exercise and aging. The review will also explore some nutraceutical and pharmaceutical agents that have been developed and enhanced to target important pathways that govern the mitochondrial profile in skeletal muscle. Together, these discussions may illuminate the portrayal of the mechanisms and targets of redundant signaling pathways to rescue skeletal muscle health during conditions that require therapeutic interventions.

1.1 Mitochondrial Turnover

The primary systems which contribute to the refreshment of the mitochondrial pool are mitochondrial biogenesis, mitochondrial autophagy (hereafter referred to as mitophagy), and antioxidant capacity. In the following section, an overview of their relevant signaling pathways with respect to endurance exercise and skeletal muscle will take place. Changes to their efficacy following signaling enhancements or impairments will be discussed in a later section (See Section 1.2).

1.1.1. Mitochondrial Biogenesis

Under healthy conditions, a series of events dedicated to the transcription, translation, import, and correct assembly of specific proteins upon the call for mitochondrial production takes place, referred to as mitochondrial biogenesis [23-25]. The physiological or environmental stimuli that may trigger biogenesis at the transcriptional level include exercise, cold temperatures, or cellular stress [26-29]. These primary signals can activate second messengers such as calcium (Ca^{2+}), ATP, NAD^{+}, cyclic AMP (cAMP), and reactive oxygen

species (ROS), which can initiate the cascade of different molecular transducers, such as signaling kinases, that will prompt the nuclear localization of transcriptional coactivators and transcription factors for the genetic transcription of nuclear genome-encoded mitochondrial proteins (NuGEMPs) [5]. These kinases converge and contribute to the activation of the meticulously studied peroxisome proliferator-activated receptor gamma co-activator 1-alpha (PGC1α), an integral responder to physiological signals for energy demand, predominantly with exercise [5,26,30]. This master regulator of mitochondrial biogenesis undergoes many transcriptional, subcellular, and post-translational modifications in skeletal muscle. Those concerning energy deprivation, however, are its direct phosphorylation by the 5' adenosine monophosphate-activated protein kinase (AMPK) [31] and deacetylation by the NAD^+-dependent protein deacetylase, Sirtuin 1 (SIRT1) [32]. Respectively, these enable the nuclear localization of PGC-1α whilst maximizing its transcriptional coactivation capabilities.

A plethora of transcription factors can associate with PGC-1α to relay the signal cascades dedicated to thermogenesis in adipose tissue, gluconeogenesis in the liver, and fibre-type switching in skeletal muscle [26]. However, those pertaining mitochondrial bioenergetics, and specifically biogenesis, include mitochondrial transcription factor A (TFAM), nuclear respiratory factor (NRF)-1 and NRF-2, and estrogen-related receptor alpha (ERRα) [26,33-34], which transcribe mitochondrially committed mRNA. Indeed, mitochondria contain their own circular DNA (mtDNA), which are predominantly transcribed by TFAM, a regulator of mtDNA transcription. Despite its obvious contribution to mitochondrially-related gene transcription, mtDNA contributes less than 1% of the total mitochondrial proteins, with 37 genes comprising 13 essential respiratory chain components along with 22 tRNAs and 2 rRNAs, [35]. Therefore, the mechanism by which mitochondrial proteins are transcribed and translated is regulated through the collaboration of both the mitochondrial and nuclear genomes, with the majority of proteins originating from outside of the mitochondrion. Thus,

handling of these precursor proteins is integral to the expansion of the mitochondrial pool, with the remainder provided by the nucleus. There exists a complex cascade of events that allow the products of either genome to shuttle to, and integrate within, the mitochondrion to facilitate in reticular expansion of the organelle. Following translation in the cytosol of the transcribed mRNA, and depending on their intended function, the unfolded precursor proteins cross the mitochondrial membranes by interacting with protein translocases. While integral in their contribution to mitochondrial biogenesis, discussions surrounding the ATP-dependent protein import machinery (PIM) are beyond the scope of this review. However, two recent and excellent reviews on this subject have been made available by Wiedemman et al. [36] and Kummer et al. [37]. Altogether, these mechanisms expand the mitochondrial network in skeletal muscle through the recruitment of mitochondrial fusion proteins Opa1 and Mfn1/2 and a concomitant reduction in fission protein Drp1 and Fis1 [5,18,22,38], thus creating a proportionate capacity for energy supply following greater energy demand.

While the dependence and focus on PGC-1α within the context of exercise-induced mitochondrial changes are evident in many studies, some have challenged its requirement for mitochondrial biogenesis. Often using knockout models, some studies have reported that changes to the mitochondrial pool can occur with exercise even in the absence of PGC-1α [39]. A potential confounding variable for these interpretations may be how knockouts are generated as residual splice variants of PGC-1α may be left intact to perform auxiliary functions [40]. With the advent of gene editing technology, it may now be possible to tailor specific deletions to PGC-1α, its isoforms, and family members to uncover their specific roles or possible redundancies that may influence these contradictory observations.

Indeed, it is imperative to acknowledge that other regulatory markers contribute to mitochondrial biogenesis in tandem with PGC-1α, especially considering that its functions in certain respects can be redundant. One example is the master regular of cellular antioxidant

response, nuclear factor erythroid 2-related factor 2 (Nrf-2), which will be discussed in detail pertaining to its mechanism and relevant antioxidant capacity in Section 1.1.3). In this context, however, Nrf-2 is also capable of binding to antioxidant response element (ARE) regions of NuGEMP promoters, including that of the NRF-1 gene [41,42] and potentially TFAM gene [41,43]. A recent study also demonstrated that Nrf-2 deficiency in middle aged and old mice showed significantly lower mRNA expression for NRF-1, TFAM, and PGC-1α, but no significant changes in young knockout mice [44]. A shift in mitochondrial dynamics to favour fission and fragmented reticula via increased Drp1 content also occurred under these conditions. Finally, reduced SDH staining as an indication of impaired complex I activity alongside reduced mtDNA copy number demonstrated the functional impact on mitochondria, as well [44]. Together, these fortify the relationship between not only Nrf-2 as a regulator of mitochondrial biogenesis signaling, but also the accelerated decline of important mitochondrial markers following Nrf-2 deficiency with age, despite the presence of PGC-1α.

Indeed, mitochondrial biogenesis is an invaluable contributor to the turnover, maintenance, and regulation of mitochondria in skeletal muscle. The pillars underneath this arc include mitochondrial content, composition, and dynamics, which can be improved or impaired, depending on the stimulus. The optimization of this mechanism relies on the availability of redundant markers as well as the tight regulation between the other arcs dedicated to mitochondrial turnover, thus beginning the next discussion on the efficient removal of suboptimal mitochondria.

1.1.2 Mitophagy: The Autophagosome-Lysosome Pathway

The next integral contributor to mitochondrial homeostasis is the selective degradation of dysfunctional mitochondria, termed mitophagy [5]. In addition to impaired biogenesis, aging, disuse, or myopathies exemplify the incapacity to clear poor functioning mitochondria.

This leads to toxic levels of ROS in these poorly respiring mitochondria, increased oxidative stress, and further to the impairment of skeletal muscle health, reduced protein synthesis [5,8,18,22]. Beneficial stimuli such as exercise, however, can enhance mitophagy in a skeletal muscle system [45,46] as this relieves the insult from ROS and enables refreshment of the mitochondrial pool. The following section will describe the mitophagy pathway and highlight important takeaways from the literature that demonstrate its relationships with PGC-1α and its roles beyond mitochondrial biogenesis.

In addition to its many roles in cellular metabolism, AMPK is also an activator of mitophagy through the phosphorylation of the outer membrane receptor, Mitochondrial Fission Factor (MFF), thus recruiting Dynamin Related Protein 1 (Drp1) and Fission Protein 1 (Fis1), to facilitate mitochondrial fragmentation, and subsequently proceed through the mitophagy system [8,45,47]. In healthy, unstressed mitochondria, PTEN-induced kinase-1 (PINK1) is regulated post-translationally by translocating across the mitochondrial membranes with the help of PIM, where PINK1 is cleaved in the matrix by mitochondrial processing peptidase (MPP) and presenilin-associated rhomboid-like protein (PARL) in the inner mitochondrial membrane (IMM). The cleaved PINK1 then dissociates from the mitochondrion and heads for rapid degradation by the ubiquitin-protease system. Disruption and reduction of mitochondrial membrane potential ($\Delta\Psi$), however, promotes stabilization of PINK1 on the outer mitochondrial membrane (OMM) through its interaction with translocase of the outer membrane (TOM), without interacting with the MPP-PARL cleaving complexes. PINK1 can then homodimerize and autophosphorylate to serve as an active kinase capable of phosphorylating and activating Parkin, an E3 Ubiquitin Ligase, as well as Ubquitin (Ub), a mitochondrial tag, to the targeted mitochondrion. Parkin attains full activation upon binding to phospho-Ub and executes its role in building poly-Ub chains on other target proteins on the OMM [5].

The adaptor protein, sequestosome 1 (SQSTM1) or p62, plays an important role in the recognition of, and binding to, ubiquitinated cargos. This occurs alongside simultaneous autophagosomal development by way of PI3K-mediated activation of PI3P, which activates the two Ub-like systems: Atg8 and Atg12 conjugating systems, forming a growing vesicular phagophore/autophagosome. Embedded in this double-membrane vesicle is one of several Atg8 family proteins: microtubule-associated protein 1A/1B-light chain 3 (LC3)-II. Following lipidation of its inactive precursor LC3-I, LC3-II anchors to p62 and facilitates the engulfment of the Ub-tagged mitochondrion [47-49]. Microtubules then facilitate the occupied autophagosome's transportation to the lysosome for fusion and organelle degradation [49].

Autophagosome-lysosomal fusion occurs by way of Rab and Arf small GTPase protein families. Their GTP-bound active membrane state (compared to their GDP-bound cytosolic state) enables recognition by effector proteins such as SNAREs, SM (Sec1/Munc-18) proteins, coat proteins, and motors to facilitate fusion [49]. In other types of autophagy pathways, such as with chaperone mediated autophagy, the transmembrane protein lysosome-associated membrane proteins (LAMP)-1 and -2 are said to aid in entry of the target protein into the lysosome for degradation. The product of autophagosome-lysosomal fusion is termed the autolysosome [50,51].

Alternatively, mitophagy can be initiated independent of PINK1 and Parkin, in receptor mediated pathways. BCL2/ adenovirus E1B interacting protein (BNIP3) and NIX are both receptors found on the outer mitochondrial membrane, previously described for their roles in apoptosis, have recently been shown to flag dysfunctional organelles for degradation [5,50]. Both BNIP3 and NIX contain LC3 interacting domains, which allow the engulfment of the damaged organelle by the growing autophagosome [51]. Therefore, mitophagy is a complex process that can be initiated by several independent pathways that strives to recycle dysfunctional mitochondria and ideally preserve the mitochondrial reticulum.

Similar to mitochondrial biogenesis, mitophagy can be stimulated during various external or environmental stressors. Exercise for example, can induce both mitochondrial biogenesis as well as mitophagy. In this context, the depletion of energy alters the ADP:ATP ratio thereby activating AMPK. Recently, it has been proposed that PGC-1α and TFEB (a member of the MiT regulatory family that promote lysosomal biogenesis) are correlated, thus likely coordinating and regulating their expression and activity [52]. A whole-body KO model of PGC-1α in mice not only showed reductions in mitochondrial biogenesis but also attenuated mitophagy flux when paired with denervation, thus reducing the capacity for targeting and removing dysfunctional mitochondria. Additionally, while LC3-II and p62 mitochondrial localization were reduced, PGC-1α overexpression still increased lysosomal capacity. This suggests that the two dichotomous processes that regulate mitochondrial turnover are highly correlated and coordinated at the upstream signaling levels that typically lead to mitochondrial biogenesis and mitophagy [52]. Furthermore, recent evidence showed that PGC-1α overexpression via *in vivo* transfection in young female mice following remobilization after two weeks of immobilization resulted in improved fusion and reduced ROS, despite attenuated levels of mitophagy proteins [53]. The coordination between PGC-1α and markers of mitophagy appears to be bidirectional, as Parkin overexpression in young and old mice has been found to increase PGC-1α content, mitochondrial density, reduce oxidative stress, and even induce hypertrophy [54]. Finally, the exercise-induced improvements in mitochondrial regulation, flux, and content were all attenuated in PGC-1α KO mice [52], fortifying the crosstalk that occurs between these markers of mitochondrial turnover.

The fascinating coordination that occurs bidirectionally between PGC-1α and markers of mitophagy suggest that its roles as a master regulator exceed those of just biogenesis as it contributes ubiquitously to mitochondrial homeostasis. While its absence does not abolish the signaling pathways for mitophagy, it is evident that these conditions can nevertheless disrupt

the efficiency of mitochondrial turnover, thus impacting the tight-knit regulation between biogenesis and mitophagy in healthy skeletal muscle. Whilst the utility of mitophagy is indisputable, the electrochemically coupled system integrated in the electron transport chain (ETC) concentrates the hub of ROS accumulation. Therefore, it is possible that triggering mitophagy each time there is a sign of elevated ROS can exhaust the cell and perhaps render inefficient mitochondrial regulation. Thankfully, intrinsic scavengers and antioxidant mechanisms are in place to attenuate elevated ROS under conditions where the mitochondrion is salvageable.

1.1.3 Mitochondrial Preservation via Antioxidant Response

Excessive electron backpressure and overwhelmed chemiosmotic gradients at the electron transport chain delegate the production of free radicals that, at toxic levels, can disrupt efficient OXPHOS, induce lipid peroxidation, and damage DNA and proteins, thus severely compromising cellular homeostasis and viability [55]. Mitochondria are primary sources of intracellular ROS production, as well as the culprits for the intracellular damage borne of excess ROS. Interestingly, and perhaps paradoxically, moderate levels of ROS are essential for the maintenance of cellular homeostasis [56-57], owing to their capacity to trigger antioxidant pathways that can attenuate intracellular damage, and preserve mitochondrial function. In fact, many disease states are borne of excessively suppressed ROS, thus requiring caution within the medical field when developing mitochondrially targeted therapeutics [58-60].

The ETC of the mitochondrion is comprised of five enzyme complexes and two electron carriers. The designations of the complexes are: Complex I, or NADH: ubiquinone reductase; Complex II, or FADH: succinate ubiquinone reductase; Complex III, or cytochrome c reductase; Complex IV, or cytochrome c oxidase, or NADH dehydrogenase; and Complex V, or F_0F_1ATP synthase [61-62]. Metabolism of free fatty acids (FFA) or glucose for bulk energy

production occurs at this formidable assembly, located on the inner mitochondrial membrane. Prerequisite steps to metabolize these fuels take place via fatty acid oxidation or glycolysis, the remaining substrates for which then localize to the mitochondrial matrix via carriers specific to each fuel type. Here, FFAs can undergo further processing via β-oxidation. These biochemical reactions ultimately produce the key intermediate, Acetyl-CoA, which can enter the tricarboxylic acid (TCA) cycle, or Krebs' Cycle to produce NADH and $FADH_2$. These substrates donate their electrons to the ETC at Complex I or II, respectively, upon which a cascade of redox reactions coupled with proton pumping take place to build the protonmotive force and potential energy that drives ATP synthesis. Excellent reviews from 2019 and 2021 describe the biochemical redox reactions that occur between and within each complex [61-62].

Mitochondria respond very well to ATP demand, driven by the presence of the rate-limiting substrate, free ADP (ADP_f). Alongside inorganic phosphate (P_i), it is liberated from the reaction that breaks down ATP, which takes place in the cytoplasm from varying ATPases including the Na^+/K^+ ATPases in cell membranes, sarcoplasmic reticulum ATPases that help in Ca^{2+} reuptake, and myosin ATPases following muscle contraction. The F_0F_1ATP synthase or Complex V responds strongly to a demand for ATP, as ADP_f must be present in the matrix for the enzyme to carry out its function. Therefore, under conditions where there is a low demand for ATP, as a result of reduced muscle contraction, loss of substrate, or poor signaling, the remaining complexes in the ETC will continue to conduct their electron transfer and build the proton gradient without its main source of dissipation, thus inducing "backpressure" [63] upon the ETC and inhibiting efficient coupled respiration [63]. Leaky uncoupling proteins can help dissipate the potential energy to generate heat and can allow for a slowed rate of oxygen consumption, but do not produce ATP. Therefore, the slower moving electrons can heighten the possibility of their escape from the ETC to instead react with electrophilic superoxide anions, ultimately forming ROS.

Although there are few explanations as to what threshold of ROS, or duration of ROS exposure, warrants mitophagy or even apoptosis, it is important to acknowledge that ROS production in skeletal muscle represents a continuum, wherein oxidative stress is continually present [64]. Therefore, it would be reasonably counterproductive to trigger extreme forms of mitochondrial quality control and disrupt the mitochondrial reticulum during reversible conditions of moderately-increased ROS levels, particularly given that they bode certain benefits to cell survival. These can activate redox signaling pathways that aid in the preservation of the mitochondria during conditions of elevated metabolic stress.

Moderate levels of ROS can promote proliferation, differentiation, and angiogenesis, alongside the activation of redox-sensitive antioxidants. While other processes that mitigate ROS-induced genomic instability, inflammation, or hypoxia are indispensable, this review will focus on the antioxidant response mediated by Nrf-2 and the Keap1/ARE axis as the predominant regulator of redox homeostasis at the transcriptional level. During homeostatic cellular conditions, the transcription factor Nrf-2 is sequestered in the cytoplasm by its negative regulator and homodimer, Kelch-like ECH-associated protein 1 (Keap1). Keap1 binds with an E3 ligase, Cullin3 (Cul3) and operates as the adaptor for the Cul3-Rbx1 ligase-mediated ubiquitination of Nrf-2. The transcription factor contains six distinct domains, which contribute differently towards its binding, transactivation, or functional repression. The domain concerning the predominant regulation of Nrf-2 activity is the Neh2 domain, containing an array of seven lysine residues upon which strong Ub-tagging takes place for its proteasomal degradation. The Neh2 domain is also characterized by its low affinity DLG motif and high affinity ETGE motif, which are bound to either molecule of the Keap1 dimer. The intermolecular affinities between Keap1 and Nrf-2 depend on these motifs as the hydrophobic- and hydrogen-binding DLG presents a lower affinity to the Keap1 double glycine (DC) COOH domain, compared to the strong hydrogen binding alone that occurs at the ETGE.

The Keap1-Nrf-2 complex serves as an electrophile sensor and antioxidant effector, respectively. Indeed, elevated ROS affect the integrity of the intermolecular bond between the Keap1 DC domains and the Nrf-2 Neh2 domain, thus inducing conformational changes upon the Keap1 homodimer that will allow Nrf-2 to carry out its response to a stressed cell. These occur by modifying the highly reactive cysteine residues on Keap1, particularly C151, which are sensitive to redox disturbance. These reactions preserve Nrf-2 binding at the high affinity ETGE motif but compromise it at the DLG motif, thus coining the "hinge and latch" concept, respectively. This ceases the Keap1-mediated sequestration and ubiquitination of nascent Nrf-2, thus bypassing Keap1, and enabling its accumulation in the cytoplasm and translocation to the nucleus. Obligatory heterodimerization with small Musculo-aponeurotic fibrosarcoma (sMaf) proteins take place with Nrf-2 to secure DNA binding at the ARE regions of promoters found upstream of phase II detoxification enzymes, including Nicotinamide Quinone Oxidoreductase 1 (NQO1) and Heme Oxygenase-1 (*HMOX1*, HO-1). Their gene expression is potently upregulated following elevated ROS and subsequent Nrf-2 activation [65-66]. In fact, NQO1 is especially dependent on Nrf-2-mediated signaling, as KO models of the transcription factor abolish its protein content [67]. Evidently, the Nrf-2-ARE pathway earns its position among mitochondrial biogenesis and mitophagy as a major contributor to mitochondrial turnover due to its complex and dynamic provision of antioxidant-mediated mitochondrial protection.

Interestingly, the contributions of Nrf-2-related antioxidant enzymes within skeletal muscle mitochondria may be more indirect than anticipated, despite their importance in preventing many disease states including type II diabetes and metabolic syndrome borne of mitochondrial dysfunction [68-69]. For example, examination of subcellular localization of NQO1 and HO-1 are scarce in the literature, although some have pointed to their cytosolic residence [70-71]. In other words, these markers do not appear to partake in feedback

mechanisms that directly target elevated intramitochondrial ROS levels. This is perhaps due to the sufficient scavenging and neutralizing capacities of markers including superoxide dismutase (SOD), catalase, and glutathione peroxidase (Gpx) [72]. Thankfully, recent literature point to the preserving roles of the antioxidants on upstream regulators that govern mitochondrial turnover and maintain oxidative fibre types in skeletal muscle, thus refining the mitochondrial pool for cellular survival and ultimately reducing ROS.

Alongside the brief discussion that revealed a correlation between Nrf-2 and PGC-1α content (Section 1.1.1), previous literature posits NQO1 as the protector of this transcriptional coactivator from proteasomal degradation by default (Ub-independent), thus proceeding with its co-regulatory roles. A 2013 study [32] showed that PGC-1α is an intrinsically disordered protein which does not contain complex tertiary or quaternary structures in its active form. The 20S proteasome, lacking a 19S subunit, targets unfolded proteins to undergo degradation by default, and PGC-1α is no exception. Interestingly, NQO1 binds to PGC-1α in an NADH-dependent manner, allowing it to bypass the 20S proteasome and undergo the AMPK/SIRT1-mediated post translational modifications that prime its regulatory roles [32]. A later study in 2021 [73] showed that NQO1 also directly binds SIRT1 to support its function as a deacetylase, as NQO1 depletion resulted in its reduced function. Although thorough evidence of the mechanistic activities that favour SIRT1-NQO1 binding have yet to emerge, a possible explanation provided points to NAD^+ hydrolysis being an essential step in the SIRT1 deacetylation reaction. Indeed, as an oxidoreductase, NQO1 is highly active in high concentrations of NAD(P)H, which can be oxidized to $NAD(P)^+$, thus providing the necessary substrate for SIRT1-mediated deacetylation [73].

Heme oxygenase-1 or HO-1 is an integral enzyme that safely metabolizes free heme released intracellularly as a result of the microtraumas that can occur in skeletal muscle during and following aerobic exercise [74]. Free heme is capable of single-electron reduction thus

synthesizing ROS including semiquinones and electrophiles, leading to cytotoxicity if in excess. The serum heme scavenger Hemopexin 1 and HO-1 localize and metabolize free heme in skeletal muscle, respectively, to avoid toxic levels of heme production, and control ROS production. It is, therefore, fitting that an HO-1 KO model impairs heme metabolism and elevates ROS, in addition to the induction of muscle atrophy and altered motor performance, in young mice [75]. Mitochondrial function and fatigue resistance were also impaired, owing to the shift from an oxidative to a glycolytic phenotype in these skeletal muscle mitochondria. Finally, satellite cell recruitment, cell differentiation, and structural integrity sealed the accelerated muscle wasting phenotype under these KO conditions [75]. Altogether, the Nrf-2-ARE mechanism evidently contributes to mitochondrial preservation and turnover in a much more ubiquitous manner to monitor and refine the mitochondrial pool at the transcriptional signaling level, in tandem with the direct ROS targeting factors that perform their acute intramitochondrial functions.

1.2 Mitochondrial Signaling Enhancements and Impairments

In healthy muscle, the presence of redundant mechanisms can preserve or modify the signaling required to maintain homeostasis or at least prevent a steep shift in the equilibrium that may favour a catabolic phenotype. Indeed, the fundamental determinants that govern these metabolic decisions are the ratio between energy supply versus energy demand, followed by the adequate signaling that can honour the appropriate metabolic response. The following section will discuss exercise, aging, and pharmacological interventions as they induce a metabolic response by influencing these fundamentals.

1.2.1 Exercise: The Ultimate Stimulus for Redundant Pathway Activation

Over 55 years of research has unanimously uncovered that exercise is muscle mitochondrial medicine. Some of the pioneering work was initiated by the late Dr. John O. Holloszy who published a ground-breaking paper in 1967 showing that endurance training

increased muscle oxygen consumption as a result of mitochondrial biogenesis [75]. Over time, it has also been shown that engaging in regular aerobic exercise improves insulin sensitivity, maintains muscle mass, regulates cardiovascular health, and even rescues the crosstalk between important mechanisms of mitochondrial turnover that are otherwise compromised with aging, disuse, or disease [5,46,76-77].

During aerobic exercise, ATP is metabolized to support the physical activity that is taking place, including muscle contraction and oxidative phosphorylation. This elicits a growing volume of ATP demand by the physiological system in order to continually support the exercise for the duration that it is conducted. Depending on the type, intensity, duration, frequency, and length of a training paradigm [78], this can result in adaptations that can endure a higher energy demand.

Patterns of metabolism as exercise adaptations continue to develop over a given period also evolve as the mitochondrial pool becomes better sensitized to exercise signals. That is, training requires less of a metabolic disturbance to achieve the same volume of ATP as sedentary cohorts [79]. The tight-knit coordination that comes about with increased and better respiring mitochondria allows for the sparing of metabolites such as phosphocreatine and glycogen, reduced AMP requirements, and improved lactate threshold. Indeed, increases in mitochondrial content are partnered with denser cristae and more ETCs to attain this metabolic efficiency. Changing and maintaining a tight mitochondrial composition requires formidable amounts of training to achieve, but it warrants appreciating the difference in fitness between individuals with a high mitochondrial content alone and those with a denser composition, as well [80-81].

Exercise is a major activator of all three mechanisms discussed in this review, with a particular emphasis on its ability to enhance the drive for mitochondrial biogenesis.

Interestingly, mitochondrial content was preserved in a skeletal muscle specific double (D)KO of PGC-1α and β in muscle tissue and cultured myotubes, but respiratory capacity is impaired as significant reductions in complexes I-V content and capacity were observed [82]. Electron microscopy (EM) images surprisingly showed preserved cristae density with the DKO [82], although they appear disorganized, which may have implications for impaired ETC assembly, as well. As such, marked reductions in the mRNA expression and protein content of the ETC subunits were paired with significant declines in maximum oxygen consumption rate [82]. Subjecting the DKO mice to an exhaustive exercise protocol showed incredible reductions in time, work, and distance to exhaustion. Therefore, it is becoming increasingly recognized that mitochondrial function, and potentially composition, can be changed without influencing mitochondrial content. These go hand-in-hand with increased ROS levels with exercise. ROS are key stimulants of exercise-induced skeletal muscle adaptations due to the activation of integral antioxidant enzymes and PGC-1α, Nrf-2, and NF-kB [83]. Consequently, redox sensitive kinases including AMPK and p38 MAPK can initiate these antioxidant responses with a particular emphasis on Nrf-2-mediated signaling. Nrf-2 KO mice showed not only impaired PGC-1α expression, but also reductions in the expression of intramitochondrial ROS scavengers including SOD2 and catalase [43].

Acute exercise can also increase mitophagy and mitophagy flux, thus contributing to the efficient clearance of fragmented mitochondria in the cell. It is important to note that mitophagy can be activated in receptor dependent and independent manners. The PINK1/Parkin system has occupied the spotlight, but a growing body of literature surrounding the latter mitophagy system shows interesting implications for stress-dependent exercise-mediated mitochondrial clearance. For example, a more moderate bout of acute exercise-induced mitophagy was recently found to not involve PINK1 in the skeletal muscle of young sedentary mice, despite successful mitochondrial clearance [84]. However, studies that

chronically administered their exercise protocol showed PINK1 stabilization and subsequent mitophagy [85,86]. Interestingly, with chronic training, the increase in PGC-1α that is typically observed in wild type mice was blunted with a Parkin KO, despite increased mitochondrial content [8], further suggesting the presence of redundant mechanisms to compensate for impaired transcriptional signaling. However, mitochondrial respiration was also blunted, and training could not attenuate ROS production. While acute exercise increases mitophagy flux, chronic training results in an adaptive response that attenuates the magnitude of mitochondrial targeting that is required due to the enhanced regulation of mitochondrial turnover. The Parkin KO, however, maintained elevations in mitophagy flux despite chronic training, likely due to elevated ROS [8]. Further to the importance of upstream signaling kinases that govern mitochondrial turnover, it was recently uncovered that specific isoforms of AMPK directly bind to the OMM (mitoAMPK) in skeletal muscle to mediate mitophagy [45]. In fact, acute exercise following competitive inhibition of mitoAMPK resulted in mitochondrial reticulum expansion but blunted mitophagy, suggesting a regulatory role of mitoAMPK that is specific to mitophagy [45]. While the signaling activity with endurance exercise is well established in healthy muscle, continued investigations are underway to characterize how exercise-induced preservation or rescuing takes place under conditions of altered redox sensing with aging, disuse, or disease.

1.2.2 The Decline in Mitochondrial Health with Aging

A plethora of metabolic signaling pathways contribute and compensate to refreshing the mitochondrial pool, attributing to the plasticity of the organelle. With aging, however, these mechanisms are often downregulated or impaired, thus compromising mitochondrial function, and overall skeletal muscle health. Sarcopenia is a typical characteristic of aging in skeletal muscle that manifests as a result of the intrinsic decrements in signal transduction, as well as physical inactivity or hospitalization, leading to progressive skeletal muscle loss and weakness

[5,87,88]. With aging, the progressive skeletal muscle wasting phenotype represents vast deviations from the tightly regulated cellular and molecular systems that typically equilibrate mass and strength in young muscle. Indeed, mitochondria are central culprits to the catabolic shifts in aged skeletal muscle, not only due to their reduction in content, but also the overall decline in respiratory capacity in the mitochondrial pool that remains, due to compromised turnover [88-89]. As mitochondrial derangements play a key role in the progression of sarcopenia, it is important to understand these shifts in mitochondrial regulation and the processes that determine the changes in content and function within muscle with age.

Electron micrographs from aged rodent muscle reveal that SS and IMF mitochondrial contents are both reduced and fragmented [90]. In aged human muscle, these decrements are reflected by changes in maximal oxygen uptake and oxidative enzyme activities [91]. Progressive declines in mitochondrial energy metabolism and mitochondrial dynamics at both the transcript and protein levels have also been observed [90,92-93]. These changes were highly associated with a reduction in muscle mass due to increased emission of pro-apoptotic factors and myonuclear decay, highlighting a role for mitochondrially-mediated muscle atrophy [94]. Further, aged skeletal muscle results in impaired ADP sensitivity, causing increased ROS emission [95].

Aging and its associative decline in muscle mass is largely due to the tissue's inability to adapt and respond to stimuli as effectively as young muscle [95]. Equally debatable is the capacity of aged muscle and mitochondria to adapt to exercise training paradigms. Endurance training was able to rescue most of the downregulated proteins associated with energy metabolism and ameliorate the decline in ATP synthesis noted with aging. Part of this reversal in gene expression with exercise can be attributed to PGC-1α [93,96]. Recent work has revealed that the overexpression of PGC-1α in aged muscle leads to molecular changes that resemble the patterns observed in muscle of younger mice [97]. Interestingly, an important part of the

intrinsic aging phenotype is faster rate of decay of important markers including PGC-1α [93]. Moreover, defects are not observed in the mitochondrial protein import machinery with age, but precursor proteins are more rapidly degraded in the cytosol, despite the same capacity for import [98]. Furthermore, aged mice with Nrf-2 KO exhibited accelerated frailty and atrophy, alongside a reduction in PGC-1α and TFAM mRNA expression as well as impaired fission:fusion dynamics [99]. Finally, mitophagy has been reported to increase with age due to the catabolic shift that leads to increased fission and ROS emission [83,100], as well as poor signal transduction to sufficiently activate sensors of cellular distress such as AMPK [101]. Additionally, the same exercise stimulus that is applied to young versus aged muscle results in lower metabolic improvements with the latter [102], demonstrating retained but diminished mitochondrial plasticity with aging. However, rigorous intervention via chronic contractile activity through surgical implantation of a stimulator is capable of restoring ROS emission to control levels and improving mitochondrial content and function [100]. Furthermore, PGC-1α overexpression attenuates the accelerated recruitment of mitophagy and apoptosis in aged mice [103]. Overall, the metabolic derangements and shortcomings with age that lead to persistent mitochondrial dysfunction and suboptimal restoration highlights this inherent aging deficit that is not solely attributed to physical inactivity [5].

Although aging is not a reversible process, its impact on skeletal muscle health can be controlled by re-establishing the upstream signaling factors that can activate important mechanisms of mitochondrial turnover. While exercise indeed induces a ubiquitous effect on mitochondrial health, varying training paradigms elicit varying restorative capacities.

1.2.3 Metabolic Mimicry: Nutraceutical and Pharmaceutical Agents

Disruption of mitochondrial homeostasis in the cell has been implicated in chronic muscle disuse, disease, and aging. Therefore, the availability of numerous divergent pathways, as well

as multiple stimuli that can activate a common pathway, together contribute to cell survival and longevity [5,41]. Examples of stimuli capable of activating redundant mechanisms include exercise or pharmacological compounds, which can target cascading events dedicated to guarding mitochondrial health and equilibrium within the cell [41]. This is the premise behind exercise mimetics, which can serve as alternatives to physical activity given their capacity to alter metabolic dynamics contributing to improving mitochondrial regulation, refining ATP production, and preserving muscle mass.

Thorough reports have uncovered the complex metabolic improvements observed in the cell following acute and chronic exercise [104-105] but reaping the benefits of drug treatments through the optimization of their metabolic mimicry remains a challenge. Nonetheless, this is an important avenue to pursue as various conditions and physiological impairments encourage intervention via nutraceutical or pharmaceutical supplementation. Exercise in young and aged muscle has been shown to reverse this catabolic phenotype, which rescues mitochondrial health and preserves muscle mass [96,99]. The true mastery of metabolic control with exercise lies with its capacity to activate redundant signaling pathways simultaneously, which all converge toward the goal of physiological sustainability in an environment of high energy demand [106]. Inducers, however, are comparatively limited as their designated function may follow with additional peripheral metabolic outcomes that complicate their characterization and true therapeutic benefits to mitochondrial health. Nonetheless, three candidates have gained considerable attention in recent literature for successful metabolic restoration in cell culture and animal models. The first agent, Sulforaphane (SFN), is a potent nutraceutical that activates the Nrf-2-antioxidant response element (ARE) pathway, which mitigates excessive ROS production [57,68,99]. The second nutraceutical, Urolithin A (UroA), has been reported to restore mitophagy, thus preventing the accumulation of unhealthy mitochondria in the cell [107-111]. Finally, the synthetic small molecule ZLN005 [112-113], activates the master

regulator of mitochondrial biogenesis, PGC-1α, which targets a series of transcription factors associated with nuclear genes encoding mitochondrial proteins, to replenish the mitochondrial pool. The integral regulator of metabolic homeostasis, AMPK, is another noteworthy marker, as reports indicate that UroA and ZLN005 activate this upstream kinase with respect to their contribution to mitochondrial turnover. Together, these agents contribute to the pillars of mitochondrial homeostasis (Figure 1,2).

Sulforaphane (SFN) is a potent nutraceutical that activates the Nrf-2-Keap1-ARE pathway (Section 1.1.3), which governs the transcriptional regulation of phase II detoxification enzymes for cytoprotection [57]. Available in cruciferous vegetables, it is deemed to be one of the most important potent cellular defense compounds readily available in natural diets. SFN is an isothiocyanate and phytochemical which has been shown to preserve the metabolic function within neurological diseases including Parkinson's and Huntington's and is a dominating agent for cancer therapeutics. Within skeletal muscle research, SFN has also been positioned as a potent metabolic preserver. Type II diabetic mice treated with the agent had restored grip strength and muscle mass, alongside the downregulation of inflammatory markers owing to its ability to increase NQO1 and HO-1 activity [114]. While it may not reverse the etiology of type II diabetes in the animals, it can mitigate some of the detrimental effects on skeletal muscle as a result of impaired insulin sensitivity and glucose uptake. Acute exhaustive exercise can induce skeletal muscle damage, which can be regulated through various antioxidant systems. With SFN pre-treatment, the exercise-induced muscle damage in rats was attenuated as a result of the upregulated Nrf-2-mediated factors as well as increased levels of lactate dehydrogenase and creatine phosphokinase [115]. Induced oxidative stress in cultured C2C12 myotubes also showed attenuated atrophy and atrophy-related markers with SFN pre-treatment [116]. While its cytoprotective effects are versatile, SFN appears to be highly specific

to Nrf-2-mediated signaling, which can uncover the pathway-specific benefits towards skeletal muscle (Figure 1, 2 **A**).

The ellagitannin, Urolithin A (UroA), has been reported to restore mitophagy starting at the upstream activating kinase, AMPK, thus preventing the accumulation of unhealthy mitochondria in the cell [107]. It gained its fame in the literature as a useful agent that restores mitochondrial clearance in aged skeletal muscle, thus promoting healthy aging of the cell. Many publications within the same groups have consistently demonstrated increased mitophagy signaling and mitophagy-related proteins with UroA treatment in *C. elegans*, C2C12 myoblasts and myotubes, young and aged mice and rats, mice with muscular dystrophy, middle-aged and aged humans, and, most recently, primary chondrocytes from aged humans with osteoarthritis [107-111]. Others who have worked with the agent showed alleviated symptoms of type II diabetes when UroA was added halfway into a 16-week high fat/high sucrose diet in mice with insulin resistance [117]. Therefore, due to the improvements in health shown in the many models used for UroA experimentation, restoring cellular redox sensing in skeletal muscle directed towards rejuvenating the mitochondrial pool by mitophagy severely lightens the oxidative burden upon the cell (Figure 1, 2 **B**).

Finally, the synthetic small molecule ZLN005 (ZLN) [112-113], activates the master regulator of mitochondrial biogenesis, PGC-1α, to replenish the mitochondrial pool. The integral regulator of metabolic homeostasis, AMPK, is another noteworthy marker, as reports indicate that ZLN (like UroA) activates this upstream kinase with respect to its contribution to mitochondrial turnover. Together, these agents uniquely contribute to the pillars of mitochondrial homeostasis. In the context of skeletal muscle mitochondria, few publications exist as the agent is quite novel in the field. Nonetheless, confirmation of its contributions to skeletal muscle came in 2013 where PGC-1α mRNA levels, glucose uptake, and FFA oxidation

were all improved. Furthermore, type II diabetic mice with ZLN administration also showed improved glucose tolerance, pyruvate tolerance, and insulin sensitivity [112] (Figure 1, 2 **C**).

Countless pharmacological agents have entered the circuit for research-based interventions that improve skeletal muscle health, some of which are characterized in Table 1. Over time, continued elucidation around skeletal muscle cellular modulation adds information to the pharmacological blueprints that can refine drug function and improve their metabolic mimicry. Since different cell lines, animals, genotypes, training paradigms, and other variables can result in varying conclusions in research, the agents that are developed to induce a metabolic change target upstream redundant signaling factors that can affect multiple mechanisms. It is likely that most agents in circulation perform secondary and tertiary functions to the cell that are unrelated or unintended, and this is potentially unavoidable. Of course, this is not necessarily a con since exercise behaves in the same fashion. However, assuming that half-life, duration, and concentration were determined, most pharmacological agents apparently do not exhibit a potent metabolic response that matches the magnitude or duration of improvement that is achieved with exercise [118]. Nevertheless, while the mechanistic changes with exercise continue to be elucidated today, its benefits to skeletal muscle health are undeniable, thus warranting the tireless efforts to mimic its influence on a physiological system through pharmacological interventions.

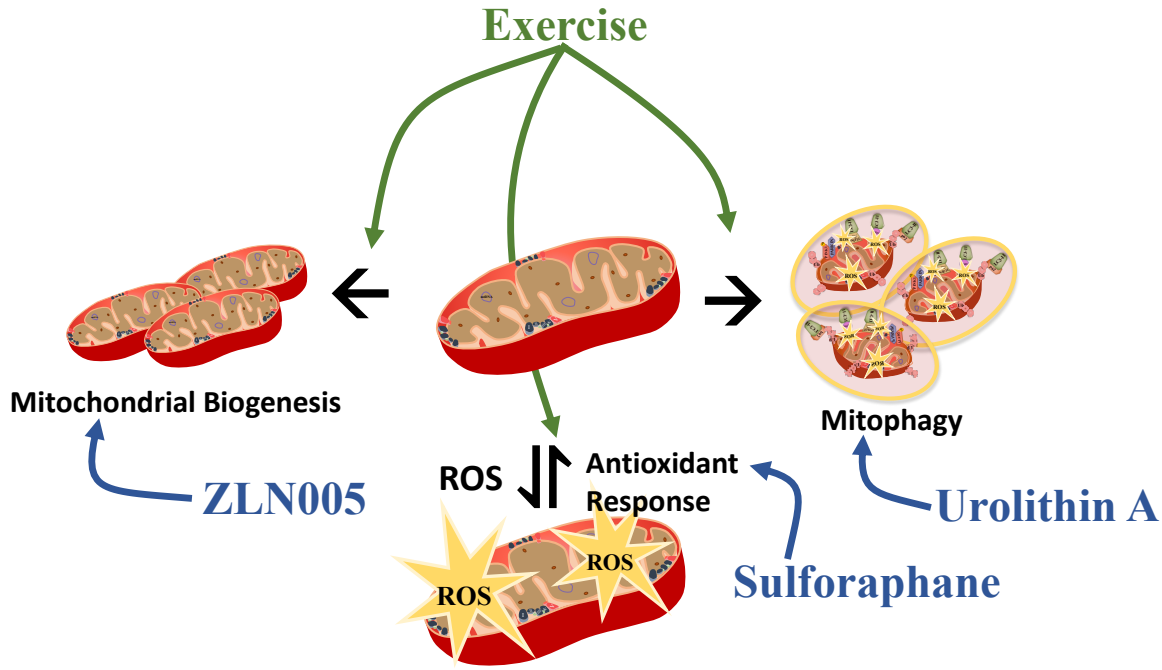

Figure 1. Mechanisms and stimuli that contribute to mitochondrial turnover and homeostasis. Mitochondrial homeostasis (depicted by the central mitochondrion) is governed by pathways that contribute to their production, degradation, and preservation. These are mitochondrial biogenesis (left), mitophagy (right), and antioxidant capacity/response (bottom). Exercise represents a strong stimulus that activates these redundant mechanisms, all of which converge towards homeostasis. The ever-expanding development of nutraceutical and pharmaceutical agents may elicit similar metabolic responses to exercise. Within this vast arena, recent literature has focused on the agents Sulforaphane, Urolithin A, and ZLN005 in their capacity to activate certain upstream markers that contribute to their corresponding mechanism.

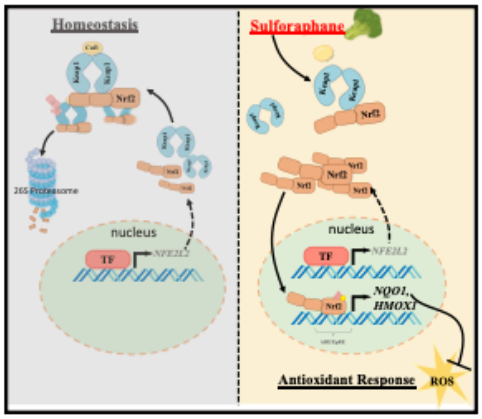

A. <u>Sulforaphane</u>: Under homeostatic conditions (**left panel, grey**), the transcription factor Nrf-2 is sequestered in the cytoplasm by its homodimeric negative regulator, Keap1. Under SFN-induced conditions (**right panel, yellow**), the sequestering capacity of Keap1 is disrupted, leading to the accumulation and nuclear localization of newly synthesized Nrf-2. It binds to the antioxidant response element in the upstream promoters for genes including *NQO1* and *HMOX1*. These eventually aid in the mitigation of excessive ROS, which can otherwise damage mitochondrial machinery and their function.

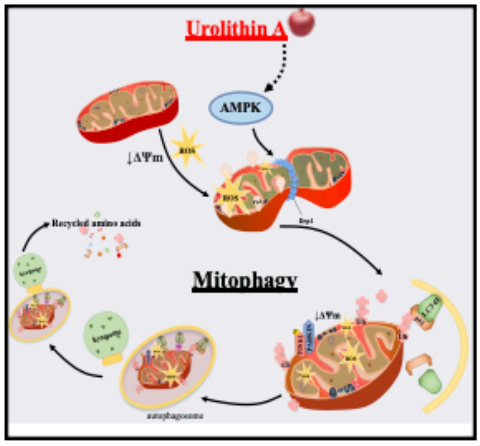

B. <u>Urolithin A:</u> AMPK is activated to cause fission and separate the stressed and poorly functioning region of the reticulum. Briefly, the mitochondrion is ubiquitinated and targeted by the adaptor protein p62, alongside simultaneous autophagosomal development, forming a growing vesicular phagophore. Embedded in this double-membrane vesicle is LC3-II, which anchors to p62 and facilitates the engulfment of the Ub-tagged mitochondrion. Microtubules then transport the occupied autophagosome to the lysosome for fusion and organelle degradation.

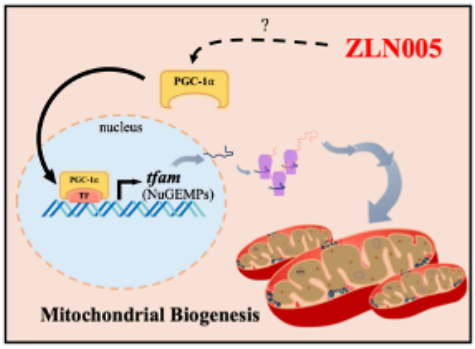

C. <u>ZLN005:</u> Shown to increase PGC-1a nuclear localization via AMPK. This initiates the transcriptional co-activation of nuclear genes encoding mitochondrial proteins, such as TFAM. Following their relevant translation and post-translational modifications, TFAM can thus bind to mtDNA to activate transcription of mitochondrially-encoded genes, which contribute to mitochondrial biogenesis.

<u>Figure 2. Schematics summarizing the documented function of the agents [A] Sulforaphane, [B] Urolithin A, and [C] ZLN005.</u>

Table 1. A few of many pharmaceutical and nutraceutical agents and their reported effects on mitochondria. Beyond and in addition to the three agents discussed in this review, more agents have been depicted in this table, each of which are complemented with characteristics, targets, action on mitochondria, and related models and pathologies. Some of these induce the same mechanisms, demonstrating the widespread thought, development, and continued efforts to refine compounds that suitably target the necessary marker(s) that can rescue metabolic health with respect to differing models, pathologies, and experimental conditions.

Drug	Characteristics	Target Mechanism or Marker	Function: Action on mitochondria	Related models and conditions/pathologies	Related Studies
Sulforaphane	Isothiocyanate; phytochemical $C_6H_{11}NOS_2$ Derivative of cruciferous vegetables	Nrf-2/Keap1/ARE antioxidant axis	NQO1: Aids PGC-1α in bypassing the 20S proteasome. HO-1: Preservation of oxidative muscle fibres, heme metabolism, and endurance Mitoprotection and cytoprotection	Model: C2C12 cell line, human hepatocytes, mouse tissue, rat tissue Related Pathologies: Cancer, Alzheimer's, Huntington's Experimental Condition: Nrf-2 KO, Keap1 KO	57, 114, 116
Urolithin A	Ellagitannin $C_{13}H_8O_4$ Derivative of pomegranates and other berries, fruits, and nuts	Mitophagy	AMPK-mediated mitophagy activation Improved clearance of suboptimally-functioning mitochondria	Model: C2C12 cell line, mouse tissue, rat tissue, human (middle-aged, aged) Related Pathologies: Aging, osteoarthritis Experimental Conditions: RNAi for bec-1, pink-1, dct-1, sqst-1, ups-34 (in *C. elegans*)	107-111, 117
ZLN005	2-[4-(1,1-dimethylethyl)phenyl]-1H-benzimidazole $C_{17}H_{18}N_2$	PGC-1α activator	Potential increase in drive for mitochondrial biogenesis	Model: C2C12, HEK293, L6 cell lines, mouse tissue Related Pathologies: diabetes Experimental Conditions: RNAi for FNDC5	112-113
AICAR	5-Aminoimidazole-4-carboxamide-ribonucleotide $C_9H_{15}N_4O_8P$	AMPK activator	AMP analog (ZMP) -> AMPK activation -> mitochondrial biogenesis and mitophagy Tighter regulation of mitochondrial turnover	Model: C2C12, mouse tissue, rat tissue Related Pathologies: Cardiotoxicity, diabetes, Alzheimer's Experimental Condition: endurance training with treatment alone in sedentary animals; mutation of human PGC-1α promoter	119-121
Edaravone	Lipophilic antioxidant 3-methyl-1-phenyl-2-pyrazolin-5-one $C_{10}H_{10}N_2O$	Nrf-2/Keap1/ARE antioxidant axis	HO-1: Preservation of oxidative muscle fibres, heme metabolism, and endurance Mitoprotection and cytoprotection Additional benefits: prevents tubular aggregate formation in skeletal muscle	Model: rodent skeletal muscle; C2C12 cell line Related Pathologies: Amyotropic lateral sclerosis (ALS), tubular aggregate myopathy (TAM) Experimental Condition: overexpression of ATPase repressor to mimic TAM	122
Resveratrol	Stilbenoid Derivative of berries and nuts $C_{14}H_{12}O_3$	Mitochondrial biogenesis	AMPKα1-mediated nuclear localization of PGC-1α Restored signal transduction for mitochondrial biogenesis Muscle regeneration	Model: rodent skeletal muscle; C2C12 cell line; human subjects Related Pathologies: obesity; insulin resistance; Duchenne's muscular dystrophy Experimental Condition: ROS-induced oxidative stress; *mdx* mice	123-125
Quercetin	Polyphenol $C_{15}H_{10}O_7$ Dietary flavenoid	Nrf-2/Keap1/ARE antioxidant axis	Nrf-2 nuclear localization leading to the expression of PGC-1α, SIRT3, TFAM, NRF-1/-2 mRNA Training blunts these effects, however	Model: hepatocytes, chontrocytes, dopaminergic neuronal cells, C2C12 cell lines; rodent skeletal muscle Related Pathologies: obesity; insulin resistance; Duchenne's muscular dystrophy Experimental Condition: mdx mice; dexamethasone-induced skeletal muscle injury	126-129

Table 1. (Continued)

Drug	Characteristics	Target Mechanism or Marker	Function: Action on mitochondria	Related models and conditions/pathologies	Related Studies
Epicatechin	Flavanol	Unclear; yet to be elucidated	Increased expression of:	Model: endothelial cells, adipocytes, rodent tissues	130-132
	$C_{15}H_{14}O_6$	Nitric oxide mechanisms implicated	signaling proteins (AMPK); Co-activators (PGC-1α); and mitochondrial proteins (TFAM)	Related Pathologies: type II diabetes, heart failure	
	Found in cocoa	Points to potential Nrf-2 involvement		Experimental Condition: reperfusion of ischemic skeletal muscle	
Elamipretide (SS-31)	Water-soluble aromatic	Unclear; yet to be elucidated	Transiently localizes to inner mitochondrial membrane	Model: animal tissue, human iPSCs	133-134
	$C_{32}H_{49}N_9O_5$	Binds to cardiolipin	Cardiolipin stabilization -> restored cristae formation, IMM stability, and mitochondrial bioenergetics	Related Pathologies: aging; Barth Syndrome	
			Restored antioxidant capacity and ROS scavenging	Experimental condition: Tafazzin mutation	
AMBMP	N4-(1,3-benzodioxol-5-ylmethyl) -6-(3-methoxyphenyl)-2,4-pyrimidinediamine hydrochloride	Calpain signaling -> targeting CAMKIIβ to promote mitochondrial biogenesis	Restores capacity for CAMKIIβ signaling with exercise -> PGC-1α-mediated mitochondrial biogenesis	Model: mouse tissue	135
	$C_{19}H_{18}N_4O_3HCl$	Activator of Wnt signaling	Improves mitochondrial respiration/function, promotes oxidative muscle phenotype	Related Pathologies: limb girdle muscular dystrophy	
				Experimental Condition: capn3 KO	
Metformin	Dimethylbiguanide	AMPK activation -> higher rates of glucose disposal and muscle glycogen concentrations in **hepatocytes**	Benefits of metformin do not appear to be skeletal-muscle specific. Some benefits in gluconeogenic and hepatic contexts.	Model: hepatocytes, adipocytes, diabetic rats, aged human subjects	132,136-137
	$C_4H_{11}N_5$		Negative effects of metformin on skeletal muscle mitochondria have been reported	Related Pathologies: diabetes, aging	
	Widely-prescribed medication for Type II diabetes			Experimental Condition: diabetes induction	
Trehalose	Non-reducing natural disaccharide	mTOR-independent autophagy (AMPK-ULK1 pathway)	Mitochondrial turnover	Model: chondrocytes, HEK293T, mouse tissue	138-140
	$C_{12}H_{22}O_{11}$		Induces AMPK-mediated autophagy -> recruits autophagic machinery for autophagosome formation	Related Pathologies: Osteoarthritis	
			Autophagosome maturation + phagophore development	Experimental Condition: co-treatment with exercise	
Curcumin	Phenolic and lipophilic compound derived from turmeric	Antioxidant capacity (ROS scavenger)	SOD2 -> Reductions in ROS	Model: C2C12, rodent and duck skeletal muscle	141-144
	$C_{21}H_{20}O_6$	Mitochondrial biogenesis	PGC-1α and SIRT3 in skeletal muscle	Related Pathologies: Diabetes, cancer, aging, neurodegenerative disease	
		Mitophagy (PINK1/Parkin-mediated)	Nrf-2 nuclear localization for mitochondrial protection	Experimental Condition: heat-induced mitochondrial dysfunction, hindlimb immobilization, high fat diet	

RESEARCH OBJECTIVES

Our research objectives are to:

- Examine Sulforaphane in its capacity to activate the Nrf-2 antioxidant pathway *in vitro;*
- Fortify Urolithin A in its capacity to activate mitophagy flux *in vitro;*
- Investigate the potential of ZLN005 to activate PGC-1α nuclear translocation as an indication of increased drive for mitochondrial biogenesis *in vitro;*
- Determine the time-dependent changes in the markers analyzed within each agent and its associated mechanism.

HYPOTHESES

We hypothesize that:

1. Sulforaphane is capable of increasing Nrf-2 content as an upstream transcription factor that leads to the increase in NQO1 and HO-1 antioxidant enzymes, in a time-dependent manner;
2. Urolithin A increases mitophagy flux via AMPK;
3. ZLN005 allows for the nuclear translocation of PGC-1α, thus leading to the upregulation of TFAM expression, and downstream mitochondrial markers as an indication of mitochondrial biogenesis.

REFERENCES

1. Hood, D. A., Uguccioni, G., Vainshtein, A., & D'souza, D. (2011). Mechanisms of exercise-induced mitochondrial biogenesis in skeletal muscle: Implications for health and disease. *Comprehensive Physiology*, 1119-1134. https://doi.org/10.1002/cphy.c100074
2. Ravera, S., Morelli, A. M., & Panfoli, I. (2020). Myelination increases chemical energy support to the axon without modifying the basic physicochemical mechanism of nerve conduction. *Neurochemistry International*, *141*, 104883. https://doi.org/10.1016/j.neuint.2020.104883
3. Braun, H. (2020). The oxidative phosphorylation system of the mitochondria in plants. *Mitochondrion*, *53*, 66-75. https://doi.org/10.1016/j.mito.2020.04.007
4. Tang, J. X., Thompson, K., Taylor, R. W., & Oláhová, M. (2020). Mitochondrial OXPHOS biogenesis: Co-regulation of protein synthesis, import, and assembly pathways. *International Journal of Molecular Sciences*, *21*(11), 3820. https://doi.org/10.3390/ijms21113820
5. Hood, D. A., Memme, J. M., Oliveira, A. N., & Triolo, M. (2019). Maintenance of skeletal muscle mitochondria in health, exercise, and aging. *Annual Review of Physiology*, *81*(1), 19-41. https://doi.org/10.1146/annurev-physiol-020518-114310
6. Protasoni, M., & Zeviani, M. (2021). Mitochondrial structure and Bioenergetics in normal and disease conditions. *International Journal of Molecular Sciences*, *22*(2), 586. https://doi.org/10.3390/ijms22020586
7. Hood, D. A., Balaban, A., Connor, M. K., Craig, E. E., Nishio, M. L., Rezvani, M., & Takahashi, M. (1994). Mitochondrial biogenesis in striated muscle. *Canadian Journal of Applied Physiology*, *19*(1), 12-48. https://doi.org/10.1139/h94-002
8. Chen, C. C., Erlich, A. T., & Hood, D. A. (2018). Role of Parkin and endurance training on mitochondrial turnover in skeletal muscle. *Skeletal Muscle*, *8*(1). https://doi.org/10.1186/s13395-018-0157-y
9. Triolo, M., Slavin, M., Moradi, N., & Hood, D. A. (2022). Time-dependent changes in autophagy, mitophagy and lysosomes in skeletal muscle during denervation-induced disuse. *The Journal of Physiology*, *600*(7), 1683-1701. https://doi.org/10.1113/jp282173
10. Bouviere, J., Fortunato, R. S., Dupuy, C., Werneck-de-Castro, J. P., Carvalho, D. P., & Louzada, R. A. (2021). Exercise-stimulated ROS sensitive signaling pathways in skeletal muscle. *Antioxidants*, *10*(4), 537. https://doi.org/10.3390/antiox10040537
11. Powers, S. K., Ozdemir, M., & Hyatt, H. (2020). Redox control of proteolysis during inactivity-induced skeletal muscle atrophy. *Antioxidants & Redox Signaling*, *33*(8), 559-569. https://doi.org/10.1089/ars.2019.8000
12. Bouviere, J., Matta, L. P., Werneck-de-Castro, J. P., Dupuy, C., Carvalho, D. P., Fortunato, R. S., & Louzada, R. A (2020). Redox signaling in widespread health benefits of exercise. *Antioxidants & Redox Signaling*, *33*(11), 745-760. https://doi.org/10.1089/ars.2019.7949
13. Coggan, A. R., Abduljalil, A. M., Swanson, S. C., Earle, M. S., Farris, J. W., Mendenhall, L. A., & Robitaille, P. M. (1993). Muscle metabolism during exercise in young and older untrained and endurance-trained men. *Journal of Applied Physiology*, *75*(5), 2125-2133. https://doi.org/10.1152/jappl.1993.75.5.2125

14. Holloszy, J. O., & Coyle, E. F. (1984). Adaptations of skeletal muscle to endurance exercise and their metabolic consequences. *Journal of Applied Physiology*, *56*(4), 831-838. https://doi.org/10.1152/jappl.1984.56.4.831
15. Dandanell, S., Meinild-Lundby, A., Andersen, A. B., Lang, P. F., Oberholzer, L., Keiser, S., Robach, P., Larsen, S., Rønnestad, B. R., & Lundby, C. (2018). Determinants of maximal whole-body fat oxidation in elite cross-country skiers: Role of skeletal muscle mitochondria. *Scandinavian Journal of Medicine & Science in Sports*, *28*(12), 2494-2504. https://doi.org/10.1111/sms.13298
16. Chen, M., Li, Y., Deng, S., Zhao, Y., Lian, Z., & Yu, K. (2022). Mitochondrial function and reactive oxygen/Nitrogen species in skeletal muscle. *Frontiers in Cell and Developmental Biology*, *10*. https://doi.org/10.3389/fcell.2022.826981
17. Hartmann, D. D., Gonçalves, D. F., Da Rosa, P. C., Martins, R. P., Courtes, A. A., Franco, J. L., A. Soares, F. A., & Puntel, G. O. (2020). A single muscle contusion promotes an immediate alteration in mitochondrial bioenergetics response in skeletal muscle fibres with different metabolism. *Free Radical Research*, *54*(2-3), 137-149. https://doi.org/10.1080/10715762.2020.1723795
18. Iqbal, S., & Hood, D. A. (2015). The role of mitochondrial fusion and fission in skeletal muscle function and dysfunction. *Frontiers in Bioscience*, *20*(1), 157-172. https://doi.org/10.2741/4303
19. Iqbal, S., & Hood, D. A. (2014). Cytoskeletal regulation of mitochondrial movements in myoblasts. *Cytoskeleton*, *71*(10), 564-572. https://doi.org/10.1002/cm.21188
20. Joseph, A., Adhihetty, P. J., & Leeuwenburgh, C. (2015). Beneficial effects of exercise on age-related mitochondrial dysfunction and oxidative stress in skeletal muscle. *The Journal of Physiology*, *594*(18), 5105-5123. https://doi.org/10.1113/jp270659
21. Iqbal, S., & Hood, D. A. (2014). Oxidative stress-induced mitochondrial fragmentation and movement in skeletal muscle myoblasts. *American Journal of Physiology-Cell Physiology*, *306*(12), C1176-C1183. https://doi.org/10.1152/ajpcell.00017.2014
22. Memme, J. M., Oliveira, A. N., & Hood, D. A. (2022). P53 regulates skeletal muscle mitophagy and mitochondrial quality control following denervation-induced muscle disuse. *Journal of Biological Chemistry*, *298*(2), 101540. https://doi.org/10.1016/j.jbc.2021.101540
23. Kim, Y., Triolo, M., & Hood, D. A. (2017). Impact of aging and exercise on mitochondrial quality control in skeletal muscle. *Oxidative Medicine and Cellular Longevity*, *2017*, 1-16. https://doi.org/10.1155/2017/3165396
24. Slavin, M. B., Memme, J. M., Oliveira, A. N., Moradi, N., & Hood, D. A. (2022). Regulatory networks coordinating mitochondrial quality control in skeletal muscle. *American Journal of Physiology-Cell Physiology*, *322*(5), C913-C926. https://doi.org/10.1152/ajpcell.00065.2022
25. Philp, A. M., Saner, N. J., Lazarou, M., Ganley, I. G., & Philp, A. (2021). The influence of aerobic exercise on mitochondrial quality control in skeletal muscle. *The Journal of Physiology*, *599*(14), 3463-3476. https://doi.org/10.1113/jp279411
26. Jannig, P. R., Dumesic, P. A., Spiegelman, B. M., & Ruas, J. L. (2022). SnapShot: Regulation and biology of PGC-1α. *Cell*, *185*(8), 1444-1444.e1. https://doi.org/10.1016/j.cell.2022.03.027

27. Puigserver, P., Wu, Z., Park, C. W., Graves, R., Wright, M., & Spiegelman, B. M. (1998). A cold-inducible Coactivator of nuclear receptors linked to adaptive thermogenesis. *Cell*, *92*(6), 829-839. https://doi.org/10.1016/s0092-8674(00)81410-5
28. MacInnis, M. J., & Gibala, M. J. (2016). Physiological adaptations to interval training and the role of exercise intensity. *The Journal of Physiology*, *595*(9), 2915-2930. https://doi.org/10.1113/jp273196
29. Rhodes, M. A., Carraway, M. S., Piantadosi, C. A., Reynolds, C. M., Cherry, A. D., Wester, T. E., Natoli, M. J., Massey, E. W., Moon, R. E., & Suliman, H. B. (2009). Carbon monoxide, skeletal muscle oxidative stress, and mitochondrial biogenesis in humans. *American Journal of Physiology-Heart and Circulatory Physiology*, *297*(1), H392-H399. https://doi.org/10.1152/ajpheart.00164.2009
30. Uguccioni, G., & Hood, D. A. (2011). The importance of PGC-1α in contractile activity-induced mitochondrial adaptations. *American Journal of Physiology-Endocrinology and Metabolism*, *300*(2), E361-E371. https://doi.org/10.1152/ajpendo.00292.2010
31. Jäger, S., Handschin, C., St.-Pierre, J., & Spiegelman, B. M. (2007). AMP-activated protein kinase (AMPK) Action in skeletal muscle via direct phosphorylation of PGC-1α. *Proceedings of the National Academy of Sciences*, *104*(29), 12017-12022. https://doi.org/10.1073/pnas.0705070104
32. Adamovich, Y., Shlomai, A., Tsvetkov, P., Umansky, K. B., Reuven, N., Estall, J. L., Spiegelman, B. M., & Shaul, Y. (2013). The protein level of PGC-1α, a key metabolic regulator, is controlled by NADH-NQO1. *Molecular and Cellular Biology*, *33*(13), 2603-2613. https://doi.org/10.1128/mcb.01672-12
33. Lin, J., Wu, H., Tarr, P. T., Zhang, C., Wu, Z., Boss, O., Michael, L. F., Puigserver, P., Isotani, E., Olson, E. N., Lowell, B. B., Bassel-Duby, R., & Spiegelman, B. M. (2002). Transcriptional Co-activator PGC-1α drives the formation of slow-Twitch muscle fibres. *Nature*, *418*(6899), 797-801. https://doi.org/10.1038/nature00904
34. Scarpulla, R. C. (2008). Transcriptional paradigms in mammalian mitochondrial biogenesis and function. *Physiological Reviews*, *88*(2), 611-638. https://doi.org/10.1152/physrev.00025.2007
35. Falkenberg, M., Larsson, N., & Gustafsson, C. M. (2007). DNA replication and transcription in mammalian mitochondria. *Annual Review of Biochemistry*, *76*(1), 679-699. https://doi.org/10.1146/annurev.biochem.76.060305.152028
36. Wiedemann, N., & Pfanner, N. (2017). Mitochondrial machineries for protein import and assembly. *Annual Review of Biochemistry*, *86*(1), 685-714. https://doi.org/10.1146/annurev-biochem-060815-014352
37. Kummer, E., & Ban, N. (2021). Mechanisms and regulation of protein synthesis in mitochondria. *Nature Reviews Molecular Cell Biology*, *22*(5), 307-325. https://doi.org/10.1038/s41580-021-00332-2
38. Memme, J. M., Slavin, M., Moradi, N., & Hood, D. A. (2021). Mitochondrial Bioenergetics and turnover during chronic muscle disuse. *International Journal of Molecular Sciences*, *22*(10), 5179. https://doi.org/10.3390/ijms22105179
39. Arany, Z., He, H., Lin, J., Hoyer, K., Handschin, C., Toka, O., Ahmad, F., Matsui, T., Chin, S., Wu, P., Rybkin, I. I., Shelton, J. M., Manieri, M., Cinti, S., Schoen, F. J., Bassel-Duby, R., Rosenzweig, A., Ingwall, J. S., & Spiegelman, B. M. (2005).

Transcriptional coactivator PGC-1α controls the energy state and contractile function of cardiac muscle. *Cell Metabolism*, *1*(4), 259-271. https://doi.org/10.1016/j.cmet.2005.03.002
40. Martínez-Redondo, V., Pettersson, A. T., & Ruas, J. L. (2015). The hitchhiker's guide to PGC-1α isoform structure and biological functions. *Diabetologia*, *58*(9), 1969-1977. https://doi.org/10.1007/s00125-015-3671-z
41. Islam, H., Hood, D. A., & Gurd, B. J. (2020). Looking beyond PGC-1α: Emerging regulators of exercise-induced skeletal muscle mitochondrial biogenesis and their activation by dietary compounds. *Applied Physiology, Nutrition, and Metabolism*, *45*(1), 11-23. https://doi.org/10.1139/apnm-2019-0069
42. Piantadosi, C. A., Carraway, M. S., Babiker, A., & Suliman, H. B. (2008). Heme oxygenase-1 regulates cardiac mitochondrial biogenesis via nrf2-mediated transcriptional control of nuclear respiratory factor-1. *Circulation Research*, *103*(11), 1232-1240. https://doi.org/10.1161/01.res.0000338597.71702.ad
43. Merry, T. L., & Ristow, M. (2016). Nuclear factor erythroid-derived 2-like 2 (NFE2L2, Nrf2) mediates exercise-induced mitochondrial biogenesis and the anti-oxidant response in mice. *The Journal of Physiology*, *594*(18), 5195-5207. https://doi.org/10.1113/jp271957
44. Huang, D., Fan, S., Chen, X., Yan, X., Zhang, X., Ma, B., Yu, D., Xiao, W., Zhuang, C., & Yu, Z. (2019). Nrf2 deficiency exacerbates frailty and sarcopenia by impairing skeletal muscle mitochondrial biogenesis and dynamics in an age-dependent Manner. *Experimental Gerontology*, *119*, 61-73. https://doi.org/10.1016/j.exger.2019.01.022
45. Drake, J. C., Wilson, R. J., Laker, R. C., Guan, Y., Spaulding, H. R., Nichenko, A. S., Shen, W., Shang, H., Dorn, M. V., Huang, K., Zhang, M., Bandara, A. B., Brisendine, M. H., Kashatus, J. A., Sharma, P. R., Young, A., Gautam, J., Cao, R., Wallrabe, H., … Yan, Z. (2021). Mitochondria-localized AMPK responds to local energetics and contributes to exercise and energetic stress-induced mitophagy. *Proceedings of the National Academy of Sciences*, *118*(37). https://doi.org/10.1073/pnas.2025932118
46. Triolo, M., Oliveira, A. N., Kumari, R., & Hood, D. A. (2022). The influence of age, sex, and exercise on autophagy, mitophagy, and lysosome biogenesis in skeletal muscle. *Skeletal Muscle*, *12*(1). https://doi.org/10.1186/s13395-022-00296-7
47. Seabright, A. P., & Lai, Y. (2020). Regulatory roles of PINK1-Parkin and AMPK in ubiquitin-dependent skeletal muscle Mitophagy. *Frontiers in Physiology*, *11*. https://doi.org/10.3389/fphys.2020.608474
48. Gumeni, S., Papanagnou, E., Manola, M. S., & Trougakos, I. P. (2021). Nrf2 activation induces mitophagy and reverses Parkin/Pink1 knock down-mediated neuronal and muscle degeneration phenotypes. *Cell Death & Disease*, *12*(7). https://doi.org/10.1038/s41419-021-03952-w
49. Onishi, M., Yamano, K., Sato, M., Matsuda, N., & Okamoto, K. (2021). Molecular mechanisms and physiological functions of mitophagy. *The EMBO Journal*, *40*(3). https://doi.org/10.15252/embj.2020104705
50. Laker, R. C., Drake, J. C., Wilson, R. J., Lira, V. A., Lewellen, B. M., Ryall, K. A., Fisher, C. C., Zhang, M., Saucerman, J. J., Goodyear, L. J., Kundu, M., & Yan, Z. (2017). Ampk phosphorylation of Ulk1 is required for targeting of mitochondria to

lysosomes in exercise-induced mitophagy. *Nature Communications*, *8*(1). https://doi.org/10.1038/s41467-017-00520-9
51. Tian, X., Teng, J., & Chen, J. (2020). New insights regarding SNARE proteins in autophagosome-lysosome fusion. *Autophagy*, *17*(10), 2680-2688. https://doi.org/10.1080/15548627.2020.1823124
52. Vainshtein, A., Desjardins, E., Armani, A., Sandri, M., & Hood, D. A. (2015). PGC-1α modulates denervation-induced mitophagy in skeletal muscle. *Skeletal Muscle*, *5*(1). https://doi.org/10.1186/s13395-015-0033-y
53. Kang, C., & Ji, L. L. (2016). PGC-1α overexpression via local transfection attenuates mitophagy pathway in muscle disuse atrophy. *Free Radical Biology and Medicine*, *93*, 32-40. https://doi.org/10.1016/j.freeradbiomed.2015.12.032
54. Leduc-Gaudet, J., Reynaud, O., Hussain, S. N., & Gouspillou, G. (2019). Parkin overexpression protects from ageing-related loss of muscle mass and strength. *The Journal of Physiology*, *597*(7), 1975-1991. https://doi.org/10.1113/jp277157
55. Hoeks, J., Hesselink, M. K., & Schrauwen, P. (2006). Involvement of UCP3 in mild uncoupling and lipotoxicity. *Experimental Gerontology*, *41*(7), 658-662. https://doi.org/10.1016/j.exger.2006.02.005
56. Broome, S. C., Woodhead, J. S., & Merry, T. L. (2018). Mitochondria-targeted antioxidants and skeletal muscle function. *Antioxidants*, *7*(8), 107. https://doi.org/10.3390/antiox7080107
57. Li, D., Shao, R., Wang, N., Zhou, N., Du, K., Shi, J., Wang, Y., Zhao, Z., Ye, X., Zhang, X., & Xu, H. (2020). Sulforaphane activates a lysosome-dependent transcriptional program to mitigate oxidative stress. *Autophagy*, *17*(4), 872-887. https://doi.org/10.1080/15548627.2020.1739442
58. Underwood, B. R., Imarisio, S., Fleming, A., Rose, C., Krishna, G., Heard, P., Quick, M., Korolchuk, V. I., Renna, M., Sarkar, S., Garcia-Arencibia, M., O'Kane, C. J., Murphy, M. P., & Rubinsztein, D. C. (2010). Antioxidants can inhibit basal autophagy and enhance neurodegeneration in models of polyglutamine disease. *Human Molecular Genetics*, *19*(17), 3413-3429. https://doi.org/10.1093/hmg/ddq253
59. Paulsen, G., Cumming, K. T., Holden, G., Hallén, J., Rønnestad, B. R., Sveen, O., Skaug, A., Paur, I., Bastani, N. E., Østgaard, H. N., Buer, C., Midttun, M., Freuchen, F., Wiig, H., Ulseth, E. T., Garthe, I., Blomhoff, R., Benestad, H. B., & Raastad, T. (2014). Vitamin C and E supplementation hampers cellular adaptation to endurance training in humans: A double-blind, randomised, controlled trial. *The Journal of Physiology*, *592*(8), 1887-1901. https://doi.org/10.1113/jphysiol.2013.267419
60. Ristow, M., Zarse, K., Oberbach, A., Klöting, N., Birringer, M., Kiehntopf, M., Stumvoll, M., Kahn, C. R., & Blüher, M. (2009). Antioxidants prevent health-promoting effects of physical exercise in humans. *Proceedings of the National Academy of Sciences*, *106*(21), 8665-8670. https://doi.org/10.1073/pnas.0903485106
61. Zhao, R., Jiang, S., Zhang, L., & Yu, Z. (2019). Mitochondrial electron transport chain, ROS generation and uncoupling (Review). *International Journal of Molecular Medicine*. https://doi.org/10.3892/ijmm.2019.4188

62. Vercellino, I., & Sazanov, L. A. (2021). The assembly, regulation and function of the mitochondrial respiratory chain. *Nature Reviews Molecular Cell Biology*, *23*(2), 141-161. https://doi.org/10.1038/s41580-021-00415-0
63. Lowell, B. B., & Spiegelman, B. M. (2000). Towards a molecular understanding of adaptive thermogenesis. *Nature*, *404*(6778), 652-660. https://doi.org/10.1038/35007527
64. Alleman, R. J., Katunga, L. A., Nelson, M. A., Brown, D. A., & Anderson, E. J. (2014). The "Goldilocks Zone" from a redox perspective - Adaptive vs. deleterious responses to oxidative stress in striated muscle. *Frontiers in Physiology*, *5*. https://doi.org/10.3389/fphys.2014.00358
65. Horie, Y., Suzuki, T., Inoue, J., Iso, T., Wells, G., Moore, T. W., Mizushima, T., Dinkova-Kostova, A. T., Kasai, T., Kamei, T., Koshiba, S., & Yamamoto, M. (2021). Molecular basis for the disruption of keap1–nrf2 interaction via hinge & Latch mechanism. *Communications Biology*, *4*(1). https://doi.org/10.1038/s42003-021-02100-6
66. Yamamoto, M., Kensler, T. W., & Motohashi, H. (2018). The KEAP1-NRF2 system: A thiol-based sensor-effector apparatus for maintaining redox homeostasis. *Physiological Reviews*, *98*(3), 1169-1203. https://doi.org/10.1152/physrev.00023.2017
67. Crilly, M. J., Tryon, L. D., Erlich, A. T., & Hood, D. A. (2016). The role of Nrf2 in skeletal muscle contractile and mitochondrial function. *Journal of Applied Physiology*, *121*(3), 730-740. https://doi.org/10.1152/japplphysiol.00042.2016
68. Zhang, Z., Wang, S., Zhou, S., Yan, X., Wang, Y., Chen, J., Mellen, N., Kong, M., Gu, J., Tan, Y., Zheng, Y., & Cai, L. (2014). Sulforaphane prevents the development of cardiomyopathy in type 2 diabetic mice probably by reversing oxidative stress-induced inhibition of LKB1/AMPK pathway. *Journal of Molecular and Cellular Cardiology*, *77*, 42-52. https://doi.org/10.1016/j.yjmcc.2014.09.022
69. Faridvand, Y., Haddadi, P., Nejabati, H. R., Ghaffari, S., Zamani-Gharehchamani, E., Nozari, S., Nouri, M., & Jodati, A. (2020). Sulforaphane modulates CX3CL1/CX3CR1 axis and inflammation in palmitic acid-induced cell injury in C2C12 skeletal muscle cells. *Molecular Biology Reports*, *47*(10), 7971-7977. https://doi.org/10.1007/s11033-020-05875-9
70. Coleman, V., Sa-Nguanmoo, P., Koenig, J., Schulz, T. J., Grune, T., Klaus, S., Kipp, A. P., & Ost, M. (2018). Partial involvement of Nrf2 in skeletal muscle mitohormesis as an adaptive response to mitochondrial uncoupling. *Scientific Reports*, *8*(1). https://doi.org/10.1038/s41598-018-20901-4
71. Yan, X., Shen, Z., Yu, D., Zhao, C., Zou, H., Ma, B., Dong, W., Chen, W., Huang, D., & Yu, Z. (2022). Nrf2 contributes to the benefits of exercise interventions on age-related skeletal muscle disorder via regulating Drp1 stability and mitochondrial fission. *Free Radical Biology and Medicine*, *178*, 59-75. https://doi.org/10.1016/j.freeradbiomed.2021.11.030
72. Irrcher, I., Ljubicic, V., & Hood, D. A. (2009). Interactions between ROS and AMP kinase activity in the regulation of PGC-1α transcription in skeletal muscle cells. *American Journal of Physiology-Cell Physiology*, *296*(1), C116-C123. https://doi.org/10.1152/ajpcell.00267.2007

73. Tsvetkov, P., Adler, J., Strobelt, R., Adamovich, Y., Asher, G., Reuven, N., & Shaul, Y. (2021). NQO1 binds and supports SIRT1 function. *Frontiers in Pharmacology*, *12*. https://doi.org/10.3389/fphar.2021.671929
74. Alves de Souza, R. W., Gallo, D., Lee, G. R., Katsuyama, E., Schaufler, A., Weber, J., Csizmadia, E., Koch, L. G., Britton, S. L., Wisloff, U., Brum, P. C., & Otterbein, L. E. (2020). Skeletal muscle heme oxygenase-1 activity regulates aerobic capacity. *SSRN Electronic Journal*. https://doi.org/10.2139/ssrn.3671735
75. Holloszy, J. O. (1967). Biochemical adaptations in muscle. *Journal of Biological Chemistry*, *242*(9), 2278-2282. https://doi.org/10.1016/s0021-9258(18)96046-1
76. Tanaka, S., Hayashi, T., Toyoda, T., Hamada, T., Shimizu, Y., Hirata, M., Ebihara, K., Masuzaki, H., Hosoda, K., Fushiki, T., & Nakao, K. (2007). High-fat diet impairs the effects of a single bout of endurance exercise on glucose transport and insulin sensitivity in rat skeletal muscle. *Metabolism*, *56*(12), 1719-1728. https://doi.org/10.1016/j.metabol.2007.07.017
77. Morinaga, M., Sako, N., Isobe, M., Lee-Hotta, S., Sugiura, H., & Kametaka, S. (2021). Aerobic exercise ameliorates cancer cachexia-induced muscle wasting through Adiponectin signaling. *International Journal of Molecular Sciences*, *22*(6), 3110. https://doi.org/10.3390/ijms22063110
78. Morinaga, M., Sako, N., Isobe, M., Lee-Hotta, S., Sugiura, H., & Kametaka, S. (2021). Aerobic exercise ameliorates cancer cachexia-induced muscle wasting through Adiponectin signaling. *International Journal of Molecular Sciences*, *22*(6), 3110. https://doi.org/10.3390/ijms22063110
79. Constable, S. H., Favier, R. J., McLane, J. A., Fell, R. D., Chen, M., & Holloszy, J. O. (1987). Energy metabolism in contracting rat skeletal muscle: Adaptation to exercise training. *American Journal of Physiology-Cell Physiology*, *253*(2), C316-C322. https://doi.org/10.1152/ajpcell.1987.253.2.c316
80. Jacobs, R. A., & Lundby, C. (2013). Mitochondria express enhanced quality as well as quantity in association with aerobic fitness across recreationally active individuals up to elite athletes. *Journal of Applied Physiology*, *114*(3), 344-350. https://doi.org/10.1152/japplphysiol.01081.2012
81. Jacobs, R. A., Flück, D., Bonne, T. C., Bürgi, S., Christensen, P. M., Toigo, M., & Lundby, C. (2013). Improvements in exercise performance with high-intensity interval training coincide with an increase in skeletal muscle mitochondrial content and function. *Journal of Applied Physiology*, *115*(6), 785-793. https://doi.org/10.1152/japplphysiol.00445.2013
82. Rowe, G., Patten, I., Zsengeller, Z., El-Khoury, R., Okutsu, M., Bampoh, S., Koulisis, N., Farrell, C., Hirshman, M., Yan, Z., Goodyear, L., Rustin, P., & Arany, Z. (2013). Disconnecting mitochondrial content from respiratory chain capacity in PGC-1-Deficient skeletal muscle. *Cell Reports*, *3*(5), 1449-1456. https://doi.org/10.1016/j.celrep.2013.04.023
83. Powers, S. K., & Schrager, M. (2022). Redox signaling regulates skeletal muscle remodeling in response to exercise and prolonged inactivity. *Redox Biology*, *54*, 102374. https://doi.org/10.1016/j.redox.2022.102374
84. Drake, J. C., Laker, R. C., Wilson, R. J., Zhang, M., & Yan, Z. (2018). Exercise-induced mitophagy in skeletal muscle occurs in the absence of stabilization of Pink1

on mitochondria. *Cell Cycle*, *18*(1), 1-6. https://doi.org/10.1080/15384101.2018.1559556
85. Arribat, Y., Broskey, N. T., Greggio, C., Boutant, M., Conde Alonso, S., Kulkarni, S. S., Lagarrigue, S., Carnero, E. A., Besson, C., Cantó, C., & Amati, F. (2018). Distinct patterns of skeletal muscle mitochondria fusion, fission and mitophagy upon duration of exercise training. *Acta Physiologica*, *225*(2), e13179. https://doi.org/10.1111/apha.13179
86. Parousis, A., Carter, H. N., Tran, C., Erlich, A. T., Mesbah Moosavi, Z. S., Pauly, M., & Hood, D. A. (2018). Contractile activity attenuates autophagy suppression and reverses mitochondrial defects in skeletal muscle cells. *Autophagy*, *14*(11), 1886-1897. https://doi.org/10.1080/15548627.2018.1491488
87. Triolo, M., & Hood, D. A. (2021). Manifestations of age on autophagy, Mitophagy and lysosomes in skeletal muscle. *Cells*, *10*(5), 1054. https://doi.org/10.3390/cells10051054
88. O'Leary, M. F., Vainshtein, A., Iqbal, S., Ostojic, O., & Hood, D. A. (2013). Adaptive plasticity of autophagic proteins to denervation in aging skeletal muscle. *American Journal of Physiology-Cell Physiology*, *304*(5), C422-C430. https://doi.org/10.1152/ajpcell.00240.2012
89. Chabi, B., Ljubicic, V., Menzies, K. J., Huang, J. H., Saleem, A., & Hood, D. A. (2008). Mitochondrial function and apoptotic susceptibility in aging skeletal muscle. *Aging Cell*, *7*(1), 2-12. https://doi.org/10.1111/j.1474-9726.2007.00347.x
90. Iqbal, S., Ostojic, O., Singh, K., Joseph, A., & Hood, D. A. (2013). Expression of mitochondrial fission and fusion regulatory proteins in skeletal muscle during chronic use and disuse. *Muscle & Nerve*, *48*(6), 963-970. https://doi.org/10.1002/mus.23838
91. Grevendonk, L., Connell, N. J., McCrum, C., Fealy, C. E., Bilet, L., Bruls, Y. M., Mevenkamp, J., Schrauwen-Hinderling, V. B., Jörgensen, J. A., Moonen-Kornips, E., Schaart, G., Havekes, B., De Vogel-van den Bosch, J., Bragt, M. C., Meijer, K., Schrauwen, P., & Hoeks, J. (2021). Impact of aging and exercise on skeletal muscle mitochondrial capacity, energy metabolism, and physical function. *Nature Communications*, *12*(1). https://doi.org/10.1038/s41467-021-24956-2
92. Kang, C., Chung, E., Diffee, G., & Ji, L. L. (2013). Exercise training attenuates aging-associated mitochondrial dysfunction in rat skeletal muscle: Role of PGC-1α. *Experimental Gerontology*, *48*(11), 1343-1350. https://doi.org/10.1016/j.exger.2013.08.004
93. Carter, H. N., Pauly, M., Tryon, L. D., & Hood, D. A. (2018). Effect of contractile activity on PGC-1α transcription in young and aged skeletal muscle. *Journal of Applied Physiology*, *124*(6), 1605-1615. https://doi.org/10.1152/japplphysiol.01110.2017
94. Ljubicic, V., Joseph, A., Adhihetty, P. J., Huang, J. H., Saleem, A., Uguccioni, G., & Hood, D. A. (2009). Molecular basis for an attenuated mitochondrial adaptive plasticity in aged skeletal muscle. *Aging*, *1*(9), 818-830. https://doi.org/10.18632/aging.100083
95. Holloway, G. P., Holwerda, A. M., Miotto, P. M., Dirks, M. L., Verdijk, L. B., & Van Loon, L. J. (2018). Age-associated impairments in mitochondrial ADP sensitivity contribute to redox stress in senescent human skeletal muscle. *Cell Reports*, *22*(11), 2837-2848. https://doi.org/10.1016/j.celrep.2018.02.069

96. Kang, C., Chung, E., Diffee, G., & Ji, L. L. (2009). Exercise training attenuates aging-associated reduction in mitochondrial biogenesis in rat skeletal muscle: role of PGC-1α. *Medicine & Science in Sports & Exercise*, *41*(5), 59. https://doi.org/10.1249/01.mss.0000353449.06824.c0
97. Garcia, S., Nissanka, N., Mareco, E. A., Rossi, S., Peralta, S., Diaz, F., Rotundo, R. L., Carvalho, R. F., & Moraes, C. T. (2018). Overexpression of PGC-1α in aging muscle enhances a subset of young-like molecular patterns. *Aging Cell*, *17*(2), e12707. https://doi.org/10.1111/acel.12707
98. Huang, J. H., Joseph, A., Ljubicic, V., Iqbal, S., & Hood, D. A. (2010). Effect of age on the processing and import of matrix-destined mitochondrial proteins in skeletal muscle. *The Journals of Gerontology Series A: Biological Sciences and Medical Sciences*, *65A*(2), 138-146. https://doi.org/10.1093/gerona/glp201
99. Yan, X., Shen, Z., Yu, D., Zhao, C., Zou, H., Ma, B., Dong, W., Chen, W., Huang, D., & Yu, Z. (2022). Nrf2 contributes to the benefits of exercise interventions on age-related skeletal muscle disorder via regulating Drp1 stability and mitochondrial fission. *Free Radical Biology and Medicine*, *178*, 59-75. https://doi.org/10.1016/j.freeradbiomed.2021.11.030
100. Carter, H. N., Kim, Y., Erlich, A. T., Zarrin-khat, D., & Hood, D. A. (2018). Autophagy and mitophagy flux in young and aged skeletal muscle following chronic contractile activity. *The Journal of Physiology*, *596*(16), 3567-3584. https://doi.org/10.1113/jp275998
101. Ljubicic, V., & Hood, D. A. (2009). Diminished contraction-induced intracellular signaling towards mitochondrial biogenesis in aged skeletal muscle. *Aging Cell*, *8*(4), 394-404. https://doi.org/10.1111/j.1474-9726.2009.00483.x
102. Ljubicic, V., Joseph, A., Adhihetty, P. J., Huang, J. H., Saleem, A., Uguccioni, G., & Hood, D. A. (2009). Molecular basis for an attenuated mitochondrial adaptive plasticity in aged skeletal muscle. *Aging*, *1*(9), 818-830. https://doi.org/10.18632/aging.100083
103. Yeo, D., Kang, C., Gomez-Cabrera, M. C., Vina, J., & Ji, L. L. (2019). Intensified mitophagy in skeletal muscle with aging is downregulated by PGC-1alpha overexpression in vivo. *Free Radical Biology and Medicine*, *130*, 361-368. https://doi.org/10.1016/j.freeradbiomed.2018.10.456
104. Picard, M., Gentil, B. J., McManus, M. J., White, K., St. Louis, K., Gartside, S. E., Wallace, D. C., & Turnbull, D. M. (2013). Acute exercise remodels mitochondrial membrane interactions in mouse skeletal muscle. *Journal of Applied Physiology*, *115*(10), 1562-1571. https://doi.org/10.1152/japplphysiol.00819.2013
105. Halling, J. F., Ringholm, S., Olesen, J., Prats, C., & Pilegaard, H. (2017). Exercise training protects against aging-induced mitochondrial fragmentation in mouse skeletal muscle in a PGC-1α dependent Manner. *Experimental Gerontology*, *96*, 1-6. https://doi.org/10.1016/j.exger.2017.05.020
106. Bhatti, J. S., Bhatti, G. K., & Reddy, P. H. (2017). Mitochondrial dysfunction and oxidative stress in metabolic disorders — A step towards mitochondria based therapeutic strategies. *Biochimica et Biophysica Acta (BBA) - Molecular Basis of Disease*, *1863*(5), 1066-1077. https://doi.org/10.1016/j.bbadis.2016.11.010
107. Ryu, D., Mouchiroud, L., Andreux, P. A., Katsyuba, E., Moullan, N., Nicolet-dit-Félix, A. A., Williams, E. G., Jha, P., Lo Sasso, G., Huzard, D., Aebischer, P.,

Sandi, C., Rinsch, C., & Auwerx, J. (2016). Urolithin a induces mitophagy and prolongs lifespan in C. elegans and increases muscle function in rodents. *Nature Medicine*, *22*(8), 879-888. https://doi.org/10.1038/nm.4132

108. Luan, P., D'Amico, D., Andreux, P. A., Laurila, P., Wohlwend, M., Li, H., Imamura de Lima, T., Place, N., Rinsch, C., Zanou, N., & Auwerx, J. (2021). Urolithin a improves muscle function by inducing mitophagy in muscular dystrophy. *Science Translational Medicine*, *13*(588). https://doi.org/10.1126/scitranslmed.abb0319
109. Andreux, P. A., Blanco-Bose, W., Ryu, D., Burdet, F., Ibberson, M., Aebischer, P., Auwerx, J., Singh, A., & Rinsch, C. (2019). The mitophagy activator urolithin a is safe and induces a molecular signature of improved mitochondrial and cellular health in humans. *Nature Metabolism*, *1*(6), 595-603. https://doi.org/10.1038/s42255-019-0073-4
110. Liu, S., D'Amico, D., Shankland, E., Bhayana, S., Garcia, J. M., Aebischer, P., Rinsch, C., Singh, A., & Marcinek, D. J. (2022). Effect of Urolithin a supplementation on muscle endurance and mitochondrial health in older adults. *JAMA Network Open*, *5*(1), e2144279. https://doi.org/10.1001/jamanetworkopen.2021.44279
111. D'Amico, D., Olmer, M., Fouassier, A. M., Valdés, P., Andreux, P. A., Rinsch, C., & Lotz, M. (2022). Urolithin a improves mitochondrial health, reduces cartilage degeneration, and alleviates pain in osteoarthritis. *Aging Cell*, *21*(8). https://doi.org/10.1111/acel.13662
112. Zhang, L., Zhou, H., Fu, Y., Li, Y., Wu, F., Gu, M., Wu, L., Xia, C., Dong, T., Li, J., Shen, J., & Li, J. (2013). Novel small-molecule PGC-1α transcriptional regulator with beneficial effects on diabetic *db/db* mice. *Diabetes*, *62*(4), 1297-1307. https://doi.org/10.2337/db12-0703
113. Liu, Y., Bai, H., Guo, F., Thai, P. N., Luo, X., Zhang, P., Yang, C., Feng, X., Zhu, D., Guo, J., Liang, P., Xu, Z., Yang, H., & Lu, X. (2020). PGC-1α activator ZLN005 promotes maturation of cardiomyocytes derived from human embryonic stem cells. *Aging*, *12*(8), 7411-7430. https://doi.org/10.18632/aging.103088
114. Wang, M., Pu, D., Zhao, Y., Chen, J., Zhu, S., Lu, A., Liao, Z., Sun, Y., & Xiao, Q. (2020). Sulforaphane protects against skeletal muscle dysfunction in spontaneous type 2 diabetic DB/DB mice. *Life Sciences*, *255*, 117823. https://doi.org/10.1016/j.lfs.2020.117823
115. Malaguti, M., Angeloni, C., Garatachea, N., Baldini, M., Leoncini, E., Collado, P. S., Teti, G., Falconi, M., Gonzalez-Gallego, J., & Hrelia, S. (2009). Sulforaphane treatment protects skeletal muscle against damage induced by exhaustive exercise in rats. *Journal of Applied Physiology*, *107*(4), 1028-1036. https://doi.org/10.1152/japplphysiol.00293.2009
116. Moon, J. Y., Kim, D. J., & Kim, H. S. (2020). Sulforaphane ameliorates serum starvation-induced muscle atrophy via activation of the Nrf2 pathway in cultured C2C12 cells. *Cell Biology International*, *44*(9), 1831-1839. https://doi.org/10.1002/cbin.11377
117. Yang, J., Guo, Y., Henning, S. M., Chan, B., Long, J., Zhong, J., Acin-Perez, R., Petcherski, A., Shirihai, O., Heber, D., & Li, Z. (2020). Ellagic acid and its microbial metabolite Urolithin a alleviate diet-induced insulin resistance in

mice. *Molecular Nutrition & Food Research*, *64*(19), 2000091. https://doi.org/10.1002/mnfr.202000091
118. Fiuza-Luces, C., Garatachea, N., Berger, N. A., & Lucia, A. (2013). Exercise is the real Polypill. *Physiology*, *28*(5), 330-358. https://doi.org/10.1152/physiol.00019.2013
119. Timm, K. N., & Tyler, D. J. (2020). The role of AMPK activation for Cardioprotection in doxorubicin-induced Cardiotoxicity. *Cardiovascular Drugs and Therapy*, *34*(2), 255-269. https://doi.org/10.1007/s10557-020-06941-x
120. Madhavi, Y., Gaikwad, N., Yerra, V. G., Kalvala, A. K., Nanduri, S., & Kumar, A. (2019). Targeting AMPK in diabetes and diabetic complications: Energy homeostasis, autophagy and mitochondrial health. *Current Medicinal Chemistry*, *26*(27), 5207-5229. https://doi.org/10.2174/0929867325666180406120051
121. Procaccio, V., Bris, C., Chao de la Barca, J., Oca, F., Chevrollier, A., Amati-Bonneau, P., Bonneau, D., & Reynier, P. (2014). Perspectives of drug-based neuroprotection targeting mitochondria. *Revue Neurologique*, *170*(5), 390-400. https://doi.org/10.1016/j.neurol.2014.03.005
122. Sánchez-González, C., Herrero Martín, J. C., Salegi Ansa, B., Núñez de Arenas, C., Stančič, B., Pereira, M. P., Contreras, L., Cuezva, J. M., & Formentini, L. (2022). Chronic inhibition of the mitochondrial ATP synthase in skeletal muscle triggers sarcoplasmic Reticulum distress and tubular aggregates. *Cell Death & Disease*, *13*(6). https://doi.org/10.1038/s41419-022-05016-z
123. Woodman, K. G., Coles, C. A., Lamandé, S. R., & White, J. D. (2021). Resveratrol promotes hypertrophy in Wildtype skeletal muscle and reduces muscle necrosis and gene expression of inflammatory markers in Mdx mice. *Molecules*, *26*(4), 853. https://doi.org/10.3390/molecules26040853
124. Springer, M., & Moco, S. (2019). Resveratrol and its human metabolites—Effects on metabolic health and obesity. *Nutrients*, *11*(1), 143. https://doi.org/10.3390/nu11010143
125. Annunziata, G. (2018). Resveratrol-based nutraceuticals for the management of diabetes and obesity: Real therapeutic potential or a Mere palliative? *Archives of Diabetes & Obesity*, *1*(2). https://doi.org/10.32474/ado.2018.01.000109
126. Feng, K., Chen, Z., Pengcheng, L., Zhang, S., & Wang, X. (2019). Quercetin attenuates oxidative stress-induced apoptosis via SIRT1/AMPK-mediated inhibition of ER stress in rat chondrocytes and prevents the progression of osteoarthritis in a rat model. *Journal of Cellular Physiology*, *234*(10), 18192-18205. https://doi.org/10.1002/jcp.28452
127. Chen, C., Yang, J., Lu, C., Chiu, Y., Chen, H., Chung, M., Wu, Y., & Chen, F. (2020). Effect of quercetin on dexamethasone-induced C2C12 skeletal muscle cell injury. *Molecules*, *25*(14), 3267. https://doi.org/10.3390/molecules25143267
128. Spaulding, H. R., Ballmann, C. G., Quindry, J. C., & Selsby, J. T. (2016). Long-term quercetin dietary enrichment partially protects dystrophic skeletal muscle. *PLOS ONE*, *11*(12), e0168293. https://doi.org/10.1371/journal.pone.0168293
129. Park, E., & Chun, H. S. (2016). Protective effects of quercetin on dieldrin-induced endoplasmic Reticulum stress and apoptosis in dopaminergic neuronal

cells. *NeuroReport*, *27*(15), 1140-1146. https://doi.org/10.1097/wnr.0000000000000667

130. Varela, C. E., Rodriguez, A., Romero-Valdovinos, M., Mendoza-Lorenzo, P., Mansour, C., Ceballos, G., Villarreal, F., & Ramirez-Sanchez, I. (2017). Browning effects of (-)-epicatechin on adipocytes and white adipose tissue. *European Journal of Pharmacology*, *811*, 48-59. https://doi.org/10.1016/j.ejphar.2017.05.051
131. Bustamante-Pozo, M., Ramirez-Sanchez, I., Garate-Carrillo, A., Ito, B., Navarrete, V., Haro, M., Garcia, R., Carson, N., Ceballos, G., & Villarreal, F. (2022). (−)-epicatechin ameliorates cardiac fibrosis in a female rat model of pre-heart failure with preserved ejection fraction. *Journal of Medicinal Food*, *25*(8), 836-844. https://doi.org/10.1089/jmf.2021.0158
132. Moreno-Ulloa, A., & Moreno-Ulloa, J. (2016). Mortality reduction among persons with type 2 diabetes: (−)-epicatechin as add-on therapy to metformin? *Medical Hypotheses*, *91*, 86-89. https://doi.org/10.1016/j.mehy.2016.04.018
133. Reid Thompson, W., Hornby, B., Manuel, R., Bradley, E., Laux, J., Carr, J., & Vernon, H. J. (2021). A phase 2/3 randomized clinical trial followed by an open-label extension to evaluate the effectiveness of elamipretide in Barth syndrome, a genetic disorder of mitochondrial cardiolipin metabolism. *Genetics in Medicine*, *23*(3), 471-478. https://doi.org/10.1038/s41436-020-01006-8
134. Whitson, J. A., Martín-Pérez, M., Zhang, T., Gaffrey, M. J., Merrihew, G. E., Huang, E., White, C. C., Kavanagh, T. J., Qian, W., Campbell, M. D., MacCoss, M. J., Marcinek, D. J., Villén, J., & Rabinovitch, P. S. (2021). Elamipretide (SS-31) treatment attenuates age-associated post-translational modifications of heart proteins. https://doi.org/10.1101/2021.08.06.455402
135. Liu, J., Campagna, J., John, V., Damoiseaux, R., Mokhonova, E., Becerra, D., Meng, H., McNally, E. M., Pyle, A. D., Kramerova, I., & Spencer, M. J. (2020). A small-molecule approach to restore a slow-oxidative phenotype and defective CaMKIIβ signaling in limb girdle muscular dystrophy. *Cell Reports Medicine*, *1*(7), 100122. https://doi.org/10.1016/j.xcrm.2020.100122
136. Sanchez-Rangel, E., & Inzucchi, S. E. (2017). Metformin: Clinical use in type 2 diabetes. *Diabetologia*, *60*(9), 1586-1593. https://doi.org/10.1007/s00125-017-4336-x
137. Bharath, L. P., Agrawal, M., McCambridge, G., Nicholas, D. A., Hasturk, H., Liu, J., Jiang, K., Liu, R., Guo, Z., Deeney, J., Apovian, C. M., Snyder-Cappione, J., Hawk, G. S., Fleeman, R. M., Pihl, R. M., Thompson, K., Belkina, A. C., Cui, L., Proctor, E. A., … Nikolajczyk, B. S. (2020). Metformin enhances autophagy and normalizes mitochondrial function to alleviate aging-associated inflammation. *Cell Metabolism*, *32*(1), 44-55.e6. https://doi.org/10.1016/j.cmet.2020.04.015
138. Tang, Q., Zheng, G., Feng, Z., Chen, Y., Lou, Y., Wang, C., Zhang, X., Zhang, Y., Xu, H., Shang, P., & Liu, H. (2017). Trehalose ameliorates oxidative stress-mediated mitochondrial dysfunction and ER stress via selective autophagy stimulation and autophagic flux restoration in osteoarthritis development. *Cell Death & Disease*, *8*(10), e3081-e3081. https://doi.org/10.1038/cddis.2017.453
139. Hamada, N., Wadazumi, T., Hirata, Y., Kuriyama, M., Watanabe, K., Watanabe, H., Hongu, N., & Arai, N. (2021). Single ingestion of Trehalose enhances prolonged

exercise performance by effective use of glucose and lipid in healthy men. *Nutrients*, *13*(5), 1439. https://doi.org/10.3390/nu13051439
140. Hamada, N., Wadazumi, T., Hirata, Y., Watanabe, H., Hongu, N., & Arai, N. (2022). Effects of Trehalose solutions at different concentrations on high-intensity intermittent exercise performance. *Nutrients*, *14*(9), 1776. https://doi.org/10.3390/nu14091776
141. Chuengsamarn, S., Rattanamongkolgul, S., Luechapudiporn, R., Phisalaphong, C., & Jirawatnotai, S. (2012). Curcumin extract for prevention of type 2 diabetes. *Diabetes Care*, *35*(11), 2121-2127. https://doi.org/10.2337/dc12-0116
142. Mañas-García, L., Bargalló, N., Gea, J., & Barreiro, E. (2020). Muscle phenotype, proteolysis, and atrophy signaling during reloading in mice: Effects of curcumin on the gastrocnemius. *Nutrients*, *12*(2), 388. https://doi.org/10.3390/nu12020388
143. Yu, T., Dohl, J., Wang, L., Chen, Y., Gasier, H. G., & Deuster, P. A. (2020). Curcumin ameliorates heat-induced injury through NADPH oxidase–dependent redox signaling and mitochondrial preservation in C2C12 myoblasts and mouse skeletal muscle. *The Journal of Nutrition*, *150*(9), 2257-2267. https://doi.org/10.1093/jn/nxaa201
144. Koboziev, I., Scoggin, S., Gong, X., Mirzaei, P., Zabet-Moghaddam, M., Yosofvand, M., Moussa, H., Jones-Hall, Y., & Moustaid-Moussa, N. (2020). Effects of curcumin in a mouse model of very high fat diet-induced obesity. *Biomolecules*, *10*(10), 1368. https://doi.org/10.3390/biom10101368

CHAPTER 2

MANUSCRIPT

MANUSCRIPT AUTHOR CONTRIBUTIONS:

Neushaw Moradi: Performed all cell culture procedures and drug treatments; transient transfections; cellular extracts for whole cell and nuclear, cytoplasmic, and mitochondrial fractions; immunoblot experiments; data analyses and interpretations; wrote the manuscript.

Dr. David A. Hood: Supervised this project and is the Principal Investigator.

SULFORAPHANE, UROLITHIN A, AND ZLN005 INDUCE TIME-DEPENDENT ALTERATIONS FOR ANTIOXIDANT CAPACITY, MITOPHAGY, AND MITOCHONDRIAL BIOGENESIS IN MUSCLE

Neushaw Moradi and David A. Hood

Muscle Health Research Centre, School of Kinesiology and Health Science, York University, Toronto, Ontario, M3J 1P3, Canada

To whom correspondence should be addressed: David A. Hood, Ph.D (dhood@yorku.ca)

Muscle Health Research Centre

School of Kinesiology and Health Science

York University, Toronto, ON M3J 1P3, Canada

ABSTRACT

Efficient signal transduction that takes place within and between important mechanisms to sustain mitochondrial turnover is a strong determinant of metabolic health in skeletal muscle. Of these pathways, our focus was aimed towards antioxidant capacity, mitophagy, and mitochondrial biogenesis. While physical activity is an excellent inducer of mitochondrial turnover and restoration of metabolic homeostasis, its ability to ubiquitously activate and enhance mitochondrial turnover prevents definitive differentiation of the contribution made by each. Therefore, we employed three agents, Sulforaphane (SFN), Urolithin A (UroA), and ZLN005 (ZLN), that are activators of important biological markers involved in the Nrf-2/ARE antioxidant system, mitophagy, or biogenesis, respectively. We investigated the time-dependent changes in proteins related to each mechanism in C2C12 myotubes. SFN treatment resulted in increased nuclear localization of the transcription factor Nrf-2 after 4 hours, with subsequent 2-fold increases in the NQO1 and HO-1 antioxidant enzymes by 24 hours and 48 hours. UroA showed a 2-fold increase in AMPK after 4 hours, which led to a modest 30% increase in whole cell mitophagy markers p62 and LC3, after 48 hours. Mitophagy flux measurements showed evidence of mitophagy activation as both LC3-II and p62 flux increased with UroA at 24 and 48-hour time points, respectively. Finally, a 2-fold increase in TFAM promoter activity was observed after 24 hours of ZLN treatment following transient transfection of a TFAM promoter-luciferase construct. While continued characterization of these agents in our *in vitro* model is required, our results suggest that early time points of treatment increase upstream pathway activity, whereas later time points represent the increased phenotypic expression of their related downstream markers. Examination of synergistic events following co-treatment with agent and contractile activity, or polypill combinations as a form of metabolic mimicry with exercise, are avenues of future work.

INTRODUCTION

While the mitochondrion fuels energy-dependent processes in the cell, its regulation and function depend on sufficient signal transduction by and for this organelle, to govern the metabolic outcomes that maintain cellular homeostasis. Metabolic derangements in skeletal muscle, borne of aging, disuse, denervation, or disease [1] can be caused by impairments in intrinsic signal transduction that typically take place in healthy muscle [2,3]. Despite the activation of mechanisms dedicated to mitochondrial turnover with exercise [4-7] full restoration of optimal organelle function is limited [2]. While exercise effectively refreshes the mitochondrial pool, this ubiquitous stimulus can blur the unique characterization of the individual pathways that contribute to an improved metabolic outcome. In this respect, nutraceutical and pharmaceutical agents that have been developed overtime for therapeutic intervention can prove useful in identifying the activation of important cellular mechanisms and illuminating their unique contributions to refreshing the mitochondrial pool.

We have gained interest in agents that target important markers that typically increase the drive for mitochondrial biogenesis, mitochondrial autophagy (hereafter referred to as mitophagy), and antioxidant capacity. Furthermore, we wished to investigate the time-dependent changes in the upstream and downstream proteins related to each pathway as an added layer of characterization. Data mining revealed three agents that have gained considerable traction in the literature and that are relevant to our experimental goals. These include the two nutraceutical agents Sulforaphane (SFN) [8-10] and Urolithin A (UroA) [11-15], alongside the third synthetic small molecule, ZLN005 [16-17].

SFN is a potent activator of the Nrf-2-Keap1-ARE antioxidant axis which governs the transcriptional regulation of phase II detoxification enzymes for cytoprotection. Available in cruciferous vegetables, this isothiocyanate and phytochemical is deemed to be one of the most

important potent cellular defence compounds readily available in natural diets. While its therapeutic application originated in neurological disease and chemoprevention [18-19], SFN has also been positioned as a metabolic preserver in skeletal muscle [8,20]. While its cytoprotective effects are versatile, SFN appears to be highly specific to Nrf-2-mediated signaling, which can uncover the pathway-specific benefits towards mitochondrial preservation.

UroA has gained a considerable reputation in the literature from *in vitro* studies to investigations in human subjects [11-15] and has been identified as a mitophagy activator. This ellagitannin has been reported to restore mitophagy starting at the upstream activating kinase, AMPK, thus preventing the accumulation of unhealthy mitochondria in the cell [11]. It gained its fame in the literature as a useful agent that restores mitochondrial clearance in aged skeletal muscle without direct targeting of mitochondrial biogenesis, thus promoting healthy aging of the cell. However, the data supporting the effects of UroA on mitophagy are not overly convincing, upon close inspection. Therefore, our goal was to characterize this agent by investigating its time-dependent ability to induce mitophagy in our *in vitro* model of skeletal muscle.

The small synthetic molecule, ZLN005 has been reported to activate PGC-1α and relieve some of the symptoms of insulin resistance [16]. ZLN005 appears to stimulate the nuclear translocation of PGC-1α and therefore may upregulate the drive for mitochondrial biogenesis [21]. For this reason, we believed this would be a suitable candidate as an activator of the expansion of the mitochondrial reticulum in skeletal muscle.

Countless pharmacological agents have entered the circuit for research-based interventions that improve skeletal muscle health. Over time, continued elucidation around skeletal muscle cellular modulation adds information to the pharmacological blueprints that

can refine drug function and improve their metabolic mimicry. While we limit our study to just these three agents, we wished to 1) examine the integrity of these agents as activators of different mitochondria-related pathways in C2C12 myotubes, and 2) expand on the characterization of these mechanisms and their unique cascade by examining the time-dependent changes of their relevant proteins.

METHODS

Mammalian cell culture and drug treatments. C2C12 murine myoblasts were seeded on six-well culture dishes (Fisher Scientific) in Dulbecco's modified Eagle's medium (DMEM) supplemented with 10% fetal bovine serum (FBS) and 1% penicillin-streptomycin (P/S). At 80-90% confluency, differentiation into myotubes was induced by switching the medium to DMEM supplemented with 5% heat-inactivated horse serum (HS) and 1% P/S. Between day 5 to 6 of differentiation, cells were treated with vehicle (DMSO) or differing concentrations of Sulforaphane (5 uM, 10 uM) (MedChemExpress), Urolithin A (20 uM, 50 uM) (MedChemExpress), or ZLN005 (10uM, 20uM). Drug treatments were followed by 4, 24, or 48 h of incubation time to examine their time-dependent effects.

Immunoblotting. Cells were lysed and proteins were extracted with 1 x passive lysis buffer dilued from a 5X stock (Promega), 1 x phosphatase cocktails, and 1 x protease inhibitor (Millipore-Sigma). Protein concentrations for each sample were determined via Bradford concentration assay. Protein samples (15-25 ug) were then loaded and separated on SDS-PAGE gels followed by transfer to nitrocellulose membranes. Membranes were then washed in Ponceau stain and cut at an appropriate range according to the molecular weight of each protein of interest. Each blot was later blocked using 5% milk or 5% bovine serum albumin at room temperature for approximately 1 hour. Western blot analyses were performed using primary antibodies against Nrf-2 (ProteinTech), Keap 1 (ProteinTech), Phospho-AMPK (Cell

Signaling), AMPK (Cell Signaling), LC3 A/B (Cell Signaling), GAPDH (Abcam), SQSTM1/p62 (Abcam), PGC-1α (Millipore-Sigma), H2B (Cell Signaling), Luciferase (Millipore-Sigma), COX IV (Abcam), and α- tubulin (Calbiochem). Blots were imaged using ECL Clarity Substrates (BIO-RAD), Invitrogen Imaging instrument, and quantification takes place using the ImageJ software. Values were normalized to each protein's corresponding loading control.

Nuclear-Cytoplasmic Fractionation. The purpose for this protocol was to examine nuclear localization of different markers of interest that may be relevant to the mechanism associated with each agent. Thus far, this concerned Nrf-2 or PGC-1α nuclear localization with SFN or ZLN005, respectively. The solutions used in this protocol were described in the work by Bhattacharya et al. [22]. Cells were harvested in cytoplasmic buffer containing 0.2% phosphatase and protease inhibitors. Samples were incubated on ice for 5 minutes and centrifuged at 2500xg for 5 minutes. The supernatant fraction of each sample was collected as the cytoplasmic fraction. Following this, each nuclear pellet was washed and resuspended with cytoplasmic buffer, followed by 3 mins of rocking in 4°C, and 3 min centrifugation at 3200xg. The wash step was repeated 10-12 times to ensure thorough clearance of cytoplasmic fraction from the nuclear pellet. Then, the pellet for each sample was resuspended in nuclear buffer, and 0.15 unit/uL of Benzonase nuclease was added to each sample. The protein content for each fraction was assessed through immunoblot analysis.

Cytoplasmic-Mitochondrial Fractionation. The purpose for this protocol was to examine the integrity of UroA as a mitophagy activator. Prior to fractionation, cells were co-treated with UroA and Bafilomycin A, an inhibitor of autophagosome-lysosome fusion [23]. Following 24 or 48 hours of treatment, cells were washed and scraped with ice cold 1xPBS. They then underwent centrifugation at 1400xg for 5 minutes. The supernatant was then aspirated, and the

cells were resuspended with resuspension buffer with an arbitrary volume that is roughly 3-4 times the pellet size. They were then transferred to smaller Eppendorf tubes for better handling and centrifugation. Cells were incubated on ice for 5 minutes prior to sonication. The sonication protocol involved 2-3 repetitions of 3-5 second sonication, with a minimum of 10 seconds rest between repetitions. Cells were centrifuged at 1000xg for 10 minutes in 4°C. The supernatant was collected and transferred to new tubes, and the pellet was discarded. It was then centrifuged at 14 000xg for 15 minutes at 4°C. The supernatant following this was collected and stored at -80°C until use, as the cytoplasmic fraction. Approximately 100 uL of resuspension buffer was then added to the remnant pellet and resuspended prior to two more centrifugation periods at 14 000xg for 10 minutes, with new resuspension buffer added between each spin. The supernatant was then discarded, and 25 – 50 uL of resuspension buffer was added to the pellet to be resuspended. Samples were freeze-thawed on dry ice 2-3 times. Each sample was then stored at -80°C until use. The protein content for each fraction was assessed through immunoblot analysis.

Promoter-Reporter Transient Transfections. A promoter-reporter Luciferase (pGL3) construct for TFAM was used to assess promoter activity for its transcription [23] as an indirect indication of activated and nuclear-localized PGC-1α following ZLN treatment. The procedure for this experiment was as described previously [23]. C2C12 myoblasts are transiently transfected at approximately 50% confluency with Lipofectamine 2000 and a pGL3-empty vector (EV), or the full TFAM promoter construct located upstream of a luciferase reporter sequence in minimal DMEM (media that does not contain antibiotics or serum). Cells were incubated in this medium for 16-18 hours and then switched to regular growth media as described earlier. Once 80% confluency was reached, cells were differentiated for 5 to 6 days prior to desired treatments.

Statistical Analysis. All data were analyzed using Prism software (GraphPad) and were standardized at Mean + S.E.M. Raw data were analyzed using a paired t-test to assess the differences between control and treated cells. One-way ANOVAs were used to assess the effect of time or concentration with treatments for the 4 and 24-hour time points. Two-way ANOVAs were used to assess the 48-hour time point as we did not take differing volumes of DMSO within each pair of concentrations into consideration when treatments were prepared. This led to each concentration having its own exclusive vehicle treatment. This was resolved for the 4- and 24-hour time points. Statistical significance was set at $P<0.05$.

RESULTS

Sulforaphane increases Nrf-2 nuclear localization at 4h, but effect dissipates by 24 and 48h. SFN is recognized for its role as an activator of the Nrf-2-Keap1 pathway (Fig. 1 **A**). We used 5 μM and 10 μM of SFN to investigate changes at 4-, 24-, and 48-hour time points in C2C12 myotubes. We hypothesized that an early time point may demonstrate early activation of the Nrf-2 transcription factor as it represents one of the initiating steps in this antioxidant axis, while later time points may show increased downstream antioxidant proteins borne of Nrf-2-ARE-mediated antioxidant activation.

A 2-fold elevation in Nrf-2 protein content was observed after 4 hours ($P<0.05$) of SFN treatment at 10 μM concentration, an approximate 1.5-fold increase by 24 hours, but this effect dissipated at 48 hours (Fig. 2 **A**-**D**). A main effect of time was observed, demonstrating the progressive restoration of Nrf-2 content back to control levels (Fig 2. **A**). The corresponding fold-change measured as the ratio of SFN over vehicle data was calculated to better observe this progression over time (Fig. 2 **C**). Conversely, changes to Keap 1 showed a trending effect of time, where 24 hours of treatment showed decreased content that was restored after 48 hours ($P=0.0558$; Fig 2. **B**, **D**). To examine Nrf-2 nuclear localization with SFN, we used cytoplasmic

and nuclear fractions of C2C12 myotubes treated with 5 μM and 10 μM concentrations after 4 hours. A near 2-fold elevation in Nrf-2 nuclear content, compared to vehicle-treated cells occurred with SFN at 5 μM (P<0.05), confirming increased localization of the transcription factor to the nucleus (Fig 2. **E**).

Sulforaphane induces time-dependent changes to antioxidant enzymes commonly related to the Nrf-2-ARE axis. Both concentrations of SFN were used to test the changes in protein content of NQO1 and HO-1 antioxidant enzymes, as well as a mitochondrial marker, COX IV (Fig. 3 **A**-**C**). While NQO1 and COX IV protein showed no change with SFN at either concentration, HO-1 exhibited an early and marked elevation of 50-60% with respect to both concentrations and this was maintained throughout the remaining time points (Fig. 3 **B**). NQO1 was increased by 2-fold at 24 hours, which was maintained at 48 hours, with a main effect of treatment and time (P<0.05; Fig. 3 **A**). COX IV showed no changes in content until 48 hours, where an approximate 40% increase occurred with either concentration (P<0.05; Fig. 3 **C**). Overall, there appeared to be no stark differences between SFN concentrations during the time points where elevations in content were observed. Thus, SFN-mediated activation of the Nrf-2-Keap1-ARE pathway was evident, with time-dependent changes in the effects of proteins, as well as in specific downstream targets.

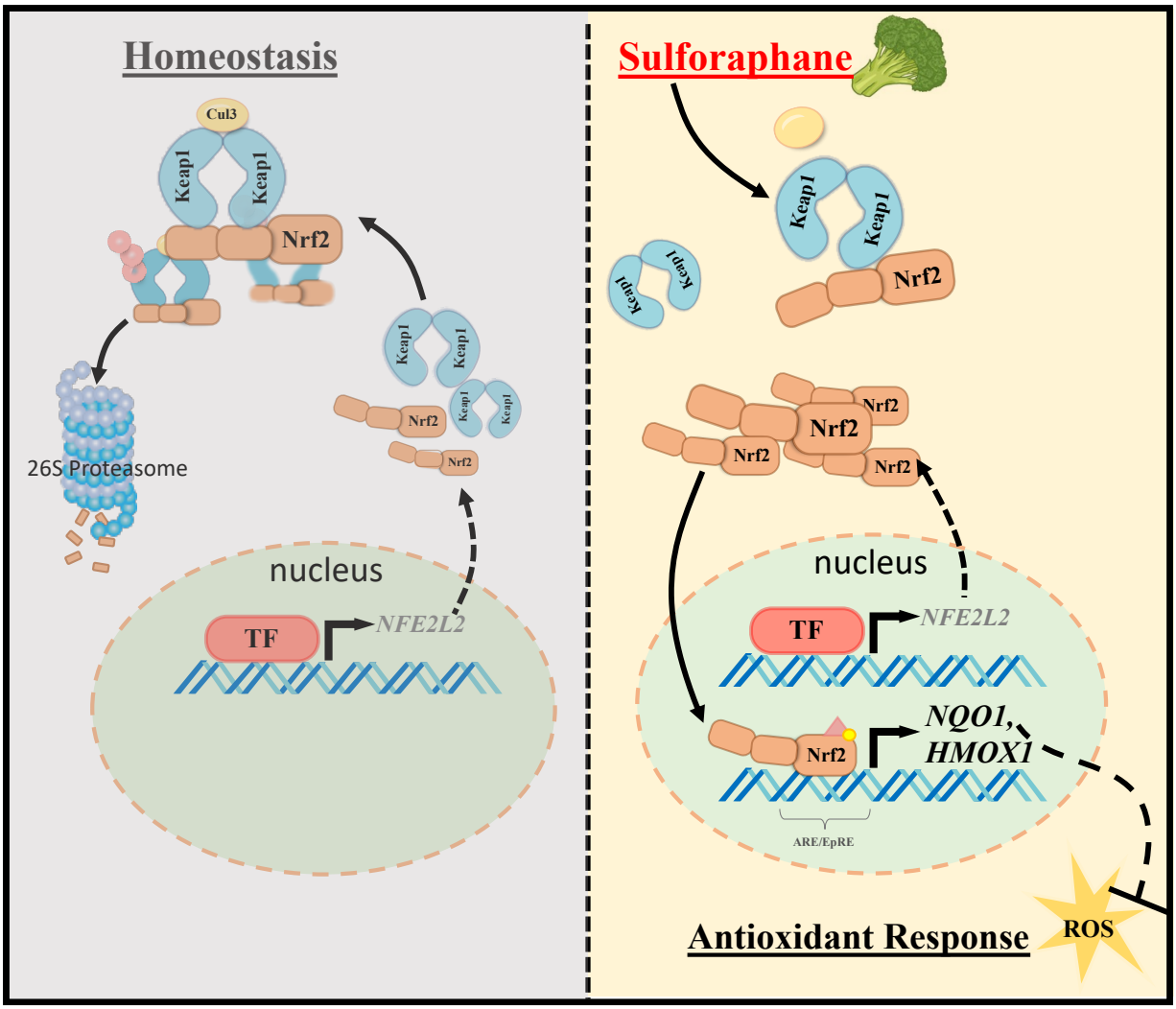

Fig 1. Schematic summarizing the documented function of Sulforaphane

Under homeostatic conditions (left panel, grey), the transcription factor Nrf-2 is sequestered in the cytoplasm by its homodimeric negative regulator, Keap1. Under SFN-induced conditions (right panel, yellow), the sequestering capacity of Keap1 is disrupted, leading to the accumulation and nuclear localization of nascent Nrf-2. It binds to the antioxidant response element in the upstream promoters for genes including *NQO1* and *HMOX1*. These eventually aid in the mitigation of excessive ROS, which can otherwise damage mitochondrial machinery and their function. Dotted lines signify additional steps to the pathway not shown.

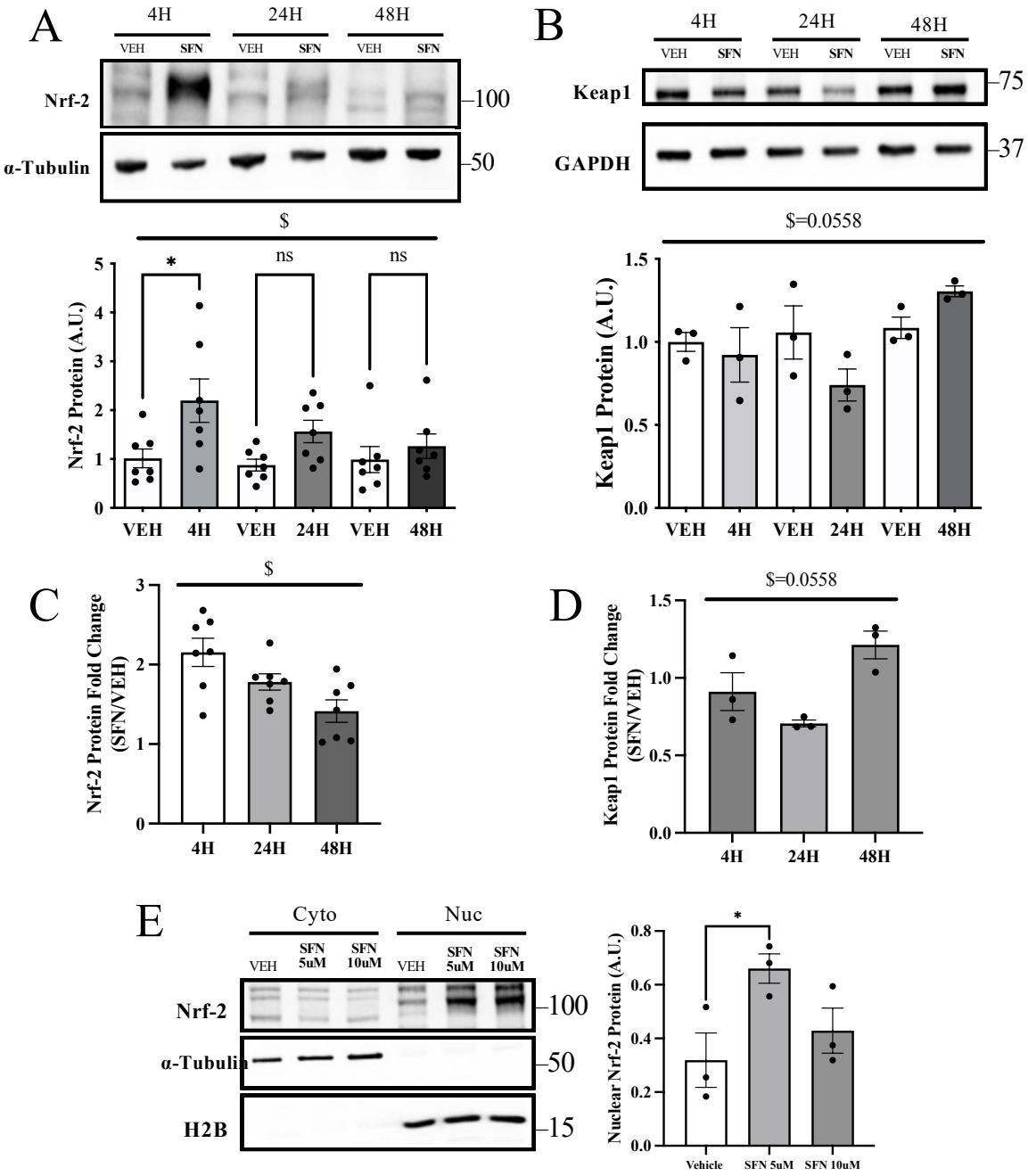

Fig 2. Upstream protein markers observed in the Nrf-2-ARE antioxidant pathway following Sulforaphane treatment. A: Progression of Nrf-2 content with time at 10 μM SFN concentration at each time point (*n*=7). One-way ANOVA, $*P*<0.05, main effect of time; **P*<0.05, treatment vs. vehicle. B: Progression of Keap1 content with time at 10 μM SFN concentration at each time point (*n*=3) One-way ANOVA, $*P*<0.05, main effect of time; **P*<0.05, treatment vs. vehicle. C,D: Fold-change (SFN/VEH) for Nrf-2 and Keap1 proteins, respectively, at each time point, related to panels A and B, respectively. E: Nuclear localization analysis using nuclear and cytosolic fractionation observing Nrf-2 protein content with SFN treatment (*n*=3); **P*<0.05, treatment vs. vehicle. *VEH,* Vehicle-treated cells with DMSO*; SFN,* Sulforaphane-treated cells. Values are means ± SEM.

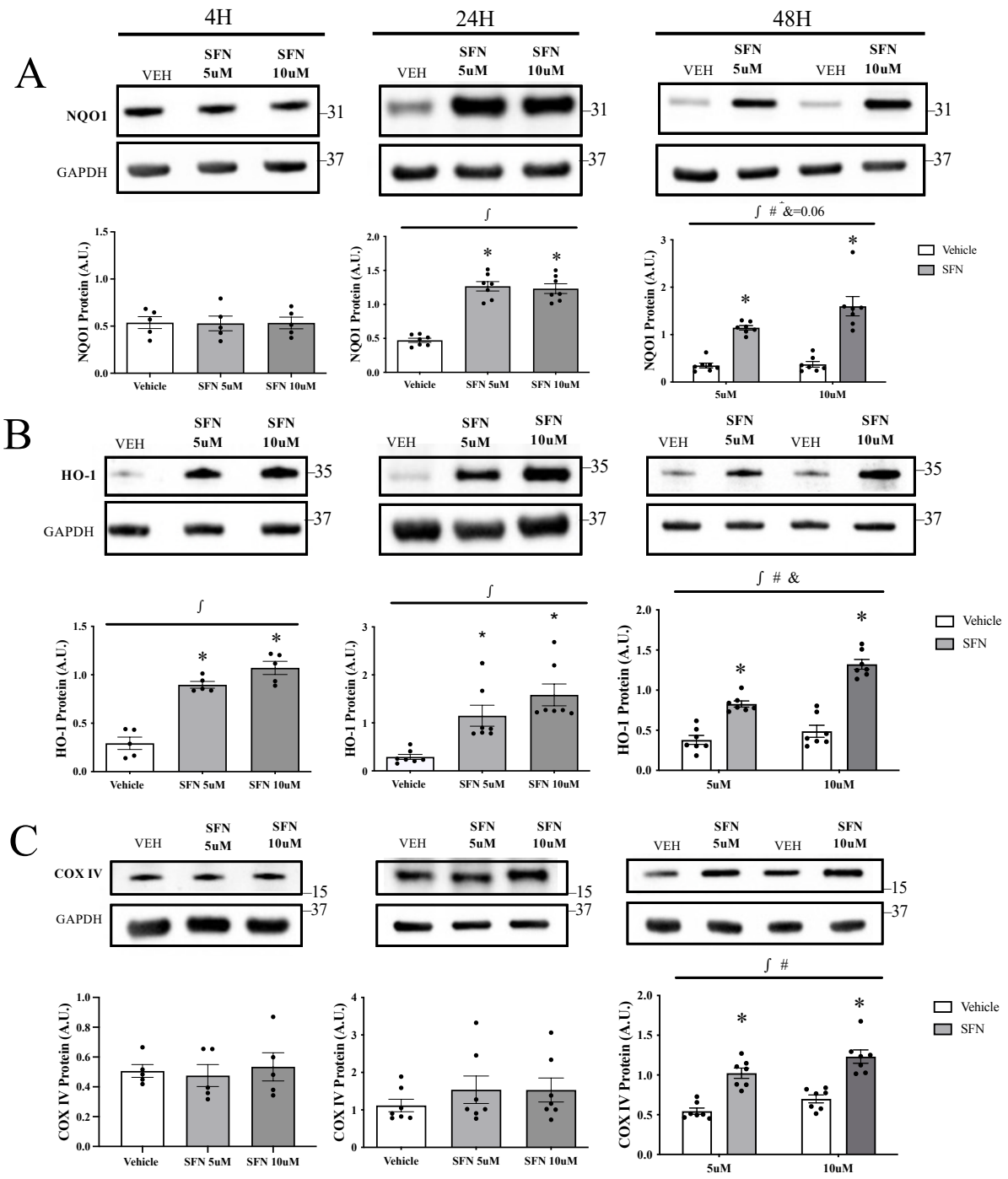

Fig 3. Downstream protein markers observed in Nrf-2-ARE antioxidant pathway following Sulforaphane treatment. Content of downstream proteins NQO1 (A), HO-1 (B), and COX IV (C), respectively, typically targeted by Nrf-2-ARE mechanism, following each given time point. Time points 4h (n=5) and 24h (n=7) underwent one-way ANOVA and 48 h (n=7) underwent two-way ANOVA, ∫P<0.05, main effect of treatment relative to control; #P<0.05, main effect of concentration; &P<0.05, interaction effect between treatment and concentration; *P<0.05, treatment vs. vehicle. *VEH,* Vehicle-treated cells with DMSO*; SFN,* Sulforaphane-treated cells. Values are means ± SEM.

Urolithin A modestly increases AMPK-mediated mitophagy markers while markedly increasing mitophagy flux. UroA has been reported to be an activator of the mitophagy pathway (Fig. 1 **B**). To evaluate this possibility, we used 20, 50, or 100 μM concentrations of UroA to investigate changes in proteins relevant to mitophagy at 4-, 24-, and 48-hour time points. At 4 hours of treatment, a 2-fold increase ($P<0.05$) in activated AMPK, represented as the ratio of phosphorylated AMPK over total AMPK, was observed at 50 μM UroA concentration. However, this effect was no longer evident at longer time points, indicating its transient activation (Fig. 5 **A**). On the other hand, p62 and total LC3, measured as the ratio LC3-II/I, showed a main effect of treatment relative to control as some increases in content occurred after 48 hours ($P<0.05$; Fig. 5 **B**, **C**).

To fortify whether UroA could activate mitophagy, we measured mitophagy flux. Western blots of cytoplasmic and mitochondrial fractions probing for p62 and total LC3 were conducted following 24 and 48 hours of UroA-Bafilomycin A or vehicle treatment (Fig. 6 **A**, **B**). The ratio of LC3-II/I for each condition at 24 and 48 hours showed a main effect of UroA, as well as an interaction effect between time, UroA, and BafA (Fig 6. **C**). A marked 50% increase in mitophagy flux was evident at 24 hours (Fig. 6 **E**). Interestingly, p62 mitochondrial localization was increased by BafA and UroA, at 24 and 48 hours ($P<0.05$; Fig. 6 **D**). However, the increase in p62 flux as a result of UroA treatment was only apparent after 48 hours (Fig. 6 **F**). Overall, the data show modest increases in whole cell mitophagy markers, and considerable increases in mitophagy flux between 24 and 48 hours of treatment.

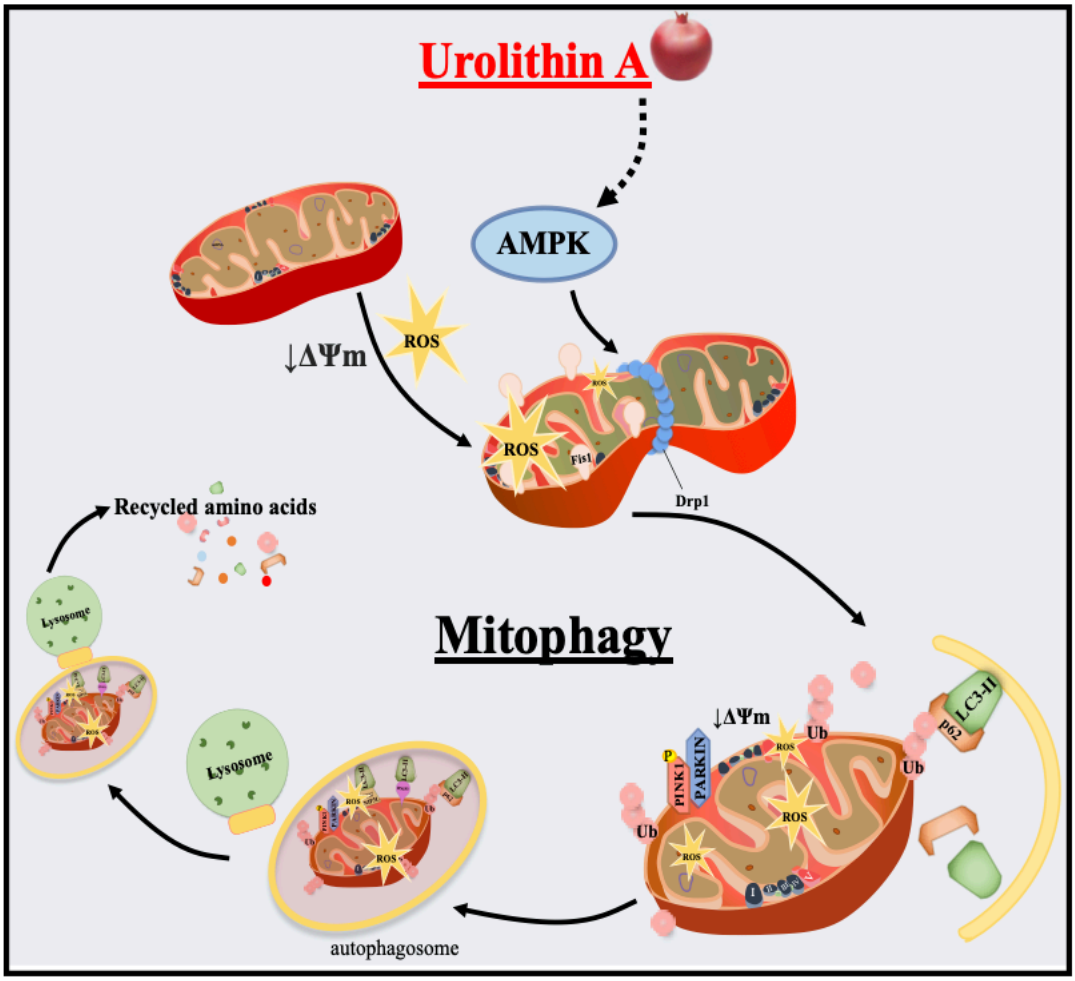

Fig 4. Schematic summarizing the documented function of Urolithin A.

AMPK is activated to cause fission and separate the stressed and poorly functioning region of the reticulum. Briefly, the mitochondrion is ubiquitinated and targeted by the adaptor protein p62, alongside simultaneous autophagosomal development, forming a growing vesicular phagophore. Embedded in this double-membrane vesicle is LC3-II, which anchors to p62 and facilitates the engulfment of the Ub-tagged mitochondrion. Microtubules then transport the occupied autophagosome to the lysosome for fusion and organelle degradation. Dotted line signifies potential steps in the pathway that have yet to be elucidated

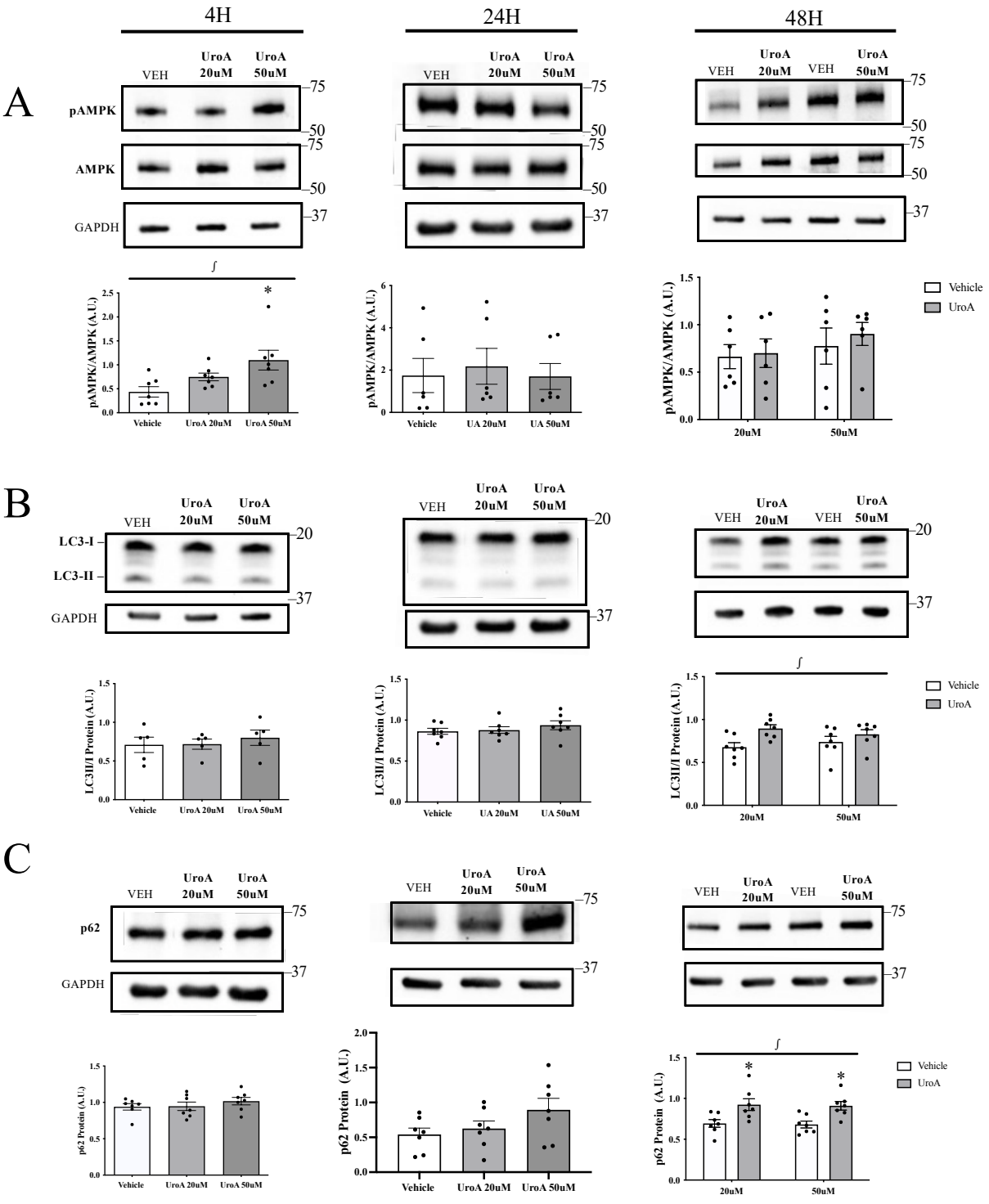

Fig 5. Whole cell mitophagy markers following Urolithin A treatment. Content of downstream proteins AMPK (A), LC3 (B), and p62 (C) respectively, typically involved in mitophagy mechanism, following each given time point. Time points 4h and 24h underwent one-way ANOVA and 48 h underwent two-way ANOVA, ∫P<0.05, main effect of treatment relative to control; *P<0.05, treatment vs. vehicle. *VEH,* Vehicle-treated cells with DMSO*; UroA,* Urolithin-A-treated cells. Values are means ± SEM.

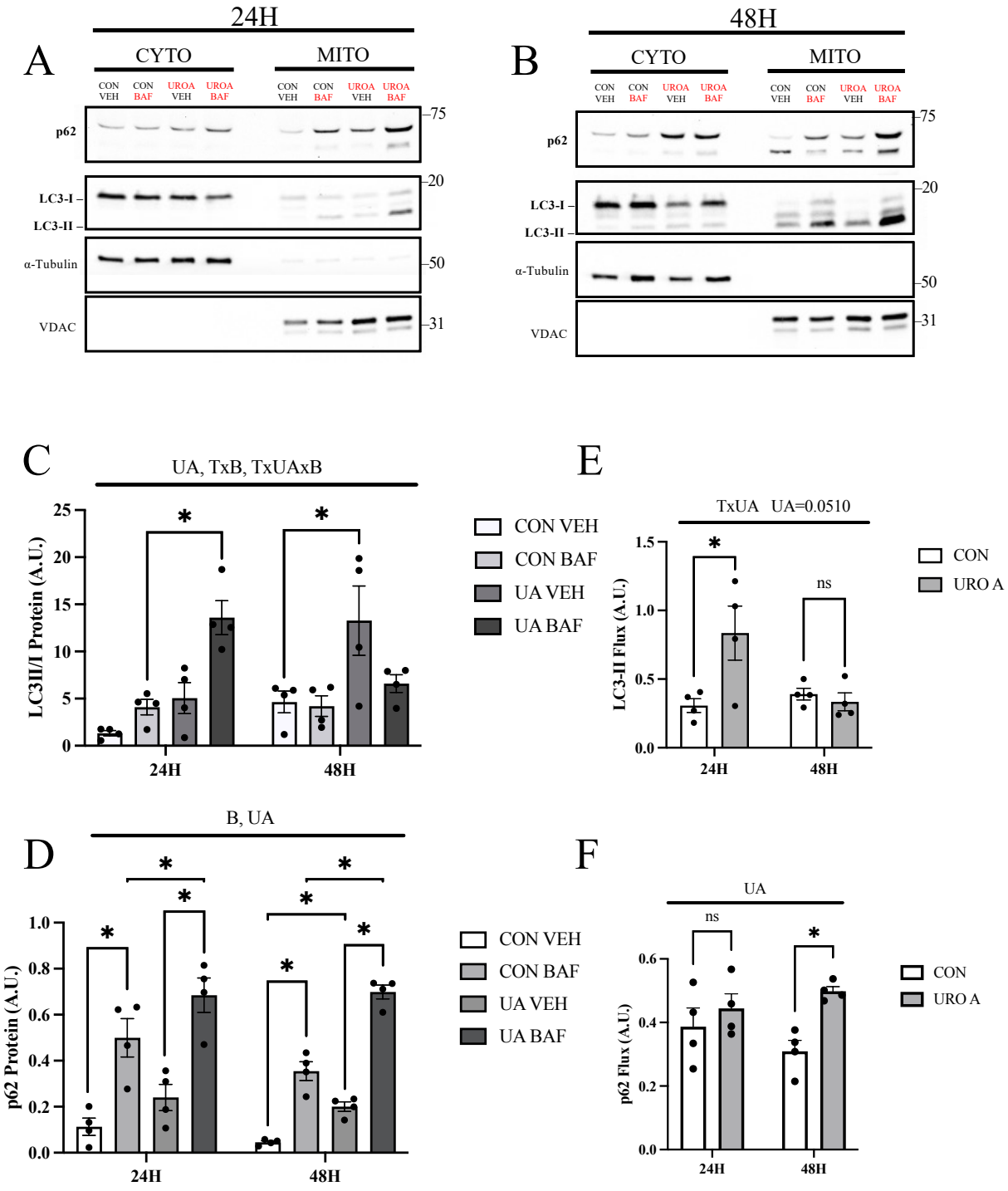

Fig 6. Mitophagy flux following Urolithin A and Bafilomycin A co-treatment. Western blots showing cytoplasmic and mitochondrial fractions following UroA (100 µM) and Baf (12 nM) co-treatment to assess mitochondrial targeting after 24 h (A) (*n*=4), and 48 h (B) (*n*=4). Mitophagy markers p62 (C) and LC3II/I ratio (D) alongside their respective p62 (E) and LC3-II (F) flux measurements were assessed to determine mitochondrial targeting for degradation (*n*=4) C, D: Three-way ANOVA between Time (T), Bafilomycin A (B), Urolithin A (UA) and E, F: Two-way ANOVA between Time (T) and Urolithin A (UA). C-E: Main effects at $P<0.05$; 'x' between conditions signifies interaction effects. *$P<0.05$, t-tests between indicated conditions. Values are means ± SEM.

ZLN005 increases TFAM promoter activity, suggesting increased PGC-1α nuclear localization. ZLN005 has been reported to increase PGC-1α expression, and therefore we speculated that it could induce mitochondrial biogenesis in C2C12 myotubes (Fig. 1 **C**). We used 10 or 20 μM concentrations to investigate changes in relevant proteins at 24 and 48 hours of treatment.

In contrast to previous reports [16-17], we were unable to confirm that ZLN could activate AMPK on increased PGC-1α at either 24 or 48 hours (Fig. 6 **A**-**D**). Nonetheless, the agent displayed some promise when we investigated the promoter activity of mitochondrial transcription factor A (TFAM), following Lipofectamine-mediated transfection of a TFAM promoter-luciferase reporter. After promoter transfection and 24 hours of ZLN treatment, a two-way ANOVA (P<0.05) revealed a main effect of both promoter and ZLN, as well as an interaction effect. This significance is attributed to the approximately 40% increase in luciferase protein content compared to that of empty vector-treated cells (Fig 6 **E**, **F**). Additionally, luciferase content corrected for empty vector results (PROM-EV) fortify the 40% increase that was observed (Fig. 6 **G**). Overall, while conclusive evidence that ZLN005 is an activator of mitochondrial biogenesis in C2C12 muscle and its time-dependent effects have yet to be uncovered, we believe that it shows promise as a result of its capacity to increase TFAM promoter activity.

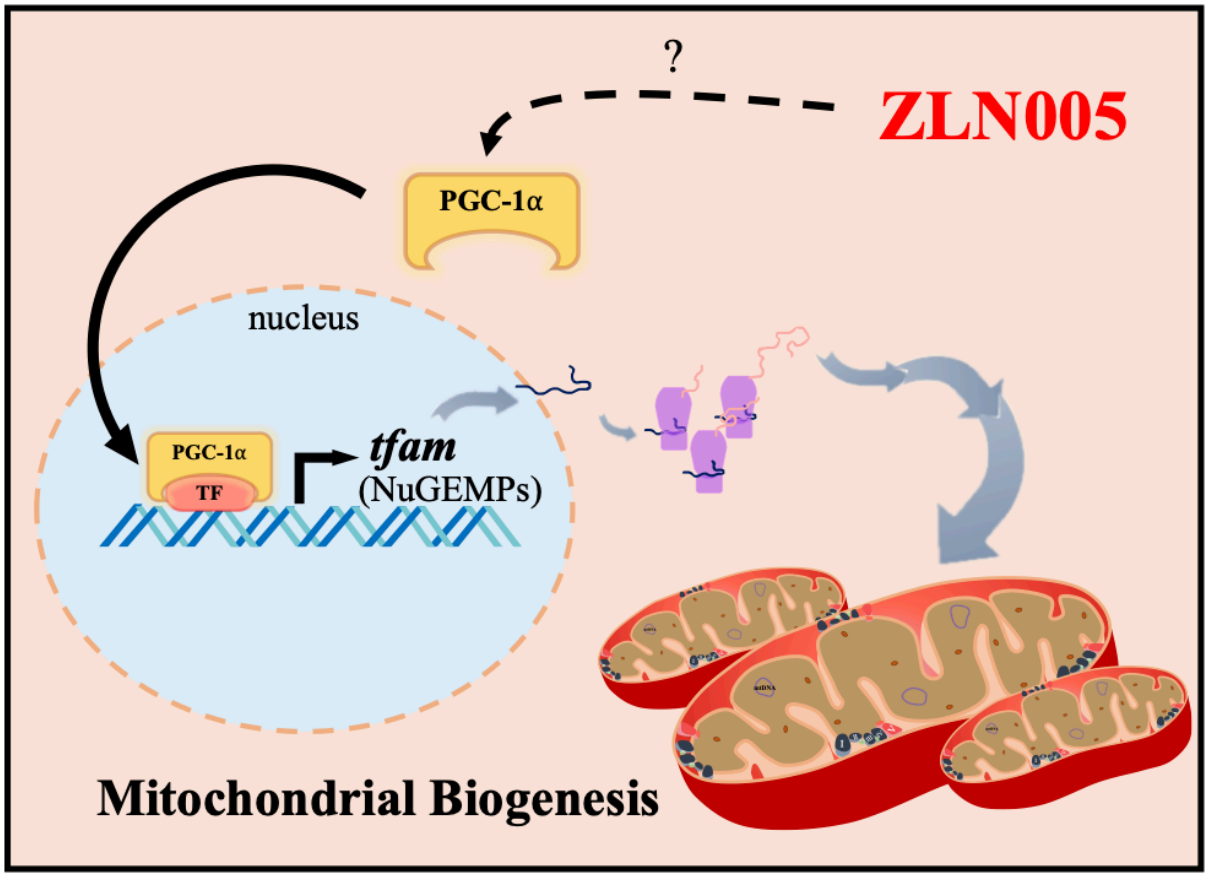

Fig 7. Schematic summarizing the documented function of ZLN005.

ZLN005 has been shown to increase PGC-1α nuclear localization. This initiates the transcriptional co-activation of nuclear genes encoding mitochondrial proteins, such as TFAM. Following their relevant translation and post-translational modifications, TFAM can thus bind to mtDNA to activate transcription of mitochondrially-encoded genes, which contribute to mitochondrial biogenesis. Dotted line signifies potential steps in the pathway that have yet to be elucidated.

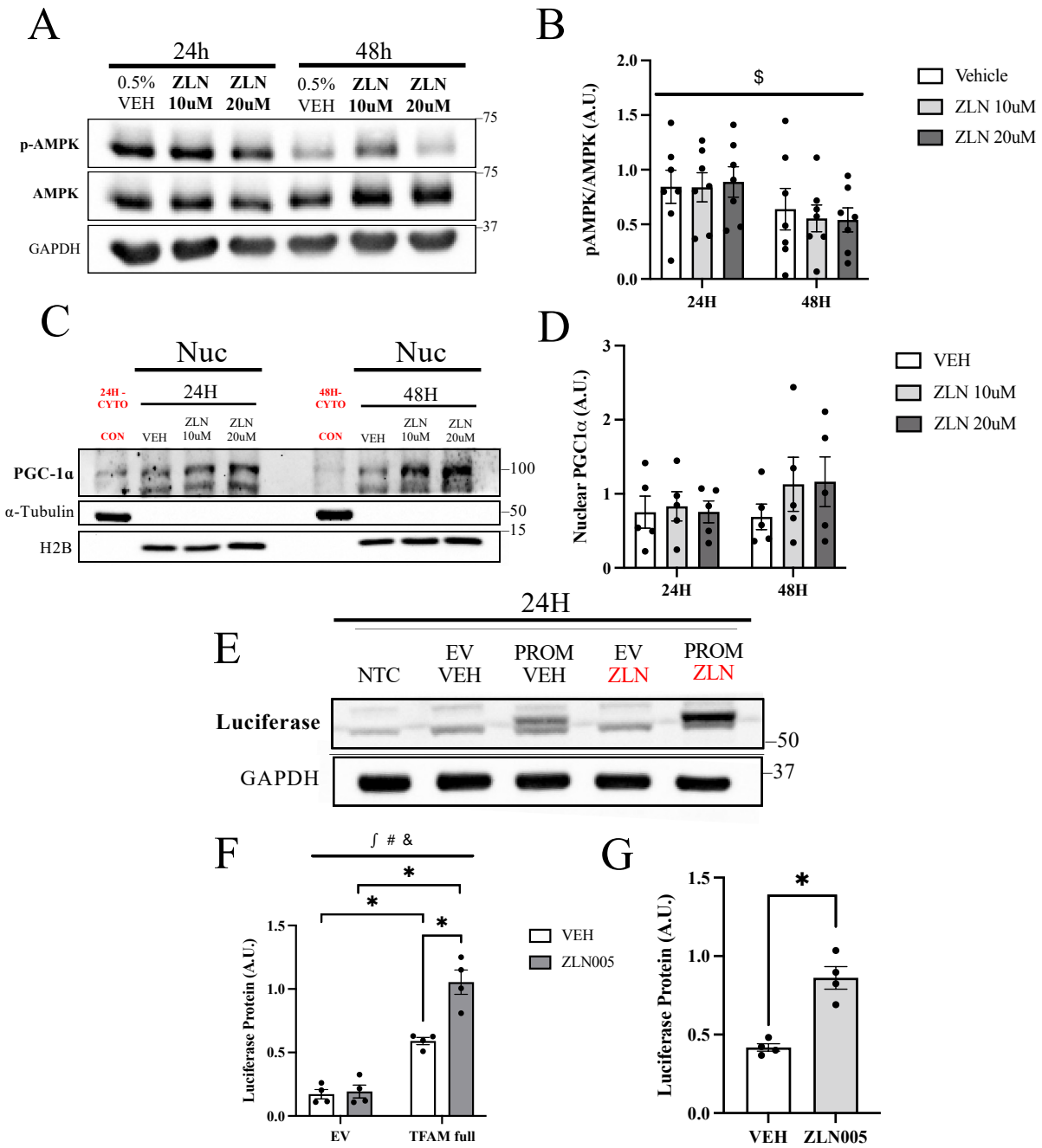

Fig 8. Analyzing the impact of ZLN005 on the drive for mitochondrial biogenesis. A: Western blot investigating whether the drive for biogenesis initiates with AMPK, tentative data are shown at 24 and 48 h (n=7). B: Corresponding quantification of pAMPK/AMPK ratio; One-way ANOVA, \$$P$<0.05, main effect of time. C: Western blot investigating nuclear PGC-1α following ZLN treatment (n=5). D. Corresponding quantification of PGC-1α localization following 24 and 48 h of treatment. E: ZLN inhibits luciferase activity, thus requiring the assessment of TFAM promoter activity to be assessed by probing for luciferase protein content. Promoter-transfected cells treated with ZLN after 24 h were assessed (n=4). F: Corresponding Luciferase quantification; two-way ANOVA, ∫P<0.05, main effect of treatment; #P<0.05, main effect of promoter; &P<0.05, interaction effect between promoter and treatment; *P<0.05, t-test between indicated conditions. Values are means ± SEM.

DISCUSSION

Mitochondria are vital for their roles in the maintenance of cellular metabolic homeostasis. The rationale for this study was to add to the continued characterization of important mechanisms dedicated to refreshing the mitochondrial pool in skeletal muscle by examining the time-dependent changes in three important arcs of mitochondrial turnover. These are mitochondrial biogenesis, mitophagy, and antioxidant capacity. Unlike the ubiquitous capacity for exercise to simultaneously activate these pathways, we used three different agents that have been reported to activate each associated pathway in order to differentiate between the cascading events that take place for organelle turnover: namely, Sulforaphane, Urolithin A, and ZLN005.

Previous reports have found that SFN activated antioxidant enzymes through the Nrf-2/Keap-1/ARE pathway [8-10], leading to important findings with chemoprevention and improvements to health within neurodegenerative diseases. Briefly, SFN aids in the cysteine modification of multiple residues on the Keap-1 homodimer, which enables nascent Nrf-2 to bypass its negative regulation and accumulate in the nucleus. Nuclear Nrf-2 then binds to ARE enhancer sequences on the promoter region of multiple target genes such as *NQO1* and *HMOX1*, resulting in their transcription [7]. A growing body of literature is documenting the use of SFN as it improves insulin sensitivity and frailty with aging in skeletal muscle [20]. To explore the time-dependent changes in SFN-mediated Nrf-2-ARE activation in our *in vitro* model of skeletal muscle, we treated C2C12 myotubes with two concentrations of SFN and analyzed markers of the Nrf-2-ARE mechanism after 4, 24, and 48 h. Not only does SFN increase Nrf-2 protein content, but it also permits nuclear localization of the transcription factor, which likely initiates the cascading events for Nrf-2/ARE-mediated antioxidant capacity. With respect to Keap 1 content, we did not expect any reciprocal events where an upregulation of nascent Nrf-2 would result in a downregulation of Keap 1. However, we

observed a main effect of time, where reductions in content were observed at 24 h compared to the other time points. Previous studies have shown that Keap 1 degradation likely takes place through the autophagy system [25-26], unlike Nrf-2 which is regularly degraded by the ubiquitin proteasome system. However, Nrf-2-mediated antioxidant activation has been reported to initiate the autophagy system [27] as well, which may attribute to the partial declines in Keap 1 content 24 hours post-induction with SFN. It is unclear whether this renders a positive feedback loop, where autophagy-mediated degradation of inactive Keap 1 also results in further activation of nascent Nrf-2. However, SFN has been demonstrated to activate autophagy where p62 competes with Nrf-2-Keap1 binding [27], suggesting a strong relationship between the antioxidant and autophagy systems as a result of SFN action.

Nrf-2 is a transcription factor that directly regulates the gene expression of antioxidant enzymes which promote the preservation of mitochondria. Thus, following Nrf-2 nuclear localization, we expected changes in the antioxidant enzymes NAD(P)H:quinone acceptor oxidoreductase (NQO1) and heme oxygenase-1 (HO-1). Consistent with the hypothesis surrounding the effect of time on upstream and downstream protein content, NQO1 increased in content starting at 24 h of treatment. Previous studies [28-29] have identified the role of NQO1 as a protective enzyme which adds complexity to “intrinsically disordered proteins” (IDP) that are regularly degraded by the 20S proteasomal system due to their intrinsic unfolded composition. PGC-1α has been identified as an IDP, and as a result, NQO1 in the presence of NADH can bind and allow the co-transcriptional regulator to bypass the proteasome and undergo the necessary post translational modifications that promote its nuclear localization and activity. While we currently do not show direct evidence to suggest NQO1 carries out this protective function, we found that by 48 hours, increased COX IV occurred, suggesting a crosstalk between the antioxidant and mitochondrial biogenesis mechanisms. Furthermore, it has been shown that Nuclear Respiratory Factors-1 (NRF1) and -2 (NRF2) contain promoter

AREs which are recognized by Nrf-2 [30]. Since NRFs are positive regulators of nuclear gene-encoded mitochondrial proteins (NuGEMPs) [1,31,32], it is possible that SFN-induced Nrf-2 activation may result in mitochondrial biogenesis via this mechanism.

Additionally, HO-1 has been reported to mediate many protective mechanisms, including mitochondrial quality control [33, and anti-inflammation [34], which were reported in the heart and cardiovasculature. The skeletal muscle-specific HO-1 animal demonstrated impairments in aerobic performance in these rats as a glycolytic phenotype was reached. That is, reduced cross-sectional area as a result of increased muscle atrophy in addition to increase mitochondrial fragmentation and reduced citrate synthase activity as an indication of mitochondrial dysfunction [35]. HO-1, in the context of skeletal muscle, serves as a neutralizer of free heme released into the muscle and plasma following microtrauma. Interestingly, the response in HO-1 protein content came as early as 4 h of SFN treatment and was maintained at 24 and 48 h. This demonstrates that, while SFN increases in HO-1 content, it is possible that the early increase of this protein occurs through an Nrf-2/ARE-independent manner, the evidence for this is that when mutations in a repressor of the HO-1 gene, Bach1, were examined in an Nrf-2-null phenotype, these mice still showed increased HO-1 expression, suggesting that it can be reliant on other activators [36]. Our data clearly show that increased HO-1 content is dependent on SFN treatment, but further investigation is required to examine its relationship with Nrf-2-mediated transcription, its earlier expression, and its relevance to cytoprotection.

The important complement to organellular production is also its efficient removal via mitophagy, to sustain a consistently healthy mitochondrial phenotype. Urolithin A has been shown to induce mitophagy in an AMPK-dependent manner, followed by the induction of mitophagy-related proteins including LC3-II and p62, in *C. elegans*, C2C12 myoblasts, rodent models, and middle-aged and elderly human subjects [11-15]. However, some of these data

remain unconvincing with respect to mitochondria-specific (mitophagy) flux [11,15], an indicator of increased mitochondrial targeting for degradation. It is prudent to present strong data on this front to fortify the efficacy of UroA as a mitophagy activator. Beginning with whole cell examination, we observed increased phospho-AMPK after 4 hours of treatment (Fig. 5 **A**), despite previous findings after 24 hours [11]. Further, while the downstream mitophagy markers p62 and LC3-II also increased significantly by 48 h, their change appeared modest compared to control levels. Through co-treatment with BafA followed by mitochondrial isolation, we were able to showcase its ability to activate mitophagy as we observed increased LC3-II and p62 flux. However, these increases occurred at 24 or at 48 hours, respectively (Fig. 6). While additional investigation is required to add to the efficacy of UroA, we can plainly suggest that based on our findings, it can increase mitophagy flux.

As we have determined candidates for antioxidant capacity and mitophagy, we wished to include an agent that might directly contribute to mitochondrial biogenesis, thus covering each approach towards mitochondrial homeostasis. Data mining and consultation of the literature uncovered the small molecule, ZLN005 [16]. It has been reported to activate the master regulator of mitochondrial biogenesis, PGC-1α, by facilitating its nuclear translocation through the upstream master regulator of cell metabolism, AMPK [16]. However, our data showed no significant changes with drug treatment, nor discernible differences with time with respect to phospho-AMPK activation. A 4-hour timepoint has not been used to investigate changes in AMPK as of yet. We acknowledge that ZLN and UroA have both been presented as activators of their relevant pathways through AMPK but identified differently as contributors to cellular metabolism. This master regulator of cellular homeostasis has been shown to regulate mitochondrial biogenesis, mitochondrial fission, and mitophagy activation [1]. Recent evidence has also shown that pools of AMPK bind to mitochondria directly as they modulate mitochondrial fate [37]. As a result, it is useful to investigate the effects of these

AMPK activators on other mitochondria-related pathways to determine why they are recognized for one particular function or mechanism.

While we used nuclear fractions after 4, 24, and 48 hours of ZLN treatment, we were unable to establish its role as a PGC-1α activator within nuclear fractions. However, we used a promoter-reporter of TFAM, a known PGC-1α co-transcriptional target [38], as a surrogate measure of an increased drive for mitochondrial biogenesis upstream. Despite lack of changes observed with time following ZLN treatment on AMPK or PGC-1α, a marked 2-fold increase in luciferase content following a transient transfection with a TFAM promoter was observed within a 24-hour time point (Fig. 8 **F**, **G**). We hope to continue fortifying the role of ZLN as an activator of mitochondrial biogenesis via PGC-1α by adding downstream mitochondrial markers borne of TFAM transcription such as COX I or IV.

CONCLUSIONS

Altogether, our results indicate that the agents SFN, UroA, and ZLN increase proteins affiliated with the three overarching mechanisms of mitochondrial turnover in a time-dependent manner. Early time points involve the activation of upstream mechanisms of action with respect to kinase phosphorylation, nuclear translocation, and transcriptional activity, whereas later time points represent the increased activity in their associated downstream markers. Continued characterization of these agents in our *in vitro* model is required to sufficiently report on their specificity for mitochondrial biogenesis, mitophagy, or antioxidant capacity. Overall, this research sets the stage for future work that can illuminate their utility as preservers of mitochondrial health in skeletal muscle.

REFERENCES

1. Hood, D. A., Memme, J. M., Oliveira, A. N., & Triolo, M. (2019). Maintenance of skeletal muscle mitochondria in health, exercise, and aging. *Annual Review of Physiology*, *81*(1), 19-41. https://doi.org/10.1146/annurev-physiol-020518-114310
2. Ljubicic, V., & Hood, D. A. (2009). Diminished contraction-induced intracellular signaling towards mitochondrial biogenesis in aged skeletal muscle. *Aging Cell*, *8*(4), 394-404. https://doi.org/10.1111/j.1474-9726.2009.00483.x
3. Ljubicic, V., Joseph, A., Adhihetty, P. J., Huang, J. H., Saleem, A., Uguccioni, G., & Hood, D. A. (2009). Molecular basis for an attenuated mitochondrial adaptive plasticity in aged skeletal muscle. *Aging*, *1*(9), 818-830. https://doi.org/10.18632/aging.100083
4. Hood, D. A., Uguccioni, G., Vainshtein, A., & D'souza, D. (2011). Mechanisms of exercise-induced mitochondrial biogenesis in skeletal muscle: Implications for health and disease. *Comprehensive Physiology*, 1119-1134. https://doi.org/10.1002/cphy.c100074
5. Chen, C. C., Erlich, A. T., & Hood, D. A. (2018). Role of Parkin and endurance training on mitochondrial turnover in skeletal muscle. *Skeletal Muscle*, *8*(1). https://doi.org/10.1186/s13395-018-0157-y
6. Holloszy, J. O., & Coyle, E. F. (1984). Adaptations of skeletal muscle to endurance exercise and their metabolic consequences. *Journal of Applied Physiology*, *56*(4), 831-838. https://doi.org/10.1152/jappl.1984.56.4.831
7. Yamamoto, M., Kensler, T. W., & Motohashi, H. (2018). The KEAP1-NRF2 system: A thiol-based sensor-effector apparatus for maintaining redox homeostasis. *Physiological Reviews*, *98*(3), 1169-1203. https://doi.org/10.1152/physrev.00023.2017
8. Li, D., Shao, R., Wang, N., Zhou, N., Du, K., Shi, J., Wang, Y., Zhao, Z., Ye, X., Zhang, X., & Xu, H. (2020). Sulforaphane activates a lysosome-dependent transcriptional program to mitigate oxidative stress. *Autophagy*, *17*(4), 872-887. https://doi.org/10.1080/15548627.2020.1739442
9. Malaguti, M., Angeloni, C., Garatachea, N., Baldini, M., Leoncini, E., Collado, P. S., Teti, G., Falconi, M., Gonzalez-Gallego, J., & Hrelia, S. (2009). Sulforaphane treatment protects skeletal muscle against damage induced by exhaustive exercise in rats. *Journal of Applied Physiology*, *107*(4), 1028-1036. https://doi.org/10.1152/japplphysiol.00293.2009
10. Moon, J. Y., Kim, D. J., & Kim, H. S. (2020). Sulforaphane ameliorates serum starvation-induced muscle atrophy via activation of the Nrf2 pathway in cultured C2C12 cells. *Cell Biology International*, *44*(9), 1831-1839. https://doi.org/10.1002/cbin.11377
11. Ryu, D., Mouchiroud, L., Andreux, P. A., Katsyuba, E., Moullan, N., Nicolet-dit-Félix, A. A., Williams, E. G., Jha, P., Lo Sasso, G., Huzard, D., Aebischer, P., Sandi, C., Rinsch, C., & Auwerx, J. (2016). Urolithin a induces mitophagy and prolongs lifespan in C. elegans and increases muscle function in rodents. *Nature Medicine*, *22*(8), 879-888. https://doi.org/10.1038/nm.4132
12. Luan, P., D'Amico, D., Andreux, P. A., Laurila, P., Wohlwend, M., Li, H., Imamura de Lima, T., Place, N., Rinsch, C., Zanou, N., & Auwerx, J. (2021). Urolithin a

improves muscle function by inducing mitophagy in muscular dystrophy. *Science Translational Medicine*, *13*(588). https://doi.org/10.1126/scitranslmed.abb0319
13. Andreux, P. A., Blanco-Bose, W., Ryu, D., Burdet, F., Ibberson, M., Aebischer, P., Auwerx, J., Singh, A., & Rinsch, C. (2019). The mitophagy activator urolithin a is safe and induces a molecular signature of improved mitochondrial and cellular health in humans. *Nature Metabolism*, *1*(6), 595-603. https://doi.org/10.1038/s42255-019-0073-4
14. Liu, S., D'Amico, D., Shankland, E., Bhayana, S., Garcia, J. M., Aebischer, P., Rinsch, C., Singh, A., & Marcinek, D. J. (2022). Effect of Urolithin a supplementation on muscle endurance and mitochondrial health in older adults. *JAMA Network Open*, *5*(1), e2144279. https://doi.org/10.1001/jamanetworkopen.2021.44279
15. D'Amico, D., Olmer, M., Fouassier, A. M., Valdés, P., Andreux, P. A., Rinsch, C., & Lotz, M. (2022). Urolithin a improves mitochondrial health, reduces cartilage degeneration, and alleviates pain in osteoarthritis. *Aging Cell*, *21*(8). https://doi.org/10.1111/acel.13662
16. Zhang, L., Zhou, H., Fu, Y., Li, Y., Wu, F., Gu, M., Wu, L., Xia, C., Dong, T., Li, J., Shen, J., & Li, J. (2013). Novel small-molecule PGC-1α transcriptional regulator with beneficial effects on diabetic *db/db* mice. *Diabetes*, *62*(4), 1297-1307. https://doi.org/10.2337/db12-0703
17. Liu, Y., Bai, H., Guo, F., Thai, P. N., Luo, X., Zhang, P., Yang, C., Feng, X., Zhu, D., Guo, J., Liang, P., Xu, Z., Yang, H., & Lu, X. (2020). PGC-1α activator ZLN005 promotes maturation of cardiomyocytes derived from human embryonic stem cells. *Aging*, *12*(8), 7411-7430. https://doi.org/10.18632/aging.103088
18. Russo, M., Spagnuolo, C., Russo, G. L., Skalicka-Woźniak, K., Daglia, M., Sobarzo-Sánchez, E., Nabavi, S. F., & Nabavi, S. M. (2017). Nrf2 targeting by sulforaphane: A potential therapy for cancer treatment. *Critical Reviews in Food Science and Nutrition*, *58*(8), 1391-1405. https://doi.org/10.1080/10408398.2016.1259983
19. Bahn, G., Park, J., Yun, U. J., Lee, Y. J., Choi, Y., Park, J. S., Baek, S. H., Choi, B. Y., Cho, Y. S., Kim, H. K., Han, J., Sul, J. H., Baik, S., Lim, J., Wakabayashi, N., Bae, S. H., Han, J., Arumugam, T. V., Mattson, M. P., … Jo, D. (2019). NRF2/ARE pathway negatively regulates BACE1 expression and ameliorates cognitive deficits in mouse Alzheimer's models. *Proceedings of the National Academy of Sciences*, *116*(25), 12516-12523. https://doi.org/10.1073/pnas.1819541116
20. Yan, X., Shen, Z., Yu, D., Zhao, C., Zou, H., Ma, B., Dong, W., Chen, W., Huang, D., & Yu, Z. (2022). Nrf2 contributes to the benefits of exercise interventions on age-related skeletal muscle disorder via regulating Drp1 stability and mitochondrial fission. *Free Radical Biology and Medicine*, *178*, 59-75. https://doi.org/10.1016/j.freeradbiomed.2021.11.030
21. Lin, J., Wu, H., Tarr, P. T., Zhang, C., Wu, Z., Boss, O., Michael, L. F., Puigserver, P., Isotani, E., Olson, E. N., Lowell, B. B., Bassel-Duby, R., & Spiegelman, B. M. (2002). Transcriptional Co-activator PGC-1α drives the formation of slow-Twitch muscle fibres. *Nature*, *418*(6899), 797-801. https://doi.org/10.1038/nature00904
22. Bhattacharya, D., Oresajo, O., & Scimè, A. (2020). P107 mediated mitochondrial function controls muscle stem cell proliferative Fates. https://doi.org/10.1101/2020.09.29.317693

23. Mauvezin, C., & Neufeld, T. P. (2015). Bafilomycin A1 disrupts autophagic flux by inhibiting both V-atpase-dependent acidification and Ca-P60A/SERCA-dependent autophagosome-lysosome fusion. *Autophagy*, *11*(8), 1437-1438. https://doi.org/10.1080/15548627.2015.1066957
24. Collu-Marchese, M., Shuen, M., Pauly, M., Saleem, A., & Hood, D. (2015). The regulation of mitochondrial transcription factor a (Tfam) expression during skeletal muscle cell differentiation. *Bioscience Reports*, *35*(3). https://doi.org/10.1042/bsr20150073
25. Jain, A., Lamark, T., Sjøttem, E., Bowitz Larsen, K., Atesoh Awuh, J., Øvervatn, A., McMahon, M., Hayes, J. D., & Johansen, T. (2010). P62/SQSTM1 is a target gene for transcription factor NRF2 and creates a positive feedback loop by inducing antioxidant response element-driven gene transcription. *Journal of Biological Chemistry*, *285*(29), 22576-22591. https://doi.org/10.1074/jbc.m110.118976
26. Taguchi, K., Fujikawa, N., Komatsu, M., Ishii, T., Unno, M., Akaike, T., Motohashi, H., & Yamamoto, M. (2012). Keap1 degradation by autophagy for the maintenance of redox homeostasis. *Proceedings of the National Academy of Sciences*, *109*(34), 13561-13566. https://doi.org/10.1073/pnas.1121572109
27. Jiang, T., Harder, B., Rojo de la Vega, M., Wong, P. K., Chapman, E., & Zhang, D. D. (2015). P62 links autophagy and Nrf2 signaling. *Free Radical Biology and Medicine*, *88*, 199-204. https://doi.org/10.1016/j.freeradbiomed.2015.06.014
28. Tsvetkov, P., Adler, J., Strobelt, R., Adamovich, Y., Asher, G., Reuven, N., & Shaul, Y. (2021). NQO1 binds and supports SIRT1 function. *Frontiers in Pharmacology*, *12*. https://doi.org/10.3389/fphar.2021.671929
29. Adamovich, Y., Shlomai, A., Tsvetkov, P., Umansky, K. B., Reuven, N., Estall, J. L., Spiegelman, B. M., & Shaul, Y. (2013). The protein level of PGC-1α, a key metabolic regulator, is controlled by NADH-NQO1. *Molecular and Cellular Biology*, *33*(13), 2603-2613. https://doi.org/10.1128/mcb.01672-12
30. Piantadosi, C. A., Carraway, M. S., Babiker, A., & Suliman, H. B. (2008). Heme oxygenase-1 regulates cardiac mitochondrial biogenesis via nrf2-mediated transcriptional control of nuclear respiratory factor-1. *Circulation Research*, *103*(11), 1232-1240. https://doi.org/10.1161/01.res.0000338597.71702.ad
31. Zhang, Y., Uguccioni, G., Ljubicic, V., Irrcher, I., Iqbal, S., Singh, K., Ding, S., & Hood, D. A. (2014). Multiple signaling pathways regulate contractile activity-mediated PGC-1*α* gene expression and activity in skeletal muscle cells. *Physiological Reports*, *2*(5), e12008. https://doi.org/10.14814/phy2.12008
32. Chabi, B., Ljubicic, V., Menzies, K. J., Huang, J. H., Saleem, A., & Hood, D. A. (2008). Mitochondrial function and apoptotic susceptibility in aging skeletal muscle. *Aging Cell*, *7*(1), 2-12. https://doi.org/10.1111/j.1474-9726.2007.00347.x
33. Hull, T. D., Boddu, R., Guo, L., Tisher, C. C., Traylor, A. M., Patel, B., Joseph, R., Prabhu, S. D., Suliman, H. B., Piantadosi, C. A., Agarwal, A., & George, J. F. (2016). Heme oxygenase-1 regulates mitochondrial quality control in the heart. *JCI Insight*, *1*(2). https://doi.org/10.1172/jci.insight.85817
34. Araujo, J. A., Zhang, M., & Yin, F. (2012). Heme oxygenase-1, oxidation, inflammation, and atherosclerosis. *Frontiers in Pharmacology*, *3*. https://doi.org/10.3389/fphar.2012.00119

35. Alves de Souza, R. W., Gallo, D., Lee, G. R., Katsuyama, E., Schaufler, A., Weber, J., Csizmadia, E., Koch, L. G., Britton, S. L., Wisloff, U., Brum, P. C., & Otterbein, L. E. (2020). Skeletal muscle heme oxygenase-1 activity regulates aerobic capacity. *SSRN Electronic Journal*. https://doi.org/10.2139/ssrn.3671735
36. Gureev, A. P., Shaforostova, E. A., & Popov, V. N. (2019). Regulation of mitochondrial biogenesis as a way for active longevity: Interaction between the Nrf2 and PGC-1α signaling pathways. *Frontiers in Genetics*, *10*. https://doi.org/10.3389/fgene.2019.00435
37. Drake, J. C., Wilson, R. J., Laker, R. C., Guan, Y., Spaulding, H. R., Nichenko, A. S., Shen, W., Shang, H., Dorn, M. V., Huang, K., Zhang, M., Bandara, A. B., Brisendine, M. H., Kashatus, J. A., Sharma, P. R., Young, A., Gautam, J., Cao, R., Wallrabe, H., … Yan, Z. (2021). Mitochondria-localized AMPK responds to local energetics and contributes to exercise and energetic stress-induced mitophagy. *Proceedings of the National Academy of Sciences*, *118*(37). https://doi.org/10.1073/pnas.2025932118
38. Jannig, P. R., Dumesic, P. A., Spiegelman, B. M., & Ruas, J. L. (2022). SnapShot: Regulation and biology of PGC-1α. *Cell*, *185*(8), 1444-1444.e1. https://doi.org/10.1016/j.cell.2022.03.027

FUTURE DIRECTIONS

1. Inducing a knockdown or knockout model for upstream master regulators such as Nrf-2, AMPK, and/or PGC-1α can determine whether the effect of their corresponding agent can be upheld.
2. Investigating the crosstalk that may occur between pathways may demonstrate the secondary and tertiary effects of each agent. For example, given the report that NQO1 protects PGC-1alpha from proteasomal degradation-by-default, it may be that SFN treatment induces mitochondrial biogenesis. Furthermore, AMPK has been reported to activate both mitophagy and mitochondrial biogenesis, which may suggest the possibility that UroA does not solely activate mitophagy.
3. Despite the possibility of redundant activation of mechanisms that are secondary to those linked with each agent, combining them together in the form of a polypill may result in a wide-ranging approach to mitochondrial refreshment.
4. Similar to the previous, comparing the functional enhancements with these agents to the known improvements observed with exercise can also elucidate their proximity to metabolic mimicry. Thus, it may be worthwhile to investigate whether synergistic outcomes take place alone or in combination with exercise.

ACKNOWLEDGMENTS

This work was supported by funding from the Natural Sciences and Engineering Research Council of Canada (NSERC) to D.A. Hood. D.A. Hood is also the holder of a Canada Research Chair in Cell Physiology.

APPENDIX A: SAMPLE DATA AND STATISTICAL ANALYSES

Table 1 **A** – Whole cell Nrf-2 protein content following 4, 24, and 48 hours of SFN treatment

Nrf-2 Protein: 4, 24, 48 H						
N	VEH	4H	VEH	24H	VEH	48H
1	0.744574	1.596074	0.440467	0.814323	0.370057	0.642683
2	0.53296	1.314702	0.694103	0.986406	0.73498	0.795501
3	0.740066	1.98367	0.835902	1.538641	0.494166	0.960508
4	1.91661	4.140545	1.141438	2.042638	0.943026	1.555789
5	1.31804	3.342917	1.358722	2.09537	1.056737	1.08097
6	1.269848	2.201999	1.037918	2.356373	2.50361	2.608985
7	0.586177	0.797094	0.637043	1.118474	0.825621	1.177808
X	1.015468	2.196714	0.877942	1.564604	0.989742	1.260321
SEM	0.191153	0.442808	0.120629	0.230634	0.268147	0.250361

Ordinary One-Way Anova		
P Value	P Value Summary	Significant? ($P \leq 0.05$)
0.013	*	Yes
	Multiple Comparisons	
	P Value Summary	Significant? ($P \leq 0.05$)
VEH vs. 4 H	*	Yes
VEH vs. 24 H	-	No
VEH vs. 48 H	-	No

Table 1 **B** – Corresponding Fold-Above-Control for whole cell Nrf-2 protein at each time point.

Nrf-2 Protein: Fold-Above-Control			
N	4H	24H	48H
1	2.143607	1.84877	1.736713
2	2.466795	1.421123	1.082344
3	2.680398	1.840696	1.943696
4	2.160348	1.78953	1.649784
5	2.536279	1.542162	1.022932
6	1.734065	2.270288	1.042089
7	1.359817	1.755728	1.426572

Table 2 – Nuclear Fraction of Nrf-2 measured after 4 hours of SFN treatment.

Nrf-2 Nuclear Fraction: 4 H			
N	VEH	SFN 5uM	SFN 10uM
1	0.517167	0.742878	0.31891
2	0.183786	0.556687	0.594243
3	0.255269	0.681178	0.374447
X	0.318741	0.660248	0.4292
SEM	0.08776	0.047422	0.072802

Unpaired T-test		
P Value	P Value Summary	Significant? ($P \leq 0.05$)
0.0414	*	Yes

One-Way ANOVA		
P Value	P Value Summary	Significant? ($P \leq 0.05$)
0.0645	ns	Trending

Table 3 **A** – Whole cell Keap-1 protein content following 4, 24, and 48 hours of SFN treatment

Keap 1 Protein Content at every time point following SFN Treatment						
N	VEH	4H	VEH	24H	VEH	48H
1	1.061274	1.212812	1.346293	0.923928	1.031631	1.366784
2	1.052237	0.905489	1.028265	0.701836	1.212603	1.257672
3	0.886032	0.646494	0.795941	0.596718	1.009611	1.287916
X	0.999848	0.921598	1.056833	0.740828	1.084615	1.304124
SEM	0.056968	0.16368	0.159514	0.096448	0.064309	0.032524

Ordinary One-Way Anova		
P Value	P Value Summary	Significant? ($P \leq 0.05$)
0.0558	ns	Trending

	Multiple Comparisons	
	P Value Summary	Significant? ($P \leq 0.05$)
VEH vs. 4 H	-	No
VEH vs. 24 H	-	No
VEH vs. 48 H	-	No

Table 3 **B** – Corresponding Fold-Above-Control for whole cell Nrf-2 protein at each time point

Keap 1 Protein: Fold-Above-Control			
N	4H	24H	48H
1	1.142789	0.686276	1.324877
2	0.860537	0.682544	1.037167
3	0.729651	0.749702	1.275656

Table 4 – Example of calculations conducted for all 3 time points for proteins related to SFN, UroA, and ZLN treatment. Example procedure provided using NQO1.

NQO1	4H			24H		
N	VEH	SFN 5uM	SFN 10uM	VEH	SFN 5uM	SFN 10uM
1	0.64561	0.59948	0.71106	0.408444	1.062827	1.014737
2	0.683267	0.793032	0.63331	0.401568	1.015624	1.143274
3	0.345418	0.340808	0.434808	0.567636	1.444706	1.41701
4	0.570355	0.48496	0.513983	0.365908	1.302144	1.054499
5	0.44107	0.427789	0.376171	0.513717	1.515287	1.503237
6				0.557666	1.31444	1.341943
7				0.487479	1.211831	1.153706
X	0.537144	0.529214	0.533866	0.471774	1.266694	1.232629
SEM	0.063328	0.078192	0.061791	0.030363	0.069801	0.071146

Ordinary One-Way Anova: 24 H		
P Value	P Value Summary	Significant? ($P \leq 0.05$)
<0.0001	****	Yes

NQO1: 48 H	Vehicle							SFN						
SFN 5uM	0.301529	0.24351	0.366074	0.221458	0.324669	0.365054	0.626105	1.104478	0.949368	1.300835	1.278688	1.066881	1.169093	1.151152
SFN 10uM	0.24094	0.314965	0.293458	0.232474	0.356877	0.508627	0.667988	1.086959	1.231097	1.431768	1.594856	1.568274	2.739258	1.547516

Two-Way ANOVA: NQO1 48 H			
Source of Variation	P Value	P Value Summary	Significant? ($P \leq 0.05$)
Interaction	0.0649	ns	Trending
Concentration	0.0419	*	Yes
Treatment	<0.0001	****	Yes

Table 5 **A** – Mitophagy Flux Data for p62

p62 Mitophagy Flux													
	CON				X	SEM	URO A				X	SEM
24H	0.254445	0.526426	0.432378	0.334101	0.386838	0.059068	0.363921	0.458937	0.3878135	0.56729748	0.444492	0.04563809
48H	0.214565	0.376372	0.337856	0.308337	0.309283	0.034508	0.468269	0.501136	0.4861591	0.53749351	0.498264	0.01470097

Two-Way ANOVA: p62 Mitophagy Flux			
Source of Variation	P Value	P Value Summary	Significant? ($P \leq 0.05$)
Interaction	0.1419	ns	No
Time	0.7807	ns	No
Bafilomycin	0.0121	*	Yes

Table 5 **B** – Mitophagy Flux Data for LC3-II

LC3-II Mitophagy Flux												
	CON				X	SEM	URO A				X	SEM
24H	0.181949	0.406107	0.36893	0.270574	0.30689	0.050516	0.304691	1.2131	1.0300774	0.79300454	0.835218	0.19663977
48H	0.293028	0.500761	0.386744	0.383908	0.39111	0.042539	0.253512	0.320641	0.5216149	0.23993769	0.333926	0.06500251

Two-Way ANOVA: LC3-II Mitophagy Flux			
Source of Variation	P Value	P Value Summary	Significant? ($P \leq 0.05$)
Interaction	0.0195	*	Yes
Time	0.0791	ns	No
Bafilomycin	0.051	ns	No

Table 6 – NTC- and EV-corrected data of ZLN-induced increases in TFAM promoter activity

ZLN005 TFAM PROM-EV corrected for Non-Transfected Control		
N	**VEH**	**ZLN005**
1	0.400242	0.896469
2	0.42338	1.035104
3	0.481945	0.690175
4	0.368199	0.824179
X	0.418442	0.861482
SEM	0.024001	0.071941

Unpaired T-test		
P Value	P Value Summary	Significant? ($P \leq 0.05$)
0.0011	**	Yes

APPENDIX B: SUPPLEMENTAL DATA

Image – Crystal Violet Staining. Diagnostic of cell viability for each treatment and corresponding concentrations using crystal violet staining assay.

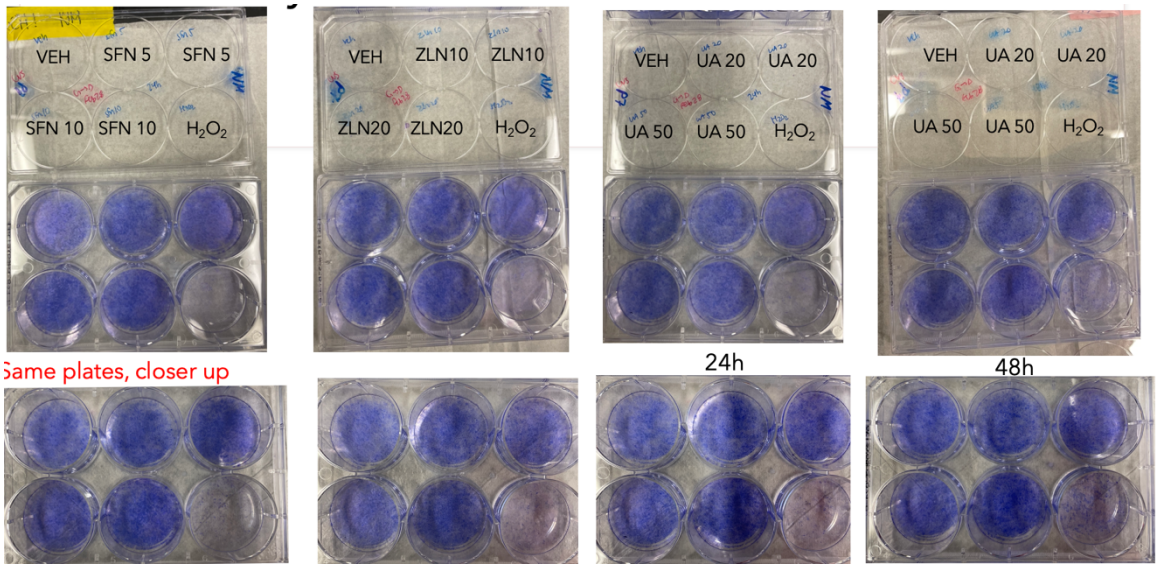

Table 1 – Luminescence reading of dual luciferase reporter assay following treatment with SFN, UroA, and ZLN005. ZLN has been reported to inhibit luciferase activity.

TFAM full transfection + treatment - SFN 5uM, UroA 50uM, ZLN 20uM - 24hTx - N1 - Jan2,22

D	SPL1	SPL2	SPL3		Well ID	
	7350	8488	2057		Luciferase activity:Lum	
	4	4	6		Renilla Activity:Lum	
	1837.5	2122	342.833		Firefly/Renilla ratio	
E	SPL4	SPL5	SPL6		Well ID	
	28	44	27		Luciferase activity:Lum	
	3	6	4		Renilla Activity:Lum	
	9.333	7.333	6.75		Firefly/Renilla ratio	
F	SPL7	SPL8	SPL9	SPL10	Well ID	
	23	11769	5	43	Luciferase activity:Lum	
	3	6	3	2	Renilla Activity:Lum	
	7.667	1961.5	1.667	21.5	Firefly/Renilla ratio	

Well ID	Name	Well	Luciferase activity:Lum	Renilla Activity:Lum	Firefly/Renilla ratio
SPL1	PROM veh	D1	7350	4	1837.5
SPL2	PROM SFN 5	D2	8488	4	2122
SPL3	PROM UroA 50	D3	2057	6	342.833
SPL4	EV VEH	E1	28	3	9.333
SPL5	EV SFN 5	E2	44	6	7.333
SPL6	EV UroA 50	E3	27	4	6.75
SPL7	VEH EV	F1	23	3	7.667
SPL8	VEH PROM	F2	11769	6	1961.5
SPL9	EV ZLN 20	F3	5	3	1.667
SPL10	PROM ZLN 20	F4	43	2	21.5

		sfn 5		uroA 50		zln 20	
		veh	tx	veh	tx	veh	tx
TFAM full	EV	9.333	7.333	9.333	6.75	7.667	1.667
	PROM	1837.5	2122	1837.5	342.833	1961.5	21.5
	Ratio	196.882	289.3768	196.882	50.79007	255.8367	12.89742

APPENDIX C: LABORATORY METHODS AND PROTOCOLS

Western/Immunoblotting Procedure

SDS POLYACRYLAMIDE GEL ELECTROPHORESIS (SDS-PAGE) PROTEAN BIO-RAD SYSTEM

Reagents

1. Acrylamide/Bis-Acrylamide, 30% Solution 37.5:1 (BioShop 10.502)
    a. Store at 4°C
2. Under Tris Buffer
    a. 1M Tris-HCl, pH 8.8 (60.5g/500ml)
    b. Store at 4°C
3. Over Tris Buffer
    a. 1M Tris-HCl, pH 6.8 (12.1g/100ml)
    b. Bromophenol Blue (for colour)
    c. Store at 4°C
4. Ammonium Persulfate (APS)
    a. 10% (w/v) APS in ddH_20 (1g/10ml)
    b. Stored at 4°C
5. Sodium Dodecyl Sulfate (SDS)
    a. 10% (w/v) in ddH_20 (1g/10ml)
    b. Store at room temperature
6. TEMED (Sigma T-9281)
7. Electrophoresis Buffer, pH 8.3 (10L)
    a. 25mM Tris 30.34g, 192mM Glycine 144g, 0.1% SDS 10g
    b. Volume to 10L with ddH_20
    c. Store at room temperature
8. 6X SDS
    a. Warm 100% glycerol in water bath at 65°C for 30 minutes
    b. Combine 1.2g SDS, 0.06g Bromophenol Blue, 3mls of 1M Tris, pH 6.8 and 1ml of ddH_20 and stir at 4°C for 5 minutes
    c. Add 3mls of 100% glycerol, stir and aliquot mixture.
    d. Store at -20°C
    e. Add 5% (v/v) ß-mercaptoethanol (Sigma M6250) to 6X SDS <u>just prior</u> to use
9. *tert*-Amyl alcohol ReagentPLus, 99% (Sigma 152463)

Procedure

1. **Prepare electrophoresis rack:**
    a. Clean glass plates thoroughly with soap followed by 95% ethanol then ddH_20.
    b. Dry carefully with a kimwipe.

c. Assemble glass plates as shown below:

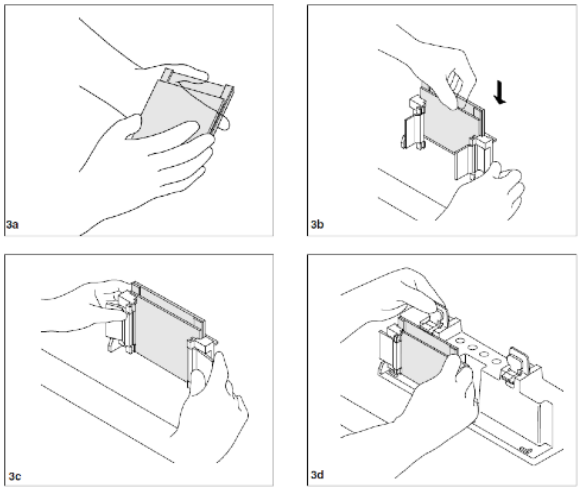

d. Check the seal y adding a small volume of ddH_20 then pour off and let dry.

2. Prepare separating gels:

a. Mini Protean 3 Bio-Rad System volumes:

	8%	**10%**	**12%**	**15%**	**18%**
Acrylamide	2.7 ml	3.3 ml	4.0 ml	5.0 ml	6.0 ml
ddH_20	4.1 ml	3.5 ml	2.8 ml	1.8 ml	0.8 ml
Under Tris	3.0 ml	3.0 ml	3.0 ml	3.0 ml	3.0 ml
SDS	100µl	100µl	100µl	100µl	100µl
APS	100µl	100µl	100µl	100µl	100µl
TEMED	10µl	10µl	10µl	10µl	10µl

b. Mix the contents of the separating gel without adding APS or TEMED. Stir.
c. Add APS and TEMED. Stir.
d. Slowly pour the entire volume of the solution into the space between the two plates while keeping plates tilted to prevent bubble formation.
e. Add *tert*-Amyl alcohol to coat top surface of gel solution.
f. Allow 30 minutes for gel polymerization.
g. Remove *tert*-Amyl alcohol by pouring it off and remove any remainder with a kimwipe. Rinse with ddH_20.

3. **Prepare stacking gel:**
    a. For a single mini gel use the following volumes:

Acrylamide	500 µl
Over Tris	625 µl
ddH_20	3.75 ml
SDS	50 µl
APS	50 µl
TEMED	7.5 µl

    b. Mix the contents of the stacking gel without adding APS or TEMED. Stir.
    c. Add APS and TEMED. Stir.
    d. Using a Pasteur pipette slowly add the entire volume from the beaker in between the plates.
    e. Add comb for desired number of wells.
    f. Allow 30 minutes for gel polymerization.

4. **Prepare samples:**
    a. Turn of the block heater to 95ºC.
    b. Pipette required volume of sample into new eppendorf with 6X SDS (1 volume of sample to 1/6 sample volume of 6X SDS). Keep samples on ice until all samples are prepared.
    c. Briefly spin each sample to bring volume to the bottom of the eppendorf.
    d. Incubate each sample at 95 ºC for 5 minutes in the heating block to denature the proteins.
    e. Briefly spin again to return volume to the bottom of the eppendorf.

5. **Assemble Mini-PROTEAN gel caster system:**
    a. See images below:

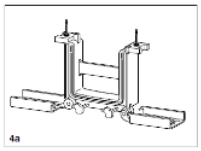

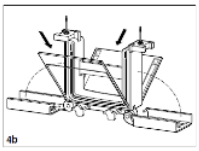

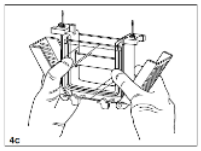

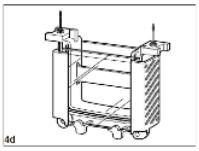

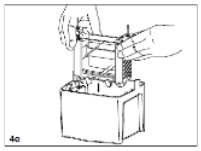

b. If you are only running one gel a plastic rectangular pseudo plate must be clamped on the other side of the caster.
c. Fill with electrophoresis buffer between the plates and outside of the plates in the chamber.
d. Slowly remove the comb using both hands (one on each side) by pulling the comb straight upwards.
e. Fix any wells that are deformed using a small spatula.
f. Clean out the wells using a syringe filled with electrophoresis buffer.
g. Withdraw the entire volume of the sample using a Hamilton syringe. Inject volume slowly into the bottom of the well.

6. **Gel electrophoresis**
   a. Immediately after all samples are loaded place the lid on the gel chamber.
   b. Place positive and negative plugs into the power supply and turn on power supply.
   c. Set power supply to 120V. Gel will run for ~2 hours depending on percent gel made.
   d. When the bromophenol blue has run off the bottom of the gel turn off the power supply. Remove plugs from power supply and remove lid.
   e. Prepare for electrotransfer of proteins from the gel to nitrocellulose membrane.

WESTERN BLOTTING AND IMMUNODETECTION

Reagents

1. Transfer Buffer
   a. 0.025M Tris-HCl pH 8.3 12.14g
   b. 0.15M Glycine 45.05g
   c. 20% Methanol 800ml
   d. make up to 4L with ddH_20
   e. store at 4°C
2. Ponceau S stain
   a. 0.1% (w/v) Ponceau S
   b. 0.5% (v/v) Acetic Acid
   c. Store at room temperature
3. Wash Buffer
   a. Tris-HCl pH 7.5 12g
   b. NaCl 58.5g
   c. 0.1% Tween 10ml

d. Store at room temperature

4. Blocking Solution
    a. 5% (w/v) skim milk power in wash buffer OR
    b. 5% (w/v) BSA in wash buffer
5. Enhanced Chemiluminescence Fluid (ECL; Santa Cruz sc-2048)
6. Film/Developer/Fixer

Procedure

1. **Transfer Procedure**
    a. Remove electrophoresis plates from chamber and separate the plates.
    b. Cut away unnecessary parts of the gel using a spatula and measure remaining gel size.
    c. Using a paper cutter cut 6 pieces of Whatman paper per gel to the same size as the gel. Wearing gloves cut nitrocellulose membrane (GE Healthcare RPN303D) to the dimensions of the gel.
    d. Assemble Whatman paper, nitrocellulose membrane and gel as shown below:

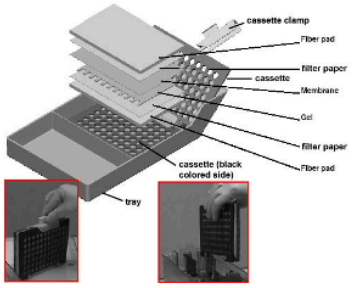

    e. Close the cassette and place in the transfer chamber with the black side of the cassette facing the back side of the chamber.
    f. Place ice pack in the chamber.
    g. Place lid on the chamber and connect the leads to the power supply.
    h. Turn on the power supply and run at 120V for 2 hours. This can vary depending on the size of the protein of interest.
2. **Removal of transfer membrane:**
    a. Turn off the power supply and disconnect leads from the power supply then remove the lid from the chamber.
    b. Remove the cassette from the chamber.
    c. With gloves on, remove the Whatman paper and gel and place the nitrocellulose membrane in a plastic dish.
    d. Add Ponceau S stain on the membrane and gently swirl.
    e. Drain off the remaining Ponceau S and save for reuse.
    f. Rinse the membrane with ddH_20 to reduce the red background. Wrap membrane in saran wrap and scan image.
    g. Cut the membrane while protein bands are still visible at the desired molecular weight.

h. Rotate membrane at room temperature in wash buffer until remaining Ponceau S has been removed.
i. Incubate membrane for 1 hour with rotation in blocking solution.
j. Incubate membrane with desired antibody diluted in blocking solution overnight at 4ºC. Membrane is placed face down into the solution on a glass plate covered in parafilm. To maintain a moist environment overnight, wet a small kimwipe and form it into a ball and place in each corner of the dish. Cover the dish with saran wrap.

3. **Immunodetection**
   a. Wash the blots in wash buffer with gentle rotation for 5 minutes 3X.
   b. Incubate the blots for 1-2 hours with the appropriate secondary antibody diluted in blocking solution.
   c. Membrane is placed face down in solution on a glass plate covered with parafilm. Place moist kimwipes in each corner of the dish and cover the dish with saran wrap.
   d. Following the incubation, wash the membrane 3X for 5 minutes with wash buffer.
4. **Enhanced Chemiluminescence Detection**
   a. Mix ECL fluids "A" and "B" in a 1:1 ratio in a disposable Rohr tube.
   b. Place blots on saran wrap face up and apply ECL solution for 2 minutes.
   c. Dab off excess ECL on a kimwipe and place blots face down on a fresh piece of saran wrap and wrap tightly.
   d. Expose blot to film (time will vary depending on protein and antibody).
   e. Place film into developer (time will vary).
   f. Once image appears place film into fixer for 2 minutes. Wash with fresh water when complete.

Isolating Cytoplasmic and Mitochondrial Fractions

Materials Required:

- Dry ice
- Ice cold 1xPBS
- Labelled 2 mL and 1.5 mL Eppendorf tubes
- Ice
- Cell scrapers (as many as conditions)
- Sonicator

Resuspension Buffer preparation:

For 10 mL:

- 100 mM KCl (0.075 g)
- 10 mM MOPS (0.021 g)
- 0.2% BSA (0.02 g)
- Top up with ddH_2O and mix thoroughly.

Procedure:

1. Culture cells at appropriate density. High cell yield is recommended for this protocol. Use two 6-well plates or one 150mm x 20mm tissue culture dish per condition. (Myoblasts can be cultured at $4x10^4$ in a 6-well plate or $8x10^4$ in a dish, and then differentiated to myotubes once 80-85% confluency has been reached).
2. After treatment, collect the cells with ice cold 1xPBS in 15 mL falcon tubes. Scraping the cells instead of trypsinizing helps maintain the pellet size. Use of trypsin-EDTA to collect cell pellet requires an additional washing step to remove the media from the suspension, which reduces pellet size and results in lesser mitochondrial yield.
3. Centrifuge at 1400xg for 5 minutes, aspirate the supernatant.
4. Resuspend each pellet with resuspension buffer at 4-5 times the size of the pellet acquired.
5. Transfer the cell suspension to labelled 2 mL Eppendorf tubes. Incubate on ice for 5 minutes.
6. Sonicate each sample at 30-40% power output for 3-5 seconds. Repeat 3x per condition. Rest the sample on ice for at least 30 seconds between each rep. Clean the sonication wand between samples/conditions.
7. Centrifuge samples at 1000xg for 10 mins at 4°C.
8. Collect the supernatant and transfer to new labelled 1.5 mL Eppendorfs. Centrifuge at 14 000xg for 15 min at 4°C.
9. Collect the supernatant and transfer to a final new labelled set of 1.5 mL Eppendorfs to be stored at -80°C as the **cytosolic fraction**.
10. Add 100-200 uL of resuspension buffer to the remaining pellet and centrifuge at 14 000xg for 10 min at 4°C. Repeat this step twice, ensuring resuspension of the pellet prior to second round of centrifugation.
11. Aspirate the supernatant and add 25-50 uL of resuspension buffer to each pellet and resuspend thoroughly. Transfer these samples to final new labelled set of 1.5 mL Eppendorfs.
12. Freeze-thaw samples 2-3 times on dry ice.
13. Store samples at -80°C as the **mitochondrial fraction**.

Isolating Cytoplasmic and Nuclear Fractions

Materials Required:

- Ice cold 1xPBS
- Labelled 2 mL and 1.5 mL Eppendorf tubes
- Ice
- Cell scrapers (as many as conditions)

Stocks

1 M Tris (200 mL) = 24.22 g

1 M NaCl (200 mL) = 11.68 g

250 mM EDTA (200 mL) = 18.61 g (Add NaOH pellets to dissolve)

250 mM DTT (30 mL) = 1.92 g

1 M $MgCl_2$ (50 mL) = 10.165 g

Cytoplasmic Buffer (200 mL)

100 mM Tris → 2 mL from 1 M stock

10 mM NaCl → 2 mL from 1 M stock

3 mM $MgCl_2$ → 600 uL from I M stock

0.5% NP-40 → 1 mL added directly

Top up with ddH_2O and mix thoroughly

Working buffer must be prepared with Cocktail [Phosphatase (Cocktail 2, 3) and Protease] Inhibitors at 0.2% concentration for each.

Nuclear Buffer (200 mL)

50 mM Tris → 10 mL from 1 M stock

5 mM $MgCl_2$ → 1 mL from 1 M stock

0.1 mM EDTA → 80 uL from 250 mM stock

1 mM DTT → 800 uL from 250 mM stock

40% glycerol → 80 mL

Top up with ddH_2O and mix thoroughly

Procedure:

1. Prepare the working cytoplasmic buffer with appropriate concentrations of cocktail inhibitors. Place on ice.
2. Culture cells at appropriate density. High cell yield is recommended for this protocol. Use two 6-well plates or one 150mm x 20mm tissue culture dish per condition. (Myoblasts can be cultured at $4x10^4$ in a 6-well plate or $8x10^4$ in a dish, and then differentiated to myotubes once 80-85% confluency has been reached).
3. After treatment, collect the cells with ice cold 1xPBS in 15 mL falcon tubes. Scraping the cells instead of trypsinizing helps maintain the pellet size. Use of trypsin-EDTA to collect cell pellet requires an additional washing step to remove the media from the suspension, which reduces pellet size and results in lesser mitochondrial yield.
4. Centrifuge at 1400xg for 5 min. Aspirate the supernatant.
5. Resuspend the pellet in cytoplasmic buffer. Volume depends on pellet size, 3x the size is adequate.
6. Incubate on ice for 5 min.
7. Rock the samples at 4°C for 5 min.
8. Centrifuge the samples at 2500xg for 5 min at 4°C.
9. Collect the supernatant and transfer to properly labelled Eppendorf tubes to be stored as the **cytoplasmic fraction** at -80°C until use.
10. Resuspend the remaining nuclear pellet with cytoplasmic buffer.

11. Rock the samples at 4°C for 3 min.
12. Centrifuge the samples at 3200xg for 3 min at 4°C.
13. Collect and discard supernatant.
14. Repeat steps 10-13 approximately 10-12 times to ensure thorough washing and purity of nuclear pellet.
15. Resuspend the final pellet following discarded cytoplasmic buffer with 150-200 uL of nuclear buffer. Transfer each sample to properly labelled Eppendorf tubes.
16. Prepare 0.15 unit/uL of Benzonase (0.5 uL Benzonase in 7.83 uL of sterile H2O)
17. Add 1.5 uL of Benzonase to each nuclear sample. Incubate on ice for 10-20 min.
18. Samples are to be stored as the **nuclear fraction** at -80°C until use.

APPENDIX D: OTHER CONTRIBUTIONS TO THE LITERATURE

Articles published or accepted in peer-reviewed journals

1. Slavin, M. B., Memme, J. M., Oliveira, A. N., **Moradi, N**., & Hood, D. A. (2022). Regulatory networks coordinating mitochondrial quality control in skeletal muscle. *American Journal of Physiology-Cell Physiology*, *322*(5), C913-C926.
2. Triolo, M., Slavin, M., **Moradi, N**., & Hood, D. A. (2022). Time-dependent changes in autophagy, mitophagy and lysosomes in skeletal muscle during denervation-induced disuse. *The Journal of Physiology*, *600*(7), 1683-1701. (BSc work)
3. Memme JM., Slavin M., **Moradi N.**, Hood DA. (2021). Mitochondrial Bioenergetics and Turnover during Chronic Muscle Disuse. *International Journal of Molecular Sciences*. 22(10): 5179. (MSc work)

Non-peer-reviewed contributions

1. **Moradi N**, Hood DA. (2022). Pharmaceutical and nutraceutical agents induce time-dependent changes in intracellular signaling for mitochondrial homeostasis in skeletal muscle cells. *International Biochemistry of Exercise Conference*. International. (Poster, MSc work).
2. **Moradi N**, Hood DA. (2022). Exercise mimicry: Characterization of nutraceutical agents that may contribute to mitochondrial homeostasis in skeletal muscle. *Experimental Biology*. International. (Poster, MSc work).
3. **Moradi N**, Hood DA. (2021). Sulforaphane and Urolithin A exert time-dependent effects on mitochondrial protein signaling in C2C12 myotubes. *Canadian Society for Exercise Physiology*, virtual. National. (Poster, MSc work).
4. **Moradi N**, Hood DA. (2021). Sulforaphane and Urolithin A induce time-dependent effects on skeletal muscle adaptation. *Broaden Horizons Conference* (virtual), YorkU, Toronto, Canada. Institutional. (Oral presentation, MSc work).
5. **Moradi N**, Hood DA. (2021). Time-dependent effects of Sulforaphane and Urolithin A on C2C12 myotubes with implications for mitochondrial regulation in muscle. Institutional. *Muscle Health Awareness Day*, virtual (Abstract, MSc work).